3.4.3

Full Length Research Papers Published in the Journals Notified on UGC Care List

2021 - 22

	2021-2022					
23.	Kavuri Satyanarayana NatikalaloSamajikaDrukpadham	Dr.B.Mary Kumari	Telugu	International Organizational of Scientific Research	July.2021	ISSN: 2279-0845
24.	Impurity Profiling and Stebility-Indicating Method Development and Validation for the Estimation of Assay and Degradation Impurities of Midostaurin in Soft Gel Capsules Using HPLC and LC - MS	Dr.PoornimaRavinathan	Political Science	Biomedical Chromatography	July.2021	DOI: 10.1002/bmc.5222
25.	Development and Validation of Liquid Chromatographic Tandem Mass Spectrometry Method for the Estimation of a Potential Genotoxic Impurity 2 (2Chloro Ethoxy) Ethanol in Hydroxyzine.	Dr.PoornimaRavinathan	Political Science	Biomedical Chromatography	Nov. 2021	DOI: 10.1002/bmc.5325
26.	The Element of Emotional Intelligence and their Impact on Social Relation	Ms.P.Hemalatha	Home Science	International Journal of Early Childhood Special Education (INT-JECSE)	Mar.2022	ISSN: 1308-5581
27.	Mahabharatham lo Sahanam KaliginaSthreeMurthulu	Dr.B.Mary Kumari	Telugu	Bhavaveena Special Eddition	Mar.2022	ISSN: 2456-4702
28.	Mucormycosis: Assessment of Risk Factors in a Subject suffering from Congenital Haemophilia	M.Aruna	Zoology	World Journal of Pharrmacy and Pharmacuitical Sciences	May.2022	ISSN 2278-4357

29.	Pesticide Spraying ROBOT : The Mechatronics Approach to Agriculture	CM Anitha	Physics	International Journal of Early Childhood Special Education	May.2022	ISSN 1308- 5581

JMJ COLLEGE FOR WOMEN (Autonomous) * TENALI *

PRINCIPAL
JMJ COLLEGE FOR WOMEN (Autonomous)
TENALI

Principal

IOSR Journal of Humanities and Social Science

IOSR Journals
International Organization of Scientific Research

e-ISSN : 2279-0837 Volume : 26 Issue : 7 Series-1 p-ISSN : 2279-0845

IOSR-JHSS

Contents:

Peer Reviewed Refereed Journal

IOSR Journal Of Humanities And Social Science (IOSR-JHSS)
Volume 26, Issue 7, Series 1 (July. 2021) 71-73
e-ISSN: 2279-0837, p-ISSN: 2279-0845.
www.iosrjournals.org

కావూరిసత్యనారాయణ నాటికలలో సామాజిక దృక్పథం

Kavuri satyanarayan natikalalo samajiaka drukadham

బి.మేరి కుమారి B.Mary kumari

జి.యం జె మహిళా కళాశాల [స్వయంప్రతిపత్తి] తెనాలి J.M.J College for women [Autonomous] Tenali

ఆధునిక నాటక రంగ చరిత్రలో పలు విజయవంతమైన నాటకాలు రచించి తన కంటూ ఒక ప్రత్యేకమైన స్థానం పొందిన రచయిత కావూరి సత్యనారాయణ

రివర్స్ మార్చ్ :

మొదటి వినోదం కోసం,పరికిని బెరుకుతనాన్నిపొగొట్టడం కోసం పుట్టిన రేజింగ్ ఈ రోజులలో రూపం దరించింది.నేటి విద్యా సంస్థలలో జరుగుతున్నా రాగింగ్ వాళ్ళ ఎందరో అమాయకుల ప్రాణాలను బలిగొంది. పెడదారి పడుతున్న యువత ఆలోచనా విధానులను.పాఠాలను బోధించి ,విజ్ఞానవంతులను తయారుచేయవలిసిన అధ్యాపకల నిర్లిప్తతనిస్సహాయ తత్వాలను అద్భుతముగా చూపించిన నాటిక

ఒక ప్రైవేటు కళాశాలలో చదువుతున్న మదన్ గోపాల్ స్నేహితుడు విరు పద్మజ అనే అమ్మాయిని మాటలతో చేతలతో హింసిస్తున్నారు.వీరి బారి నుండి తప్పించుకోవటానికి పద్మజ పై అంతస్తు నుడి దూకి చనిపోయింది.ఆ కళాశాల ప్రెసిడెంట్ మదన్ తండ్రి ప్రజాహితరావు పద్మజ ప్రమాదవశాత్తు జారిపడినట్లు పిర్యాదుచెయవలిసిందిగా ప్రిన్సిపాల్ ను ఒత్తిడి తెస్తాడుస్తూపై అనునిత్యం జరుగుతున్నా అమానుష దాడులను గూర్చి నాలుగా ఎందరో సభ్యజనులును సిగ్గుతో మాన వేదన అనుబావిస్తున్నారే గాని నేరస్తుడు మన కళ్ళ ముందే తిరుగుతుంటి ఇదేమిటి అని ఒక్కడు కూడా ప్రశ్నించలేనిదుర్భర స్థితిఅంటూ ప్రిన్సిపాల్ ఎదురుతిరుగుతాడు తప్పించుకోవడానికి ప్రయంతించినగోపాల్ జనం నన్ను పట్టు కున్నారు. శవాన్ని నాకు అప్పగించారు. తప్పించుకోవడానికి ఎక్కడ కుట్ర జరుగుతుందో అక్కడ నుండి సవం మాయాలంటి మన ముగ్గురంసవాన్ని మాయాలంటు ఆ తర్వాత చట్టానికి లొంగిపవలంటూ అని జనం శాసించారు అంటుడు దానితో ప్రెసిడెంట్

ప్రజాహితరావు అని పేరు పెట్టడం రచయిత వ్యంగ్యధోరణి కనిపిస్తుంది. ఈ నాటిక [illegible] దృష్టి స్పష్టమౌగా తెలుస్తుంది .

శ్వేతా పత్రం ;

శ్రీధర్ రావు కొడుకును చదివిస్కోవటానికి పట్నానికి వస్తాడు కొడుకు [illegible] అడ్డదారులలో ప్రశ్నాపత్రాలనుతెస్తాడు తెలివి లేని శంకర్ ఫస్ట్ క్లాస్ తెలివిగల [illegible] మారలాడు. హితస్సునైన శ్రీధరరావు పవర్తిస్తున్న [illegible] మార్క్రమే ఫలితాలను తారుమారు చేస్తుందని గ్రహించలేకపోయాను [illegible] బజారులో పట్టగల వస్తువాగితాల మాదిరి అమ్ముడు పోతుంటే ఇంకా [illegible] యమ సెట్ హోల్ ఇండియా ఏఅసి ఇంటికెగి . [illegible] ప్రచారిస్తుంటే సామాన్యుడికి చదువెందుకు అంటాడు.చదుకునే రోజులు [illegible] , టక్నిషియన్లతో ఈ దేశం నిది ఉండ కూడదని సందేశాన్ని అందించాడు

ముఖ చిత్రం:

వార్తపత్రికలలో వచ్చే వార్త జనలకు స్పందింప నాటకీకరించే సంప్రదాయంతో నాటిక [illegible] సంతానం రఘు కష్ట పడకుండా అర్జంటుగా కోటీశ్వరుడు కావాలనుకొని రఘు ఒక [illegible] దోచుకుంటాడు .ఆ విష్యం తెలుసుకున్న చలపతి రఘుని పోలీసుకి అప్పచెప్పుతాడు [illegible] వచ్చిన రఘు తల్లి తండ్రులను కులనాడ వారిని కత్తితో గాయపరుస్తాడు. నేటి సమాజంలో [illegible] పొడాబుద్ధి విసిరిన వాళ్ళే ఈ సమాజం జను అంటుంది బాబ్బు విసిరిన వాళ్ళే [illegible] గడించిన వాళ్ళను దైవంస సంభూతుడని భావించి భజనలు చేస్తున్నారు జైల్లో మగ్గవలసిన నేరస్థులు [illegible] అధికార పీటం మీద కుర్చుని రాజ్యాంగాన్ని రక్షిస్తున్నారునిరుద్యోగులగారోడ్ల మీద తిరుగుతున్నా యువకులు [illegible] సంస్కృతి వైపు ఆసర్కితులవుతున్నారు నేరస్థుడితో స్నేహం చేయడం రఘు కూడా నేరాలు [illegible]

ఆపాదిన్చుకుంటున్నారు . ఒరెయ్ ని లాంటి నేరస్తులు సృష్టించెది పోలసులు చట్టాలు కోర్టులు ప్రభుత్వాలు కవుర సామాజక బహిష్కరణ నీకు తగిన శిక్ష . ఎదో ఒక రోజున కడుపు మండిన జనంచెతిలో కుక్క చావు చస్తవురా అంటూ తండ్రి రమును చెల్లగొడతాడు పడదరి పడుతున్న యువతరం వికృతమైన దుర్మార్గ లకు ఈ నాటక ముఖ చిత్రంగా ఉంది

జానుడు మెట్లు :

లాభాటి కాని మోగు నాకొద్దు అంటూ లాభం లని పెళ్ళాం నకక్కర లదు అంటూ విడాకులు తమలపాకులు తీసుకున్నంత తేలికగా తీసుకుంటున్నారు మీరు ఇలా చెస్తున్నరనుకుంతేతరతరాల పవిత్రమైన వివాహ బంధాన్ని ఇంతదాకా మోసుకోచ్చెవారము కాదు .నిన్నటి సతి సహగమనం రోజే సమాది చేసి ఉండెవారము నైతిక విలువలు అన్నటికి విలువలు ఉన్ని వివాహబంధాన్ని తొక్కేస్తూ పైకి ఎక్కేస్తునం అంటూ వివాహ బంధాన్ని వ్యాపార బంధముగా మార్చుకుంటున్న మిమ్మల్ని మా పిల్లలని చెప్పుకోవటానికి సిగ్గుపడుతున్నాము వివాహ బంధం సారీరక మానసిక ఆర్థిక పరిరక్షణకు అనకట్ట ఈ బంధం సక్రమముగా ఉంటె దెశం సక్రమముగా ఉంటుంది అనాగరిక కృత్రిమ విలువలు తల్లక్రిందులై నియమాలు విద్వాసమై పోతే రేపటి భవిష్య లదు అని ప్రపంచానికి రచయిత తెలియజెస్తున్నాడు

రాచఱ కాష్టం:

కార్గిల్ యుద్ధంలో కొడుకు చనిపొనప్పుడు హృదయవికరముగ్ ఏడుస్తున్న భార్యతో ఎదవుకు నువ్వు ఏడిస్తె వాడికి అవమానం వాడు చురకేంచి చంద కోట్ల భారతీయ హృదయాలలో జీవించాడు. వాడు అమరుడు మర పిరంగికి గుండైని గుడుగా అడ్డుపెట్టి కోట్లాది జాతిజనుల గుండ్లమీద చెర్స్ వెసుకుని నిద్రపోయెల చెసాడు మన బిడ్డ తల్లి, తండ్రి భార్య బిడ్డలు బందులు అనుబందులు రంటి విలువైనది సైనికుడి బాద్యత ఈ యుద్ధంలో ఎన్ని కులాల మతాలు జాతులు ప్రాంతాలు పాల్గొన్నారు తెలుగు వారు చిందించి రక్తం తో త్రి వర్ణ పతాకం తడిసింది శాంతి కోసం జరుగె యుద్ధం ఆగదు ఇది రాచఱ కాష్టం భారత సైనిక శక్తి ఆజెయమని లొకనింకి చాటుడు రచయిత

ఈ విదముగ్ రచయిత సమాజానికి అవసరమైన్న విషయాన్ని సునిసిత దృష్టి తో చూసు ముందు కాలానికి ఉపయోగపడే రచనలు చెసాడు

IOSR Journal of Humanities and Social Science (IOSR-JHSS)

Contact Us

Website URL : www.iosrjournals.org
Email : Support@iosrmail.org

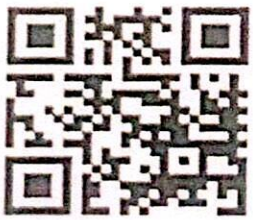

Qatar Office:

IOSR Journals
Salwa Road
Near to KFC and Aziz
Petrol Station,
DOHA, Qatar

India Office:

EHTP, National Highway
8, Block A, Sector 3
Gurugram, Haryana
122001

Australia Office:

53, Ring Road,
Richmond Vic 3121
Australia

New York Office:

8th floor, Straight hub,
NS Road, New York,
NY 10003-9595

Received: 4 May 2021 | Revised: 8 July 2021 | Accepted: 23 July 2021

DOI: 10.1002/bmc.5222

RESEARCH ARTICLE

Biomedical Chromatography WILEY

Impurity profiling and stability-indicating method development and validation for the estimation of assay and degradation impurities of midostaurin in softgel capsules using HPLC and LC–MS

Narasimha Swamy Lakka[1] | Chandrasekar Kuppan[1] | Poornima Ravinathan[2]

[1]Division of Chemistry, Department of Science and Humanities, VIGNAN'S Foundation for Science, Technology and Research (VFSTR), Vadlamudi, Guntur, India

[2]Department of Science and Humanities, JMJ College for Women, Tenali, India

Correspondence
Chandrasekar Kuppan, Division of Chemistry, Department of Science and Humanities, VIGNAN'S Foundation for Science, Technology and Research (VFSTR), Vadlamudi, Guntur 522213, India.
Email: drcsk_sh@vignan.ac.in

Abstract

Midostaurin (MDS) is used for the treatment of acute myeloid leukemia, myelodysplastic syndrome, and advanced systemic mastocytosis. MDS softgel capsule samples were subjected to stress testing per International Conference on Harmonisation of Technical Requirements for Registration of Pharmaceuticals for Human Use guidelines for impurity profiling study. MDS underwent extensive degradation under stress testing (acid, alkaline, oxidative, photolytic, thermolytic, and hydrolysis conditions) and formed four degradation products (DPs). MDS and its DPs were separated well from one another with good resolution using reserved-phase HPLC using an Inertsil ODS-3V column (250 × 4.6 mm, 5 μm) and a mobile phase of ammonium formate (40 mM) and acetonitrile. The stability-indicating characteristic of the newly developed method was proven for the estimation of MDS assay, and its organic impurities were free from interference. The validated method exhibited excellent linearity, accuracy, precision, specificity, detection limit, and quantitation limit within 25 min run time. Stress testing, robustness, and solution stability were performed to ensure the continuous performance of the developed method. The peak fractions of DPs formed under stress testing were isolated and characterized using LC–MS, ^{1}H and ^{13}C NMR, IR, and UV–Vis. The structure of the major DPs was predicted as DP1 based on the spectral data. The proposed method is effectively used for MDS in bulk drug and finished formulations in the pharmaceutical industry.

KEYWORDS

degradation product, impurity profiling, LC–MS/MS, method development and validation, midostaurin, reversed phase-HPLC, stress testing

1 | INTRODUCTION

Midostaurin (MDS) is a multitargeted protein kinase inhibitor that is used in the treatment of acute myeloid leukemia (AML), myelodysplastic syndrome, and advanced systemic mastocytosis. MDS is a semisynthetic derivative of staurosporine, an alkaloid from the bacterium Streptomyces 'Staurosporeus'. MDS possesses four chiral centers held between a rigid bicyclic ring system and exists as a single enantiomer. The IUPAC named MDS as *N*-[(2*S*,3*R*,4*R*,6*R*)-3-methoxy-2-methyl-16-oxo-29-oxa-1,7,17-triazaoctacyclo [12.12.2.12,6.07,28.08,13.015,19.020,27.021,26]nonacosa-8,10,12,14,19,21,23,25,27-nonaen-4-yl]-*N*-methyl benzamide, with molecular formula $C_{35}H_{30}N_4O_4$ and molecular weight 570.649 g/mol (Scheme 1a).

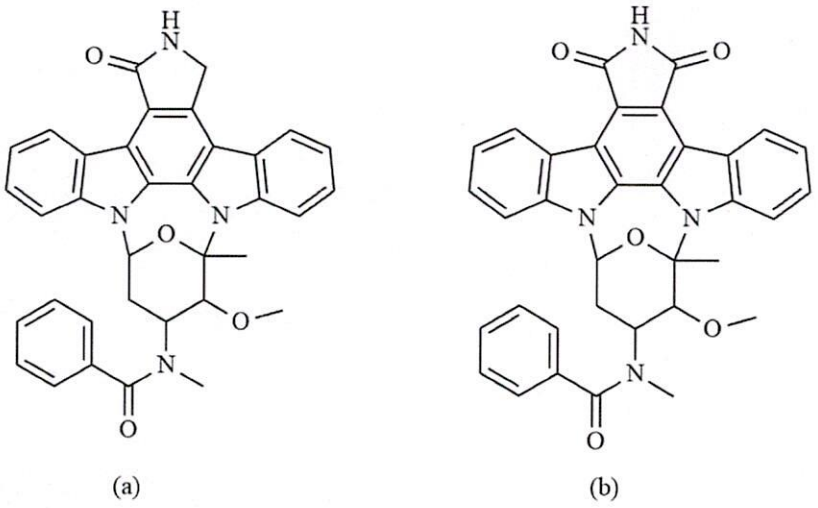

(a) (b)

SCHEME 1 Chemical structure of (a) midostaurin (MDS) and (b) degradation product 1 (DP1)

MDS is a white to light yellowish-green hygroscopic powder that forms three benzyl alcohol crystalline solvates: form II, form SA, and form SB [RYDAPT (midostaurin)—FDA, 2017]. MDS in softgel capsules form [brand: RYDAPT (MDS form II)] was developed by Novartis Pharmaceuticals Corporation (East Hanover, NJ, USA) and recently approved as an orphan drug by the U.S. Food and Drug Administration (FDA, on April 28, 2017), which is commercially available as 25 mg softgel capsules. The recommended dosage of MDS is 50 mg twice a day for AML and 100 mg orally twice with food for patients with aggressive systemic mastocytosis, systemic mastocytosis with an associated clonal hematological nonmast cell lineage disease, and mast cell leukemia disorders. MDS was also found to inhibit multiple receptor tyrosine kinases (Richard & Sabine, 2018). MDS and its major human active metabolites, *O*-desmethyl midostaurin (CGP62221) and 3-hydroxy midostaurin (CGP52421), inhibit the activity of mutant kinases [wild-type FLT3, ITD, TKD, KIT (wild type and D816V mutant), PDGFR α/β, and VEGFR2], as well as members of the serine/threonine kinase protein kinase C family.

Preliminary literature survey revealed that there is no official monograph (United States Pharmacopoeia (USP); European Pharmacopoeia (Ph.Eur.); International Pharmacopoeia (IP), etc.) available either for the active pharmaceutical ingredient (API) or for the drug product of MDS. A variety of HPLC–MS methods are available for the determination of MDS individually and in combination with its metabolites in plasma samples [Handan et al., 2017; Philippe et al., 2014; Thomas et al., 2007; Van Gijn, Havik, et al., 1995; Van Gijn, van Tellingen, et al., 1995, Table S1 (Supporting Information)]. Only a few HPLC methods were reported for the assay testing of MDS in API and drug products [Ahmed et al., 2018; Narayanaswamy et al., 2020, Table S1 (Supporting Information)]. An extensive literature search revealed that no specific method has been developed to suit HPLC and LC–MS techniques for the determination of MDS assay and its organic impurities that are present in MDS soft gelatin capsule formulations. Furthermore, to the best of our knowledge, none of the research papers have reported on the impurity profiling study of MDS and characterization of the degradation products (DPs) or degradation impurities that are most likely to be formed under various stress conditions of MDS.

In recent times, global regulatory agencies and their forums (ICH, U.S. FDA, The European Directorate for the Quality of Medicines & HealthCare, etc.) have made it mandatory to set stringent strategies to decrease the amount of unknown impurities or DPs to less than 0.1% in drugs to improve their quality and to ensure the safety of patients using the stability-indicating method (SIM) and stress testing [ICH, Q1A(R2), 2003; Narasimha et al., 2019; Q3A(R2), 2006a; Q3B (R2), 2006b].

Stress testing a drug is necessary to investigate and identify the potential impurities through the degradation pathways and to understand the intrinsic stability of a drug to assess its shelf life (Bhaskar et al., 2020; Blessy et al., 2014; Deepti & Pawan, 2013; ICH, Q1B., 1996; Kumar et al., 2016; Nageswara et al., 2013; Narasimha & Chandrasekar, 2019; Narasimha et al., 2020; Roberto de Alvarenga & Lajarim, 2019; Saranjit et al., 2013; Venkataraman & Manasa, 2018). Therefore, the proposed method specifically focuses on (a) the forced degradation studies on MDS at different stress conditions, (b) separating the DPs from the reagent and excipients using HPLC, (c) isolating and characterizing the DPs, and (d) predicting the possible structure of the DPs with the aid of spectral data.

The current contribution focuses on the development of a new SIM suitable for the routine quality control testing of the MDS assay and its organic impurities (impurity profiling) for MDS softgel capsules in the pharmaceutical industry. The developed method exhibited the stability-indicating characteristic (defined as an analytical procedure that measures the target analyte so-called drug compound accurately and precisely free from interference), and it was successfully applied for the estimation of the MDS assay and its organic impurities without any interference from the DPs, process impurities, and excipients in the isocratic elution mode with a reduced run time (25 min). The developed method provided a good resolution (>1.5) between the closely eluting peaks with a base-to-base separation in the presence of the pharmaceutical formulation. In addition, the developed method was used for the isolation and characterization of potential DPs of MDS

(i.e., four DPs of MDS formed during the stress-testing conditions of acid, alkali, and oxidation were isolated). The chemical structure of the major formed DPs (mentioned as DP1 in the manuscript) under the oxidation stress condition was confirmed using various spectral techniques like HPLC–UV, LC–MS, LC–MS/MS, FT–IR (Fourier-transform infrared spectroscopy), and NMR (nuclear magnetic resonance). The spectral data of the other three DPs (DP2, DP3, and DP4) obtained using UV and LC–MS/MS were discussed and presented.

The proposed HPLC method was validated and it exhibited excellent linearity, accuracy, precision, specificity, stress testing, detection limit (DL), and quantitation limit (QL) [ICH, Q2(R1), 1995; USP < 1225>, 2020]. The robustness and solution stability studies were carried out to ensure the continuous performance of the developed HPLC method [ICH, Q2(R1), 1995], and the results were within acceptable limits.

2 | EXPERIMENTAL

2.1 | Reagents and materials

MDS standards (purity ≥99%), samples of MDS drug substance, formulated drug product (MDS soft gelatin capsules), and their placebo (all the excipients without drug) were provided by Dr. SLN Laboratories Pvt. Ltd. (Hyderabad, India). Extra-pure analytical-grade ammonium formate was purchased from SRL (Taloja, Maharashtra, India); HPLC-grade acetonitrile was purchased from Qualigens (Thermo Fisher Scientific India Pvt. Ltd., Mumbai, India); analytical-grade sodium hydroxide (NaOH), hydrochloric acid (HCl), potassium nitrate (KNO_3), and hydrogen peroxide (30%, H_2O_2) were purchased from Rankem (Thane, Maharashtra, India). HPLC-grade methanol was purchased from Rankem (Thane, Maharashtra, India).

2.2 | Standard solution

MDS standard solution, with a concentration of 0.4 mg/mL, was prepared for assay testing by dissolving 4.0 mg of the MDS standard in 10 mL of diluent (40 mM ammonium formate buffer, acetonitrile, and methanol, 40:40:20, v/v/v) and stored at room temperature (25°C). A diluted standard of MDS at a concentration 0.8 µg/mL (0.2%, w/w, with respect to the sample concentration 0.4 mg/mL) was prepared using the same diluent from the stock for organic impurity analysis.

2.3 | Sample preparation

MDS softgel capsules (25 mg × 4, which is equivalent to 100 mg) were opened using a capsule cutter and were directly transferred into a 100-mL glass beaker. The cutter was rinsed with 10–15 mL of diluent directly into the beaker to remove any drug adhering to the cutter blade. The solution was transferred into a 250-mL volumetric flask, and a diluent was added up to the mark. The drug was extracted by keeping the flask in an ultrasonic bath for ~5 min with intermittent shaking. The sample solution prepared was filtered using a 0.22-µm PVDF membrane filter (diameter: 30 mm, Allpure Biotechnology, TX, USA). The concentration of MDS in the resulting sample solution was 0.4 mg/mL, and the same was used for the estimation of assay and organic impurities of MDS in softgel capsules. The placebo solution along with the soft gelatin capsule shell of MDS capsules was prepared using the same procedure as that for the sample solution.

2.4 | Instruments

HPLC coupled with a photodiode array (PDA) detector and a UV detector was utilized for the separation, identification, and quantitative determination of MDS and its DPs (Waters e2695 with 2998 PDA and 2489 UV detectors). The stationary phase used was a C_{18} column from Inertsil ODS-3V (250 × 4.6 mm, 5 µm) (GL Sciences, Tokyo, Japan). The output signal was monitored and processed using Empower 2 software. Ultrasonic bath used for sample preparation was obtained from PCI (Mumbai, India). The samples and standards were weighed using an analytical balance (RADWAG, model: AS82/220.X2, Polska, Poland). Ultrapure water (electrical resistivity ≥18.2 MΩ cm at 25°C) was obtained using a Millipore Milli Q IQ-7000 (Merck, Molsheim, France) water purification system. The forced degradation studies were carried out in a forced degradation unit at 100 rpm (Electrothermal, UK) inside the fume hood (Citizen Industries, Gujarat, India). The *m/z* values of the MDS and its four DPs were analyzed using LC–MS (Waters HPLC e2695 system equipped with a 2998 PDA detector and a Qda mass detector (Milford, MA, USA) and UPLC–MS/MS (Waters Acquity Quattro Premier XE, Micromass MS Technologies, Manchester, UK).

2.5 | HPLC

HPLC separation of MDS and its four DPs was achieved on a C_{18} column (Inertsil ODS-3V, 250 × 4.6 mm, 5 µm) using an isocratic elution mode, with a mixture of 40-mM ammonium formate buffer and acetonitrile (35:65, v/v) as the mobile phase. The autosampler was set to an ambient temperature, and the column oven temperature was maintained at 40°C for all the analyses unless otherwise specified. The injection volume of the standard and sample solutions for analysis was 10 µL, and the flow rate was maintained at 0.9 mL/min. The eluted analytes (MDS and its DPs) were identified and estimated using a UV detector at a wavelength of 293.5 nm.

2.6 | MS

2.6.1 | LC–MS conditions

The molecular mass of the newly formed DPs was found using a Waters HPLC e2695 system equipped with a 2998 PDA detector and

a QDA mass detector (MS). The mass detector parameters used were cone voltage, 15 V; capillary voltage, 0.8 kV; and probe temperature, 600°C. Empower 3 software was used for data acquisition and processing. Inertsil ODS-3V (250 × 4.6 mm, 5-µm particle size) was used for chromatographic separation. The mobile phase used is a mixture of 40 mM ammonium formate buffer and acetonitrile (35:65, v/v). The flow rate used was 0.8 mL/min, and the injection volume was 10 µL; the other conditions used for LC–MS analysis were the same as those for the HPLC method.

2.6.2 | LC–MS/MS conditions

The molecular mass (*m/z*) and fragmentation pattern of the eluted fraction of four unknown degradation impurities along with the MDS were obtained using flow injection analysis on a Waters Acquity UPLC coupled with a tandem-quadrupole mass spectrometer MS/MS detector (Quattro Premier XE, Micromass MS Technologies) with a 0.2 mL/min flow rate of the mobile phase (a mixture of ammonium formate and acetonitrile, 50:50, v/v). The final optimized UPLC–MS/MS conditions for the MS scan with positive electrospray ionization (ESI) source are as follows: capillary, cone, and extractor voltages are 3.0 kV, 40 V, and 3.0 V, respectively. The temperature used for the source and desolvation were 150 and 400°C, respectively. The gas flow of high-purity nitrogen used for the cone and desolvation was 50 and 200 L/h, respectively. The collision cell pressure of high-purity argon gas used was 11.1 bar. The aforementioned conditions were applied for the mass (*m/z*) confirmation of MDS and all four DPs.

2.7 | FT-IR and NMR spectroscopy

The vibrational stretching frequency of the standards and degraded products was studied using infrared spectroscopy recorded on an Alpha II Compact FT-IR (Brucker, Ettlingen, Germany) using the KBr technique. The structure of the drug and degradation product 1 (DP1) was further confirmed by nuclear magnetic resonance spectroscopy (^{1}H-NMR and ^{13}C-NMR) recorded using an SA Varian 400 MHz NMR instrument (Walnut Creek, California, USA) with d^{6}-DMSO (dimethylsulfoxide, Sigma-Aldrich, Bengalore, India) as the solvent.

2.8 | Stress-testing study

To identify the degradation pathways and evaluate the stability-indicating characteristics of the developed HPLC method and also to determine the intrinsic stability and impurity profiling of the drug, forced degradation or stress testing was performed by hydrolyzing at different conditions (acid, alkali, neutral, and humidity), by oxidation and by thermal and photolytic degradation. For the study, 0.4 mg/mL MDS was subjected to stress-testing conditions as follows: *acidic hydrolysis*: stirred at 100 rpm in 5N HCl solution at 60°C for 1 h; *alkaline hydrolysis*: stirred at 100 rpm in 5N NaOH solution at 60°C for 1 h; *neutral hydrolysis*: stirred at 100 rpm in water at 60°C for 1 h; *oxidative degradation*: stirred at 100 rpm in 3% H_2O_2 solution at 25°C for 4 h; *thermal degradation*: exposed the softgel capsules to dry heat at 105°C for 6 h; *photolytic degradation under ultraviolet light*: exposed the softgel capsules under near-UV light for ~200 W h/m^2 at 25°C; and *photolytic degradation under visible light:* the softgel capsules exposed under cool white fluorescent lamp for ~1.2 million lux-hours at 25°C.

All the stressed sample solutions were neutralized (for acidic hydrolysis, alkali hydrolysis, and oxidation) and diluted to obtain a concentration of 40 µg/mL before assay testing. For acidic, alkali, and neutral hydrolyses and oxidation, the respective blank solutions were prepared in the same manner as that for the sample preparation and analyzed using the same procedure. The corresponding placebo solutions for each stress condition were also prepared and analyzed together with the sample and blank solutions.

2.9 | Method validation

The developed HPLC method for the related organic impurities of MDS and its assay was validated as per ICH guidelines and the USP for specificity, linearity, DL, QL, accuracy, precision, and robustness [Narasimha et al., 2019; Q2(R1), 1995; USP <1225>, 2020].

3 | RESULTS AND DISCUSSION

3.1 | Optimization of chromatographic conditions

The stress-testing samples were prepared using the procedure mentioned in the 'Experimental' section and were analyzed using the HPLC technique with different C_{18} columns and different mobile phases containing buffers like trifluoroacetic acid, sodium phosphate, potassium phosphate, and ammonium formate with organic modifiers, that is, acetonitrile and methanol (Narasimha et al., 2019). The optimized conditions of the developed SIM are specified in Section 2.5. Some of the experimental trials performed to optimize the HPLC conditions are summarized (Table 1).

3.1.1 | Selection of diluent

The soft gelatin capsule shell was freely dissolved in aqueous solution; MDS and other excipients used in the formulation of MDS softgel capsules were also found to be spontaneously soluble in methanol and acetonitrile (Rampurna, 2010). Based on the solubility profile of the drug and its associated impurities, a homogeneous solvent mixture of ammonium formate buffer (40 mM), methanol, and acetonitrile (40:40:20, v/v/v) was selected as the extracting solvent (diluent). With this solvent mixture and based on the trial runs, it was observed that the MDS and its impurity components were completely solubilized and were extracted completely from the MDS softgel capsules. This

TABLE 1 Optimization trials of HPLC method used for estimation of assay and organic impurities of MDS

Column name	Mobile phase	Elution mode, flow rate	Observation	Results
Inertsil ODS-3V, 5 µm, 25 × 4.6 mm	Buffer and MeCN—1:1	Isocratic, 1.0 mL/min	MDS and its DPs in stressed samples (hydrolysis and oxidation) were not eluted	Rejected
Inertsil ODS-3V, 5 µm, 25 × 4.6 mm	A: buffer, B: MeCN	Gradient [time (min)/%B: 0.01/30, 15/70, 22/70, 23/30. 25/30], 1.0 mL/min	Late elution. All peaks were not separated well. MDS (Rt 18.3 m), DP2 (Rt 21.6 m), DP1 (Rt 22.9 m)	Rejected
Inertsil ODS-3V, 5 µm, 25 × 4.6 mm	A: buffer, B: MeCN	Gradient [time (min)/%B: 0.01/50, 6/70, 15/80, 22/80, 23/50, 25/50], 1.0 mL/min	Resolution was found to be less than 1.5 between the MDS (Rt 10.3 m), DP2 (Rt 13.0 m), DP1 (Rt 13.8 m), and other unknown impurities	Rejected
Inertsil ODS-3V, 5 µm, 25 × 4.6 mm	A: buffer, B: MeCN	Gradient [time (min)/%B: 0.01/70, 14/75, 15/80, 22/80, 23/70. 25/30], 1.0 mL/min	All peaks eluted, but the unknown impurity is eluted closely with DP1 (Rt 10.3 m) and MDS (Rt 6.7 m)	Rejected
Inertsil ODS-3V, 5 µm, 25 × 4.6 mm	A: buffer, B: MeCN	Gradient [time (min)/%B: 0.01/65, 10/70, 16/70, 17/65, 20/65], 1.0 mL/min	All peaks eluted and separated. MDS (Rt 8.2 m), DP1 (Rt 12.8 m), DP2 (Rt 11.7 m)	Rejected
Inertsil ODS-3V, 5 µm, 25 × 4.6 mm	Buffer and MeCN—7:3	Isocratic, 1.0 mL/min	All peaks eluted, but an unknown peak was co-eluted at the peak end of MDS (Rt 7.4 m), DP1 (Rt 11.3)	Tentatively accepted
Inertsil ODS-3V, 5 µm, 25 × 4.6 mm	Buffer and MeCN—35:65	Isocratic, 1.0 mL/min	All peaks eluted and separated. MDS (Rt 8.6 m), DP1 (Rt 14.9 m), DP2 (Rt 13.2 m)	Tentatively accepted
Inertsil ODS-3V, 5 µm, 25 × 4.6 mm	Buffer and MeCN—35:65	Isocratic, 0.9 mL/min	All peaks eluted and separated. MDS (Rt 9.6 m), DP1 (Rt 16.6 m), DP2 (Rt 14.6 m)	Accepted
Inertsil ODS-3V, 5 µm, 25 × 4.6 mm	Buffer and MeCN—35:65	Isocratic, 0.8 mL/min	All peaks eluted and separated. MDS (Rt 10.4 m), DP1 (Rt 18.6 m), DP2 (Rt 16.5 m)	Accepted

Notes: DP, degradation product; MDS, midostaurin; Rt, retention time.

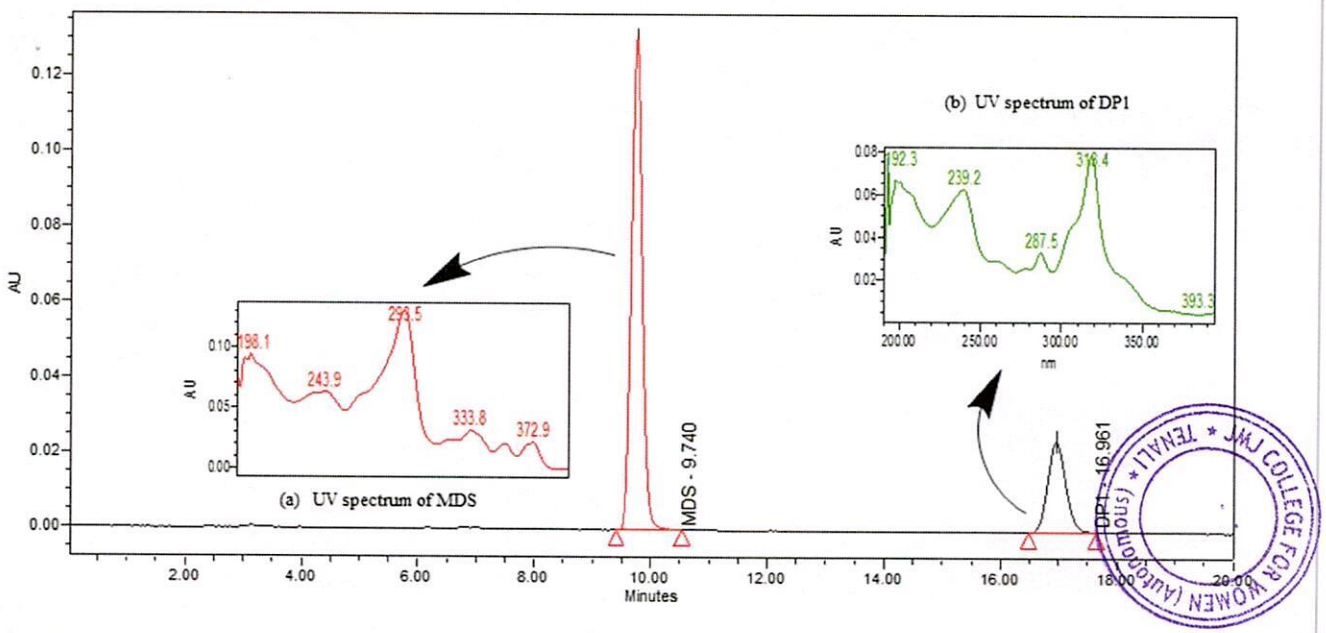

FIGURE 1 HPLC chromatogram of MDS (midostaurin) and its DP1 (optimized HPLC method); in-site view: (a) ultraviolet spectrum of MDS; (b) ultraviolet spectrum of MDS-DP1

confirmed that the chosen diluent did not interference with MDS and its organic impurities (DPs).

3.1.2 | Selection of wavelength

The ultraviolet absorbance of MDS and its DPs was scanned from 190 to 400 nm using the HPLC-PDA detector with a 20μg/mL diluent. The absorption spectrum of MDS and its DPs exhibited the maximum at different wavelengths, and all the maximums are presented in Figure S1 and Table S2 (Supporting Information). From the wide range of wavelength maximum for the drug and its associated compounds, the detection wavelength for quantitative determination and monitoring was fixed at 293.5 nm, as the drug MDS showed the maximum absorbance at 293.5 nm (Figure 1). The DP1 of MDS showed absorbance at three wavelengths: 239.2, 287.5, and 318.4 nm with a blue shift.

3.1.3 | Selection of mobile phase

For selecting the mobile phase, different buffers were used (i.e., trifluoroacetic acid, sodium phosphate, potassium phosphate, and ammonium formate) with different ratios of organic modifiers (acetonitrile and methanol), but the desired separation, especially with a resolution greater than 1.5 between the closely eluting DP and MDS peaks along with good peak symmetry (tailing factor: ~1.0), was achieved with a combination of 40-mM ammonium formate and acetonitrile (35:65, v/v, Figure 1). As the MDS peak and other DPs were eluted within 20 min under isocratic elution mode, further trials were not performed using a gradient run. The total elution time was fixed as 25 min for the separation of MDS and its four DPs.

3.1.4 | Selection of columns and oven temperature

The stationary phase C_{18} column (Inertsil ODS-3V, 250 × 4.6 mm, 5 μm) chosen for the chromatographic analysis was crucial in base-to-base separation between closely eluting and adjacent peaks and also to detect low levels of degraded impurities (≤0.1% of MDS at a concentration of 0.4 mg/mL). The column oven temperature was maintained at 40°C based on the preliminary work as it showed good response and sharp peaks with a symmetry factor of ≤2.0 and better resolution (R > 1.5) between the closely eluting peaks of MDS and its DPs (Figure 2).

3.2 | Results of stress testing

All stress-testing samples of MDS were analyzed using HPLC coupled with a PDA detector, and the relative percentage of degradation was assessed based on the elution data. Four DPs were formed from MDS during the stress degradation study. The DPs of MDS were denoted as DP1–DP4 in line with the order of retention time obtained in the HPLC chromatograms. Of these, DP1 and DP4 were the major DPs, whereas DP2 and DP3 were the minor DPs. DP1 was formed mostly during oxidation stress conditions, and DP4 was formed as a major degradation impurity during acid and oxidation stress conditions, whereas DP2 and DP3 are minor DPs of acid hydrolysis, alkali hydrolysis, and oxidation stress conditions. A total of 30% degradation was observed in acid stress, whereas only 5% degradation was observed in alkaline stress and oxidation stress conditions. The chromatograms showing the separation of MDS and all the DPs are depicted in Figure 2, and the stress-testing results are presented in Table 2.

The schematic representation of DP1 formation from MDS under oxidative degradation condition is provided in Scheme 2. The

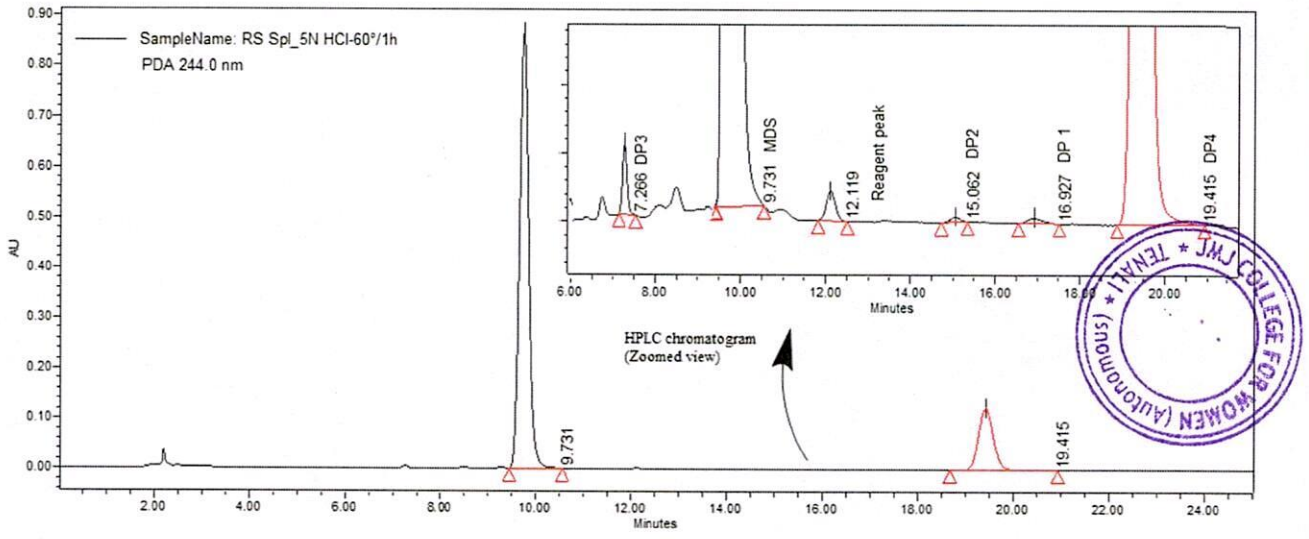

FIGURE 2 HPLC chromatogram of acid hydrolysis stress sample (in-sight view) shows all closely eluting degradation products (DPs) and MDS (midostaurin) peak

TABLE 2 Stress-testing results of MDS in softgel capsules

Stress condition	Temperature/time	Degradation (%)	Assay (%)	MB (%)[a]	Degradation product (DP) formed (%)
5N HCl (acid hydrolysis)	60°C/1 h	30.0	70.3	100.3	DP1(0.04%), DP2(0.1%), DP3(0.3%), DP4(28.5%)
5N NaOH (alkali hydrolysis)	60°C/1 h	5.0	94.2	99.2	DP1(0.2%), DP2(0.3%), DP3(0.3%), DP4(4.2%)
Water hydrolysis (H_2O)	60°C/1 h	0.08	99.8	100.0	–
Oxidation by 3% H_2O_2	25°C/4 h	5.0	95.1	100.1	DP1(4.8%), DP3(0.2%) formed
Thermolytic stress	105°C/6 h	0.1	100.1	100.2	–
Photolight	UV–Vis.[b]	0.1	99.8	99.9	–

Note: MDS, midostaurin.
[a]Mass balance: % total degradation (sum of known and unknown impurities) + % assay.
[b]UV light (200 W h/m^2) and fluorescent light (1.2 million lux-h).

SCHEME 2 Degradation pathway of midostaurin (MDS, oxidation stress condition): (a) midostaurin; (b) MDS-DP1 (degradation product 1)

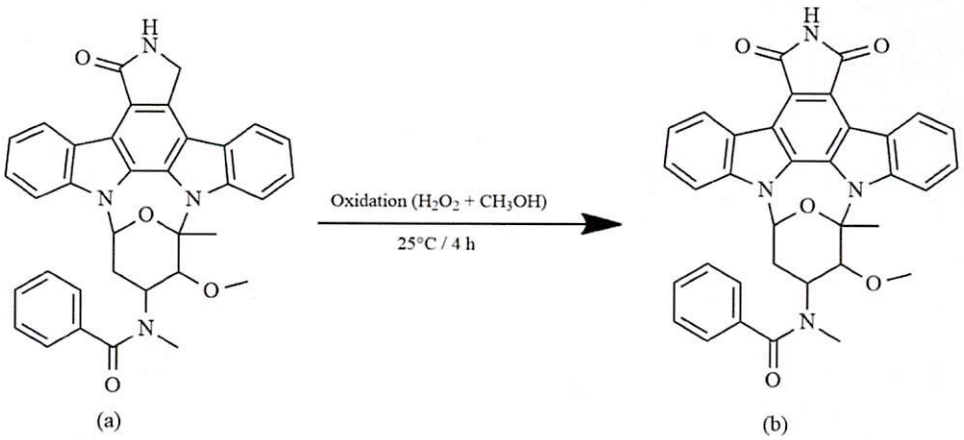

stress studies revealed that MDS was more susceptible to acid, alkaline, and oxidation stress conditions when compared to other stresses. The peak responses of the oxidation stress sample were monitored and extracted using three different wavelengths (293.5, 244, and 318 nm) to assess and identify the new DPs of MDS (Figure 3), but no new impurity was observed other than four DPs (DP1–DP4).

The stress samples were further diluted to a concentration of 40 µg/mL and were assayed against the same concentration of MDS standard. The mass balance for each stressed sample was calculated using the sum of the percentage assay value and percentage DPs (total impurities) formed under stress testing, and the results are presented in Table 2. The peak purity of MDS was evaluated in each stress condition using the HPLC-PDA detector. As shown in Figure 4(b,c), the peak purity plots confirmed that the MDS and its DP1 were pure and do not have any other unknown moiety; that is, the purity angle of MDS and DP1 was found to be less than the purity threshold value, and no flag was observed). The stress-testing study and the separation process confirmed that the proposed isocratic HPLC method for the related organic impurities of MDS and its assay showed the stability-indicating characteristic as it proved that the separation between the closely eluting peaks was good and well resolved with a resolution >1.5 (USP < 621>, 2020).

3.3 | Isolation of DPs formed during stress testing

Reversed-phase LC with an isocratic solvent delivery system discussed under HPLC was used for the isolation of four unknown DPs (DP1–DP4) of MDS [retention time (RT): 9.731 min]. As shown in Figure 2, the peak fractions of four DPs were observed at RT 7.2, 15.0, 16.9, and 19.4 min corresponding to DP3, DP2, DP1, and DP4, respectively, under severe stress conditions, which were individually isolated and concentrated using a rotary evaporator (Büchi rotary evaporator, model: R-200).

3.4 | Structure elucidation

The isolated solids obtained from the concentrated fractions of DPs were used for structural analysis using LC–MS, LC–MS/MS, UV, FT-IR, and NMR.

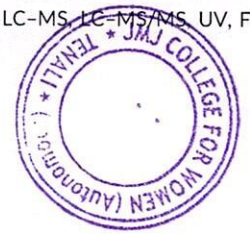

3.4.1 | Results of MS

MDS (m/z 570.6)

The ESI mass spectrum (positive mode) of the MDS fraction obtained using LC–MS/MS (at an RT of 9.74 min) showed a molecular ion peak

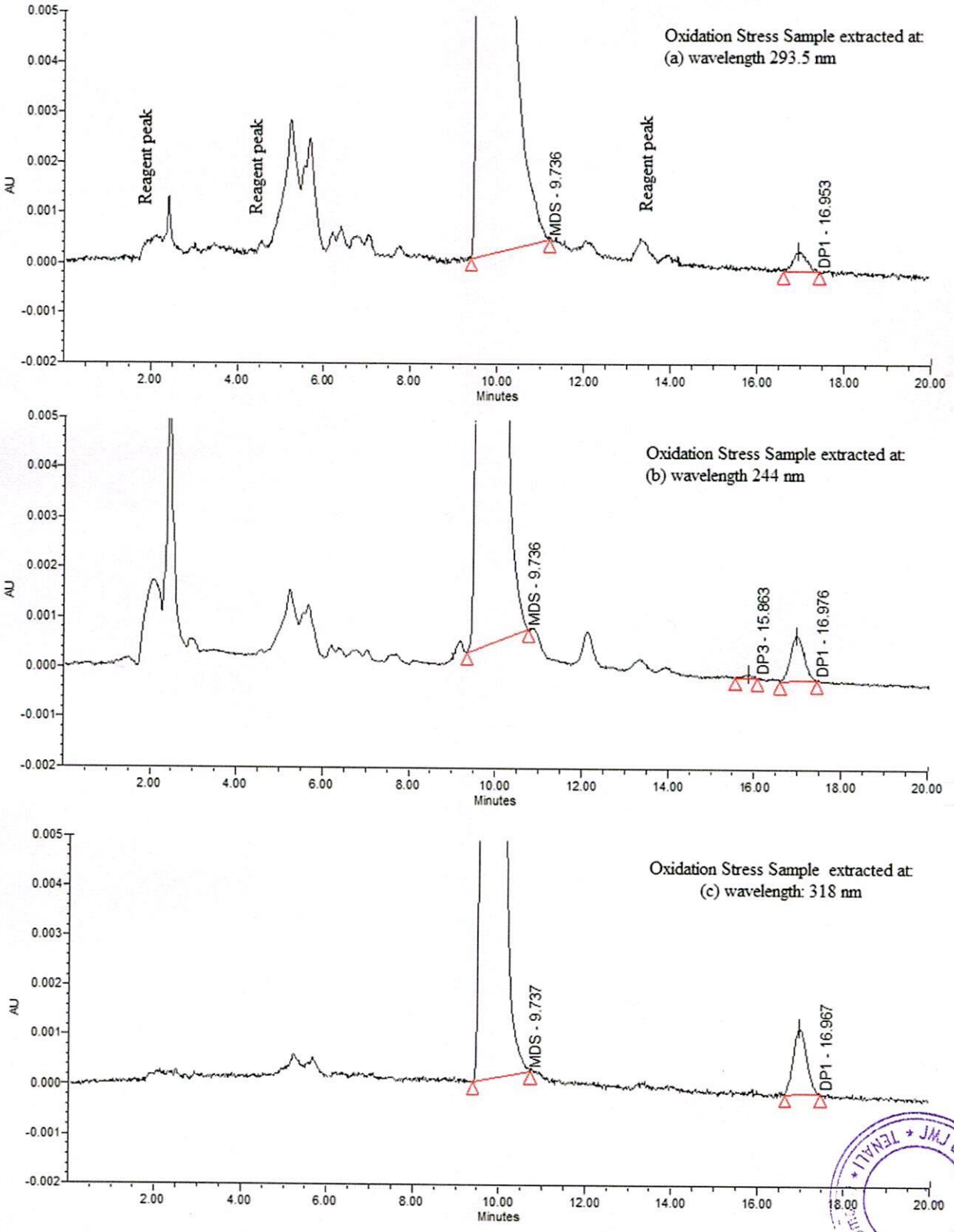

FIGURE 3 Oxidation stress sample solution: HPLC chromatogram extracted at wavelength (a) 293.5 nm (optimized condition), (b) 244 nm, and (c) 318 nm

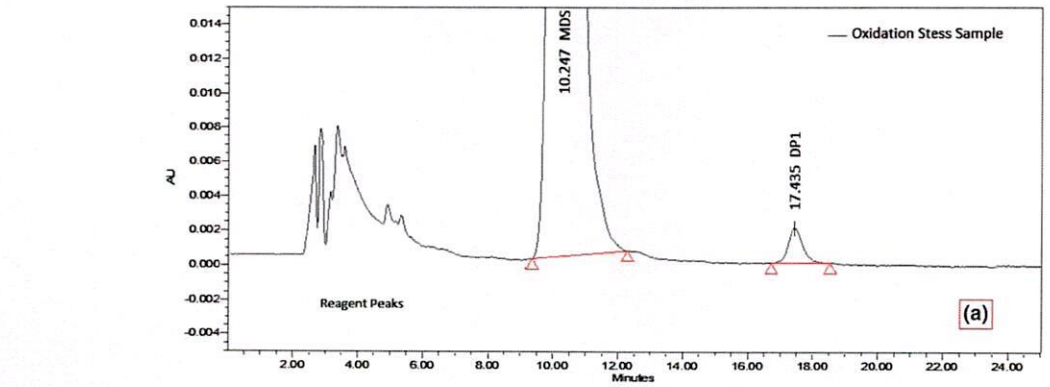

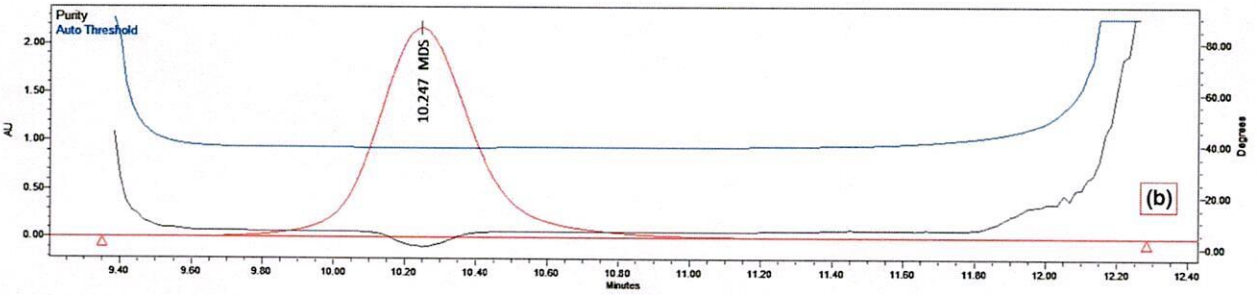

Name	Retention Time	Purity1 Angle	Purity1 Threshold	Purity1 Flag
MDS	10.247	3.511	39.077	No

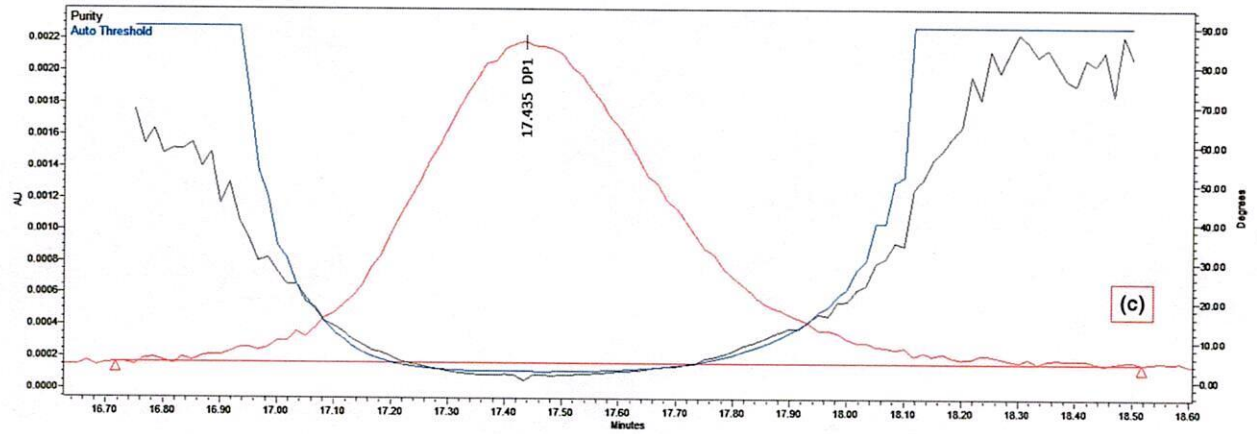

Name	Retention Time	Purity1 Angle	Purity1 Threshold	Purity1 Flag
DP1	17.435	3.842	4.307	No

FIGURE 4 A representative chromatogram and peak purity plots of MDS (midostaurin) and its DP1 obtained from an assay sample of oxidation stress study: (a) HPLC chromatogram; (b) peak purity plot of MDS; and (c) peak purity plot of DP1

at *m/z* 571.18 [M + H] with molecular formula $C_{35}H_{30}N_4O_4$ and molecular weight 570.6 g/mol of standard MDS (Figure 5a). The fragmentation pattern of MDS obtained using LC–MS/MS is shown in Figure S2 (Supporting Information).

DP1 (m/z 584.6)

The mass spectra (LC–MS) of DP1 (RT: 16.95 min, Figure 1) exhibited a molecular ion peak at *m/z* 584.93 (Figure 5b). The ammonium adduct data of MDS-DP1obtained using LC–MS/MS are shown in Figure S4. The molecular formula of DP1 was calculated to be $C_{35}H_{28}N_4O_5$ with the support of degradation patterns from the spectral data [Scheme S1 (Supporting Information)]. On comparing the *m/z* data of DP1 and MDS, a difference of 14 *m/z* was obtained, which can be interpreted for a conversion of methylene ($-CH_2$) in MDS to carbonyl ($-C{=}O$) group during stress condition at the fifth position of pyrrolidine ring on DP1 structure.

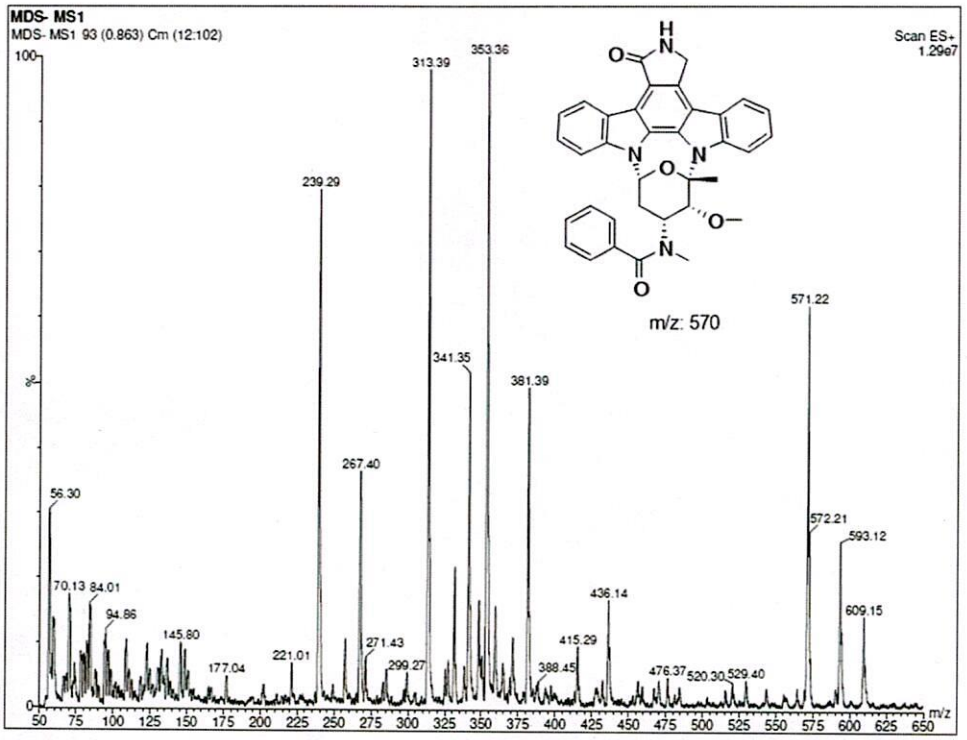

(a) Mass spectra of MDS (obtained from LC-MS/MS)

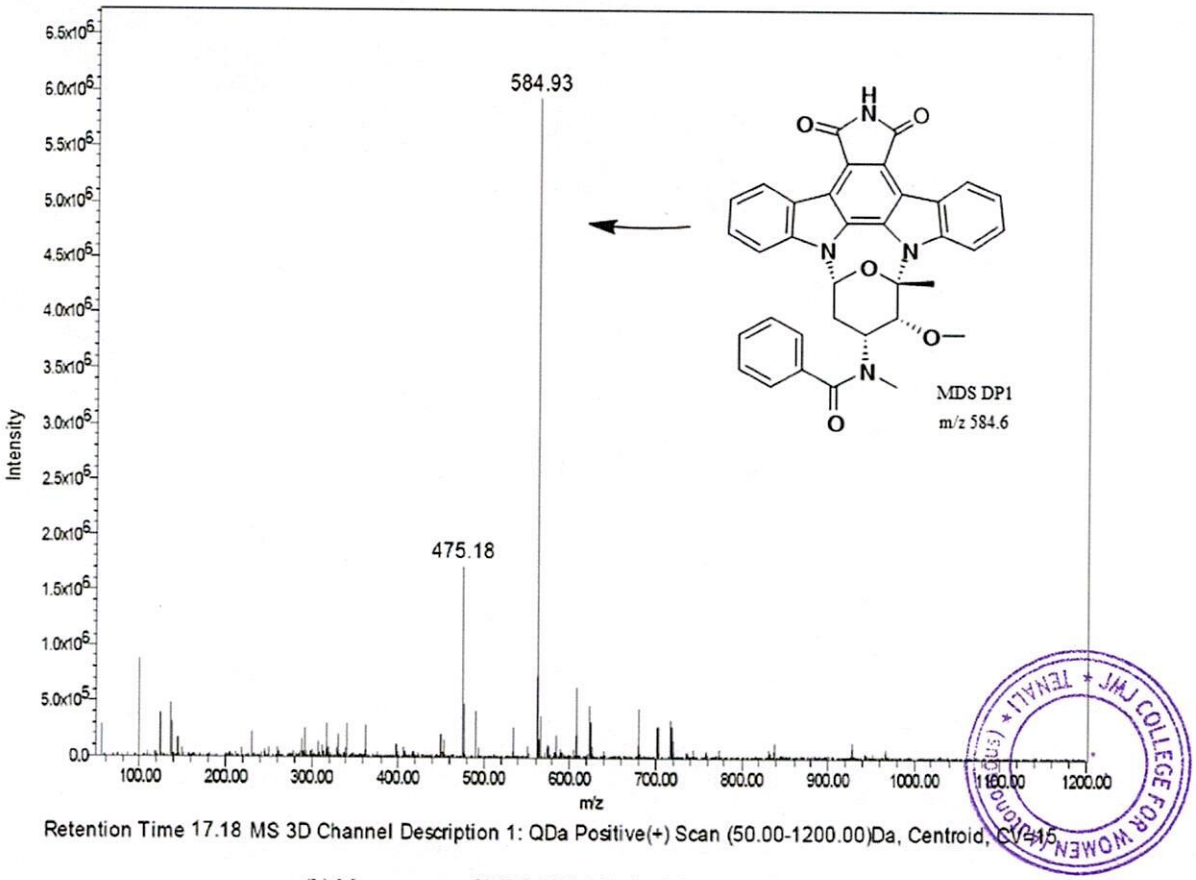

(b) Mass spectra of MDS-DP1 (obtained from the LC-MS)

FIGURE 5 (a) Mass spectra of MDS (midostaurin) (obtained using LC–MS/MS). (b) Mass spectra of MDS-DP1 (obtained using LC–MS)

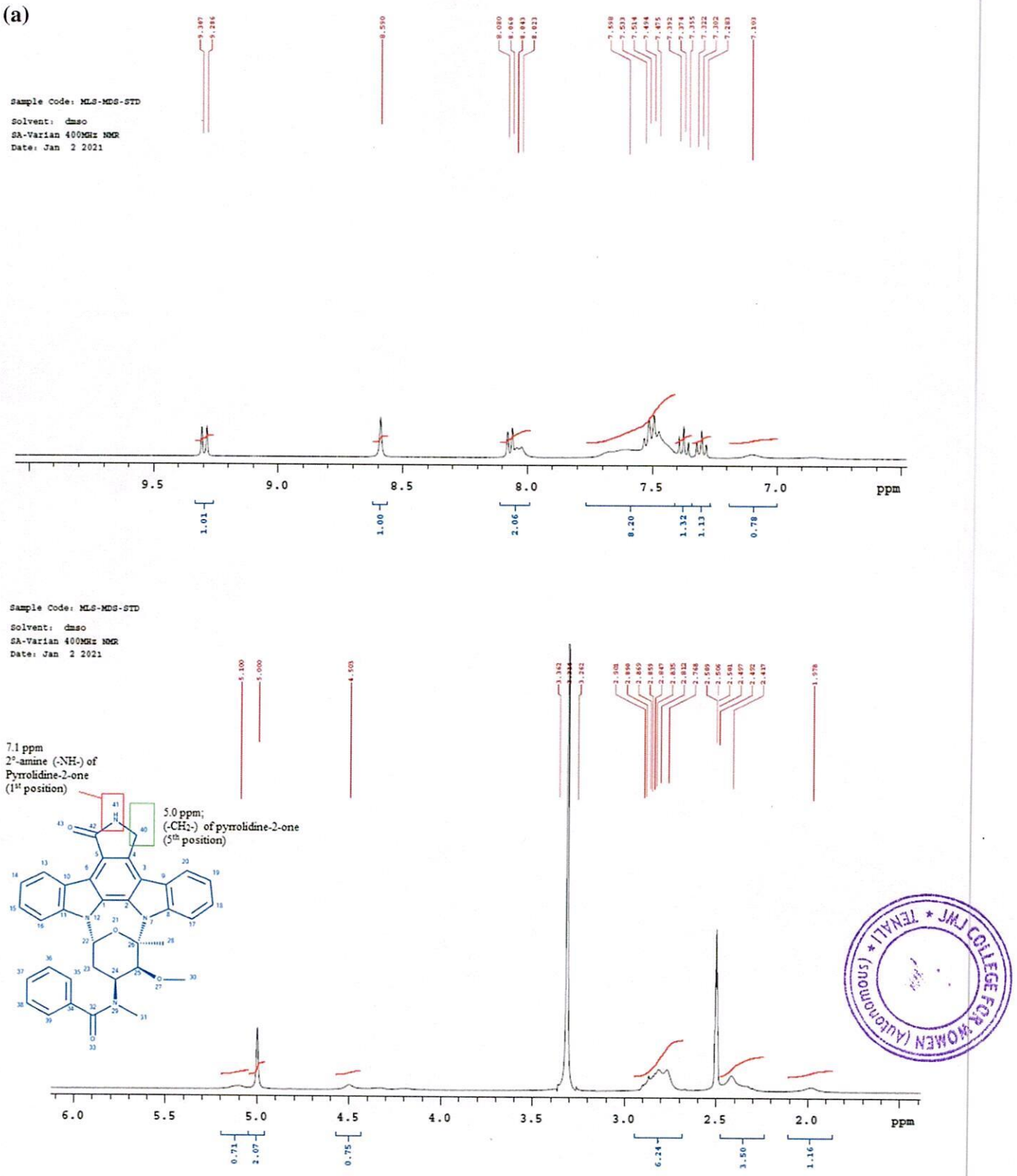

FIGURE 6 (a) ^{1}H-NMR spectra of MDS (midostaurin) (zoomed view). (b) ^{1}H-NMR spectra of MDS-DP1 (zoomed view)

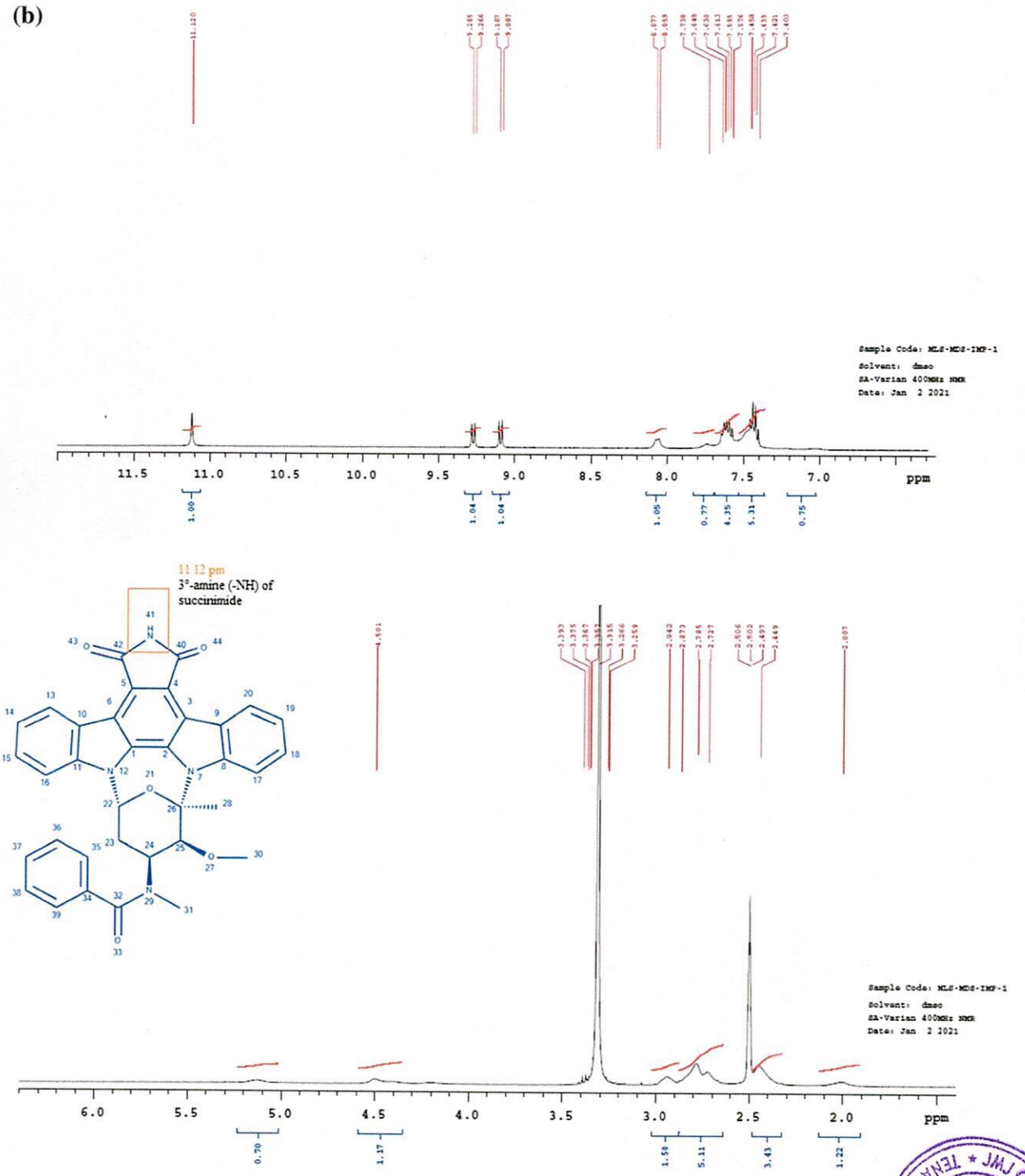

FIGURE 6 (Continued)

The mass value and molecular formula proposed for DP1 of MDS were compared against the literature data, and it revealed that the chemical structure (formula and mass) matched exactly with *stauprimide* (Giorgio et al., 1994; Shoutian et al., 2009). The spectral data of FT-IR and NMR confirmed the structure of DP1 as stauprimide (Scheme 1b).

Stauprimide is a semisynthetic analog of the staurosporine family of indolocarbazoles (Giorgio et al., 1994). It is chemically known as [*N*-[(2*S*,3*R*,4*R*,6*R*)-3-methoxy-2-methyl-16,18-dioxo-29-oxa-1,7,17-triazaoctacyclo[12.12.2.12,6.07,28.08,13.015,19.020,27.021,26]nonacosa-8,10,12,14,19,21,23,25,27-nonaen-4-yl]-*N*-methylbenzamide] (Scheme 1b). Stauprimide specifically inhibits the nuclear

localization of NME2, which results in the suppression of c-MYC—a key regulator of pluripotency thereby priming cells for differentiation.

Other DPs (DP2–DP4)

The chemical structure of other DPs (DP2–DP4) of MDS that were formed under acid, alkali, and oxidation stress conditions was not elucidated as they were not the major fractions and moreover the fractions were found to be unstable. However, the UV spectra of all the DPs were measured and are shown in Figures S5–S7 (Supporting Information).

3.4.2 | Structure confirmation using NMR and FT-IR spectroscopy

The structure of the MDS and DP1 fractions was further confirmed by ^{1}H-NMR and ^{13}C-NMR recorded using an SA Varian 400 MHz NMR instrument in d^{6}-DMSO, and the respective spectra are shown in Figures 6 and 7. The chemical shift for all the protons of MDS and DP1 is found to be the same except for the change in the pyrrolidine ring where the methylene (-CH_2-) group of MDS converts to the carbonyl (-C=O) group due to oxidation reaction. The conversion is confirmed by the absence of singlets at 5 ppm in the ^{1}H-NMR spectra of DP1. The associated spectral change in the region from 8 to 11 ppm for DP1 further confirms the conversion by oxidation of MDS. The spectral data shown in Figure 6(a,b) are summarized in Table S3 (Supporting Information), with support of Scheme 2. The formation of the carbonyl group is further confirmed by ^{13}C-NMR spectra where a doublet for the newly formed succinimide carbonyl is obtained at 170 and 171 ppm (Scheme 2; Figure 7). These characteristic peaks confirmed the proposed structure for DP1.

The proposed structure was further confirmed using the vibrational stretching frequency of the degraded product 1 (DP1) and MDS using FT-IR recorded on an Alpha II Compact FT-IR instrument (Brucker) using the KBr pellet technique (Figure 8). The newly formed succinimide ring exhibited peaks for the two carbonyl groups (-C=O) at 1754 and 1718 cm^{-1}, which were absent in the MDS spectra. The

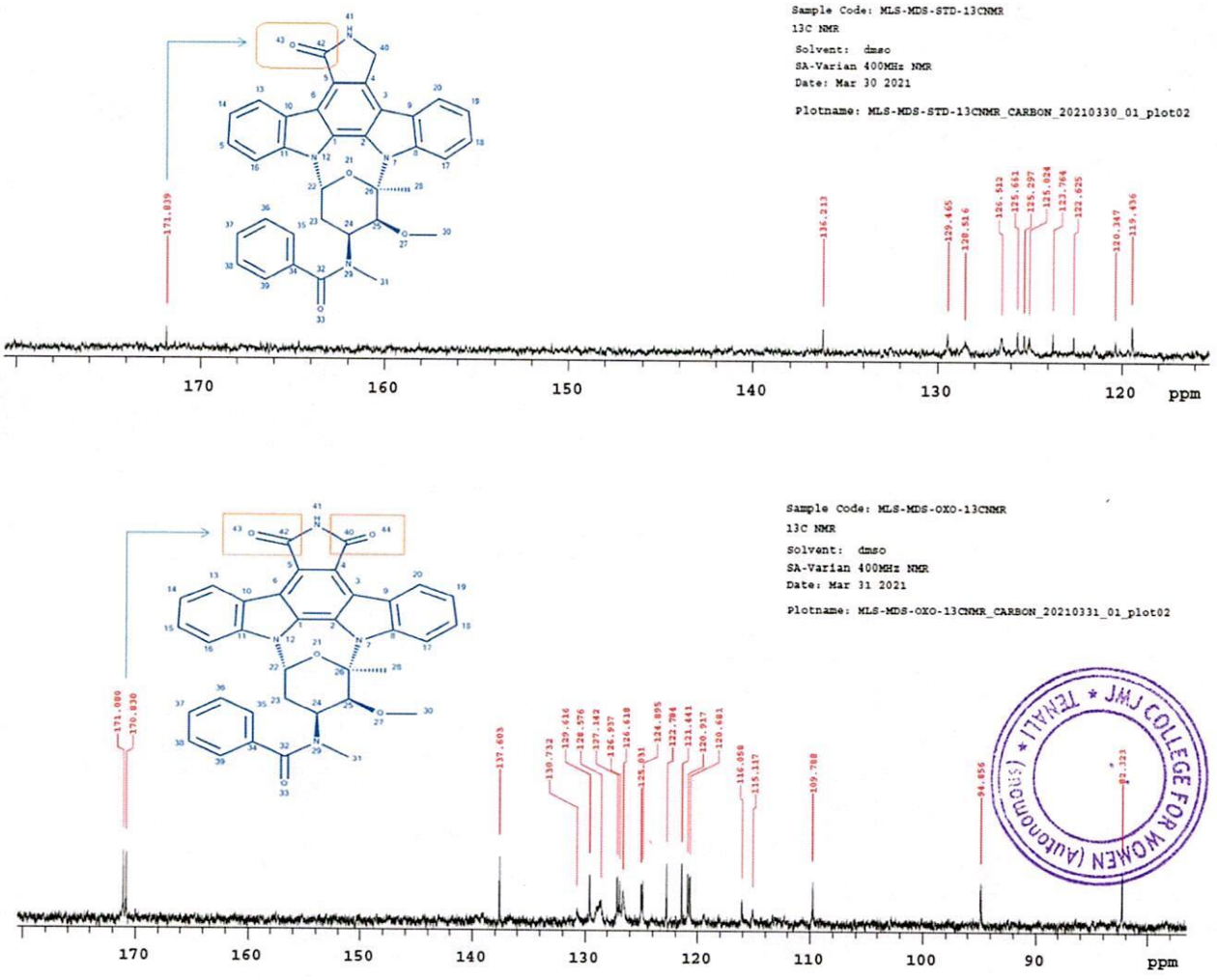

FIGURE 7 ^{13}C-NMR spectra of MDS (midostaurin) and DP1 (zoomed view)

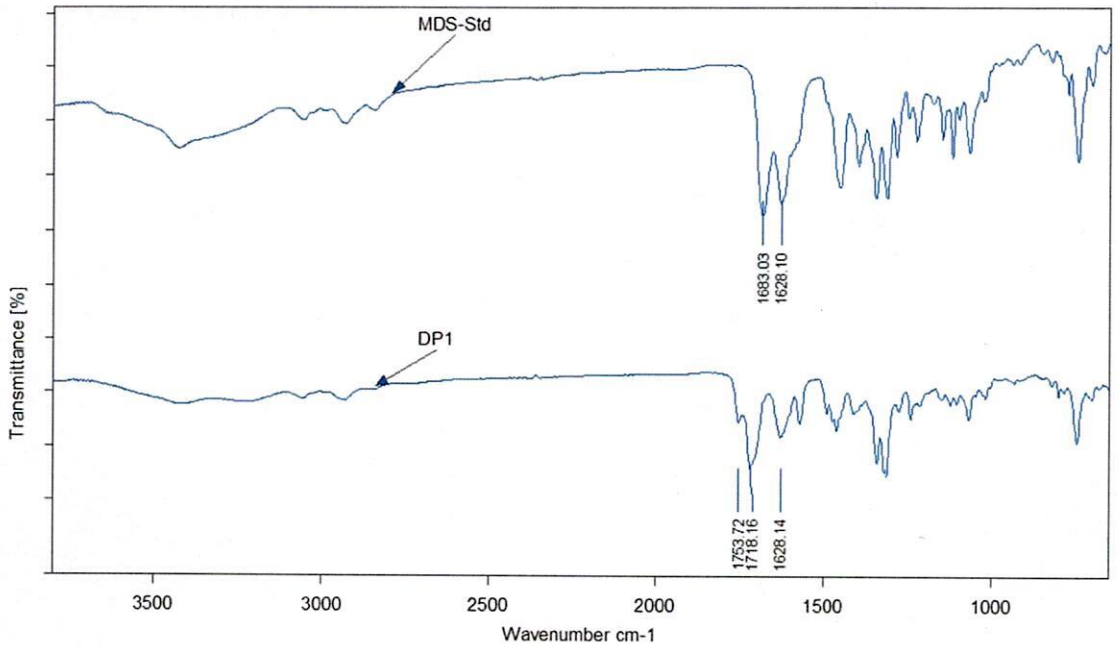

FIGURE 8 FT-IR (Fourier-transform infrared spectroscopy) spectra of MDS (midostaurin) and its DP1

peaks at 1683 and 1628 cm^{-1} are attributed to the two amide stretching present in the MDS structure. The spectral data confirmed that the oxidation of MDS leads to DP1. The details of the other stretching frequency are shown in Figure 8 and Table S4 (Supporting Information).

3.5 | Method validation

The proposed SIM was validated per ICH guidelines for the quantitative determination of related impurities of MDS and its assay in softgel capsules [ICH, Q2(R1), 1995; Narasimha et al., 2019; USP <1225>, 2020]. The observations from the validation study results are discussed in the following sections.

3.5.1 | Specificity

The specificity of the developed test method was demonstrated by analyzing the blank (diluent) solution (used for sample and standard preparations), placebo solution (amount of excipients used for the formulated MDS softgel capsules), and soft gelatin capsule shell (used for drug filling). The results prove that the blank, placebo, and capsule shell did not interfere with the retention time (RT) of MDS and its four DPs formed under stress testing. The developed HPLC method separated all the four DP and MDS peaks without any overlapping. The peak purity of the stressed samples was evaluated using the HPLC-PDA detector, and all DP (DP1–DP4) and MDS peaks were found pure. The developed test method is specific and exhibited the stability-indicating characteristic.

3.5.2 | Detection limit and quantitation limit

The concentration for DL and QL of MDS and DP1 was demonstrated with respect to the test concentration of 0.4 mg/mL. Based on the visualization method as recommended in the ICH guidelines [Q2 (R1), 1995], the concentrations of QL and DL were found to be 0.05% (0.20 µg/mL), which was less than the ICH reporting threshold and 0.025% (0.10 µg/mL), respectively [Q3A(R2), 2006a; Q3B (R2), 2006b]. The concentrations of DL and QL were confirmed by analyzing three individual standard solutions of MDS and DP1 at the established level, and the respective data are presented in Table 3 (Figure 9).

3.5.3 | Linearity

The linearity of the proposed method was determined using a series of standard solutions (six), with concentrations ranging from 0.101 to 505.0 µg/mL covering 0.025–125% of the MDS test concentration (0.4 mg/mL). The calibration curve of MDS showed a good correlation between the different concentrations and the respective peak areas [Figures S8 and S9 (Supporting Information)]. The linear regression equation and regression coefficients of MDS were found to be $y = 70{,}864x - 47{,}239$ and 0.9988, respectively (Table 3; Figure 9).

According to ICH guidelines [Q3A(R2), 2006a; Q3B(R2), 2006b], the specification limit for the identified DP1 was 0.2% (based on the identification threshold), and the method validation (linearity) was determined by analyzing a series of DP1 solutions at five different concentrations ranging from 0.10 to 1.66 µg/mL covering 0.05–0.4% of

TABLE 3 Linearity results of MDS and its DP1

Name	Concentration range (µg/mL)	Trend line[a]	Correl (*r*)[b]	R^2[c]	RRF[d]	DL concentration (µg/mL)[e]	QL concentration (µg/mL)[f]
MDS	0.101–505.0	$y = 70{,}864x - 47{,}239$	0.9994	0.9988	1.00	0.101	0.202
DP1	0.104–1.664	$y = 37{,}996x - 1622.1$	0.9977	0.9953	0.54	0.104	0.208

Notes: DP, degradation product; MDS, midostaurin.
[a]$y = mx + c$, where '*m*' is the slope, '*c*' is the intercept that is obtained from the linear regression line (concentration vs. peak response), and '*x*' is the unknown concentration of the target analyte.
[b]Correl (*r*) is the correlation coefficient obtained from the linear regression plot of the respective component.
[c]R^2 is the linear regression coefficient obtained from the linear regression plot of the respective component.
[d]RRF is the relative response factor calculated using the slope of DP1 divided by the slope of MDS, which were obtained from the linear regression plot of the respective component.
[e]The concentration of the detection limit (DL, 0.025%; 0.10 µg/mL) is determined using the visualization method per ICH guidelines.
[f]The concentration of the quantification limit (QL, 0.05%; 0.20 µg/mL) using the visualization method per ICH guidelines.

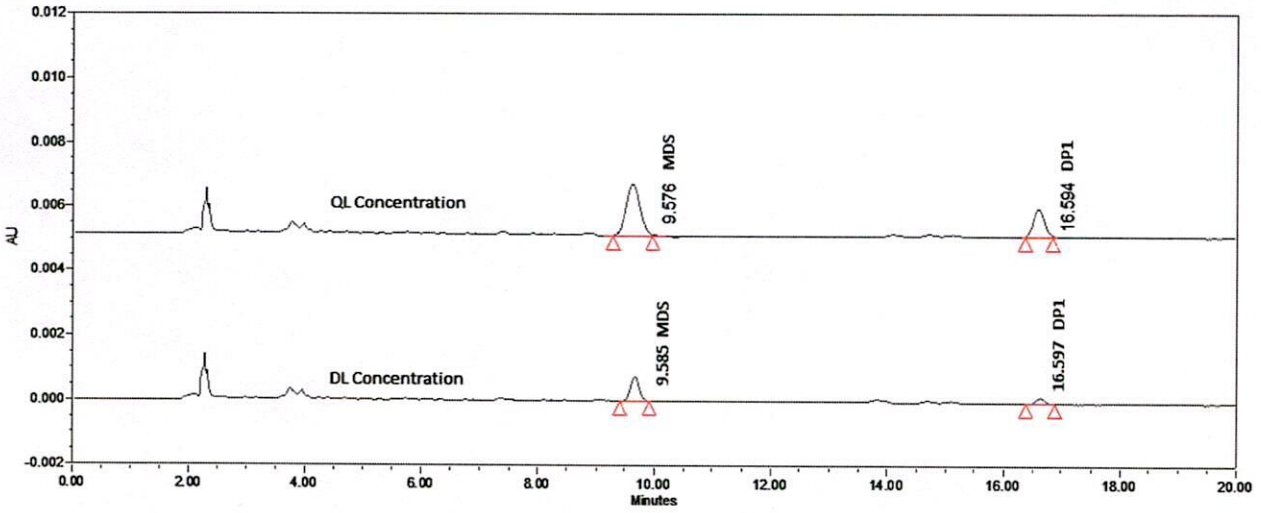

FIGURE 9 HPLC chromatograms of MDS (midostaurin) and DP1 at DL (detection limit) and QL (quantitation limit) concentrations

TABLE 4 Accuracy and precision results of MDS and DP1 in softgel capsules

	MDS recovery (%), $n = 3$[a]			DP1 recovery (%), $n = 3$[b]		
Number	5%	100%	125%	QL	0.2%	0.4%
1	99.0	100.5	101.0	95.2	99.9	105.4
2	98.6	101.0	100.8	94.7	100.2	106.1
3	100.6	100.5	100.8	94.3	99.8	104.7
Mean	99.4	100.7	100.8	94.8	100.0	105.4
%RSD	1.08	0.28	0.11	0.49	0.23	0.67

Notes: DP, degradation product; MDS, midostaurin, QL, quantitation limit.
[a]MDS concentrations (with respect to sample 0.4 mg/mL): R1: 0.02 mg/mL (5%), R2: 0.4 mg/mL (100%), and R3: 0.5 mg/mL (125%).
[b]DP1 concentrations (with respect to sample 0.4 mg/mL): 0.10 µg/mL (0.05%), 0.8 mg/mL (0.2%), and 0.4% (1.6 µg/mL).

the proposed limit of DP1. The calibration curve of DP1 showed a good correlation between the different concentrations and the respective peak areas (linear regression equation: $y = 37{,}996x - 1622.1$, and regression coefficients: 0.9977) (Table 3). The relative response factor of the newly identified impurity (DP1) observed at 16.96 min ($\lambda_{293.5}$) was determined as 0.54 by using the slope of DP1 versus the slope of MDS obtained from the linearity study.

3.5.4 | Accuracy and precision

The accuracy of the test method was estimated by spiking a known amount of MDS on placebo samples. Triplicate sample solutions were prepared for MDS at each accuracy level [R1: 0.02 mg/mL (5%), R2: 0.4 mg/mL (100%), and R3: 0.5 mg/mL (125%)], and the recoveries of MDS from the spiked samples were

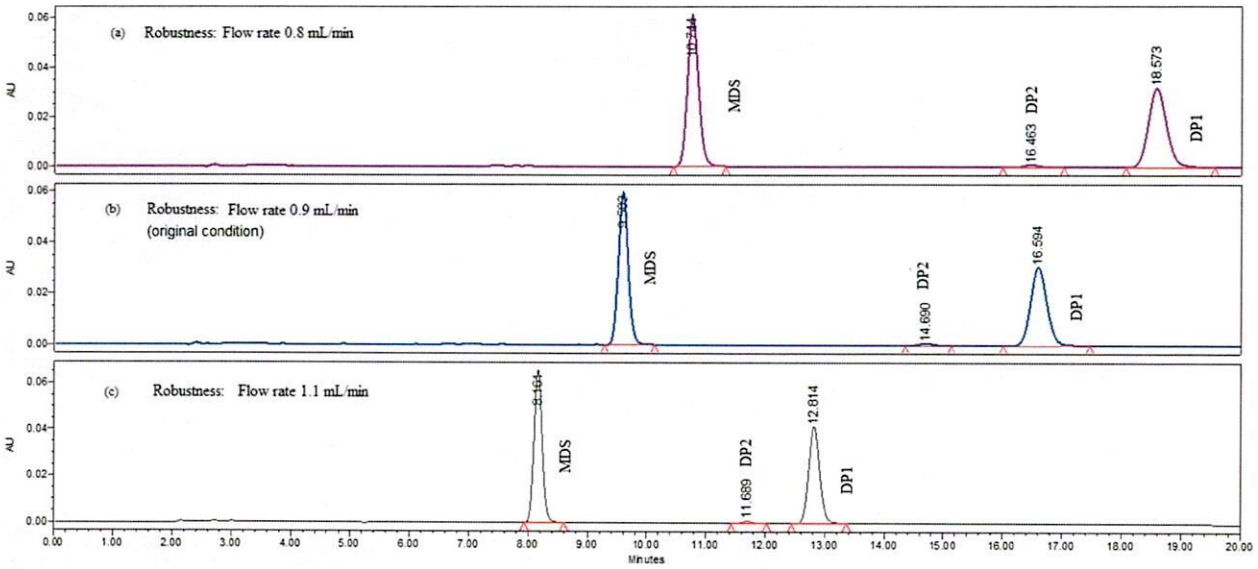

FIGURE 10 HPLC chromatograms for robustness study as a function of change in flow rate of the mobile phase: (a) 0.8 mL/min; (b) 0.9 mL/min; and (c) 1.1 mL/min

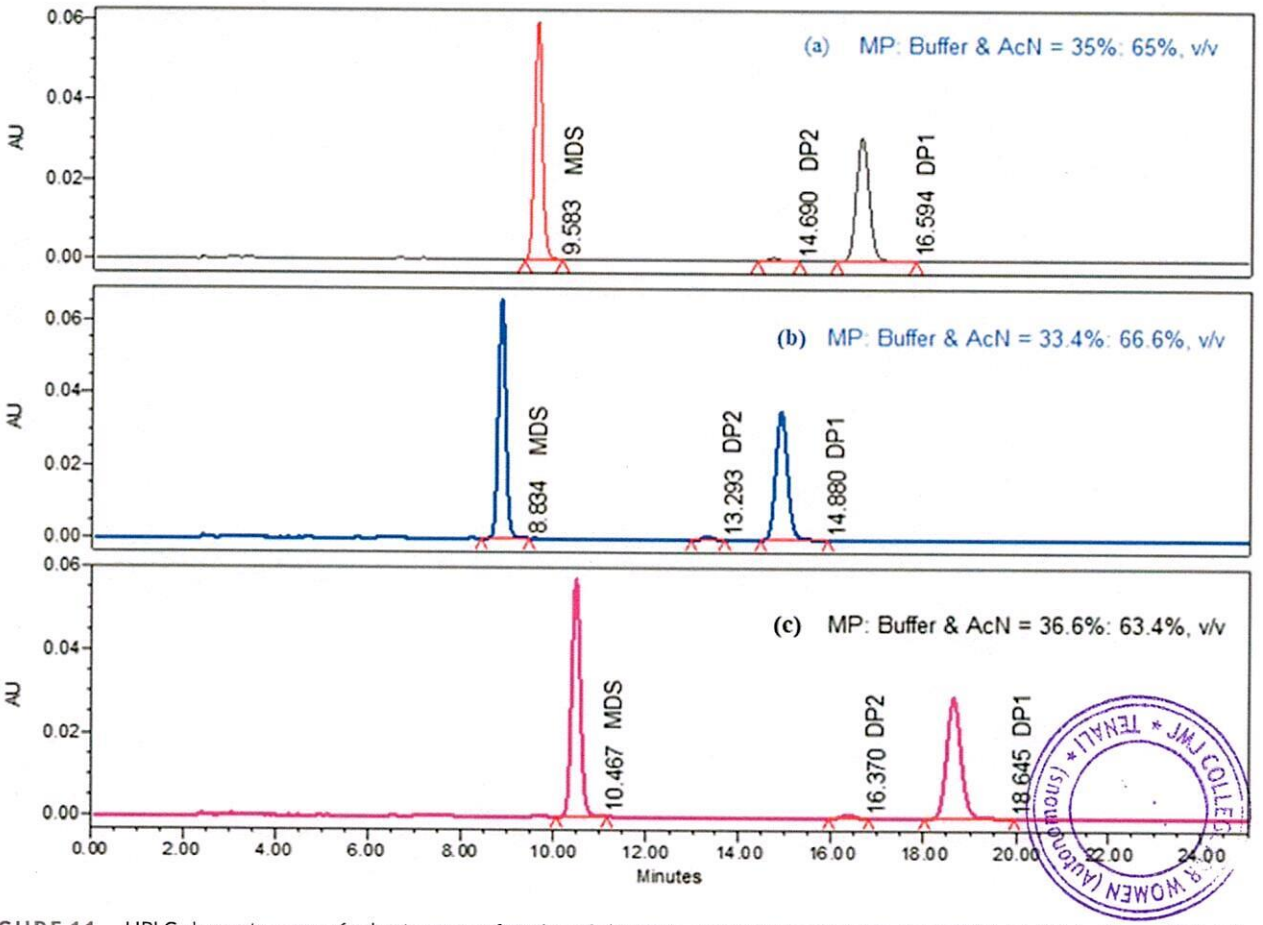

FIGURE 11 HPLC chromatograms of robustness as a function of change in organic ratio of mobile phase (MP): (a) MP: buffer and CH_3CN—35:65 (%, v/v); (b) MP: buffer and CH_3CN—33.4:66.6 (%, v/v); and (c) MP: buffer and CH_3CN—36.6:63.4 (%, v/v)

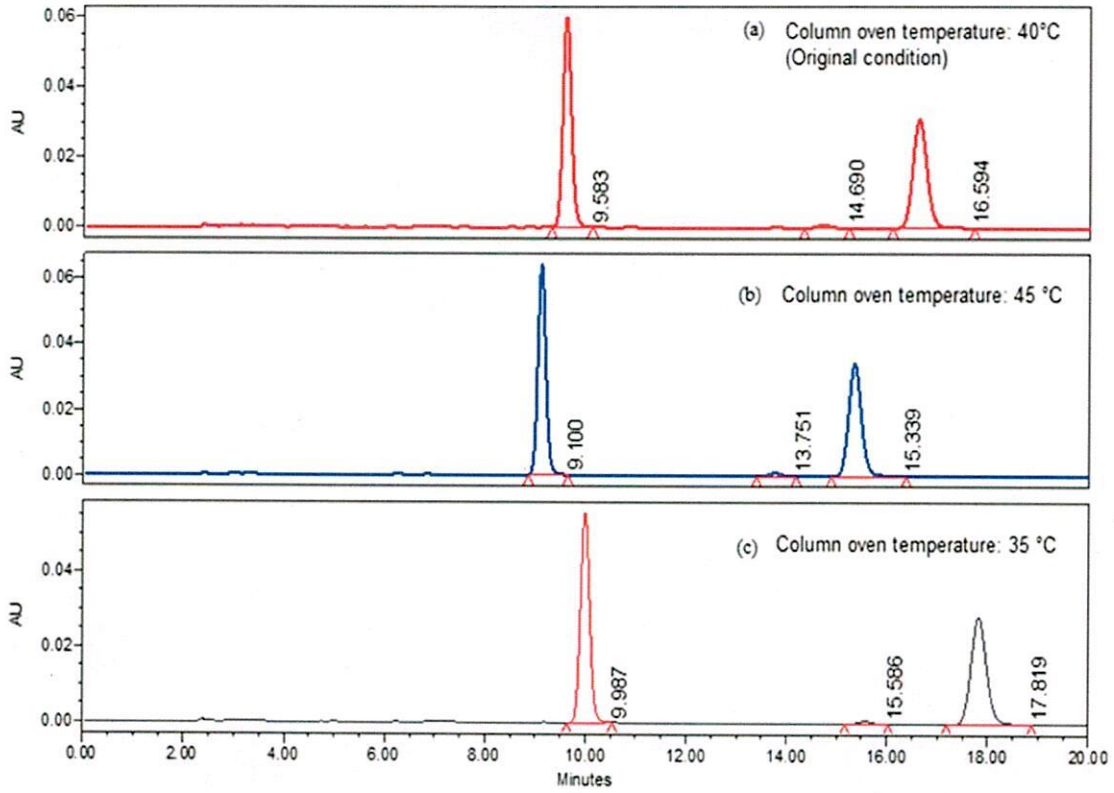

FIGURE 12 HPLC chromatograms from robustness study as a function of column oven temperature: (a) at 40°C; (b) at 45°C; and (c) at 35°C

calculated against the MDS standard and are summarized in Table 4. Similarly, the accuracy study of DP1 was assessed by spiking the DP1 stock on sample at three different concentration levels, that is, QL (0.05%, w/w), 100% (0.2%, w/w), and 200% (0.4%, w/w). The percentage recovery, mean percentage recovery, and %relative standard deviation (RSD) were calculated and are summarized in Table 4. All nine preparations ($n = 9$) were considered and reported for precision study per ICH guidelines [Q2 (R1), 1995]. This study proves that the developed method is precise and accurate.

3.5.5 | Robustness

A mixed solution of DP1 and DP2 obtained from peak fractions and MDS was prepared at certain concentration (unknown), and the robustness of the proposed test method was demonstrated by changing the chromatographic conditions, that is, change in flow rate of mobile phase: 0.9 ± 0.1 mL/min (Figure 10), change in organic phase (acetonitrile) of mobile phase composition: 35 ± 2.5% absolute change (Figure 11), and change in column oven temperature: 40.0 ± 5.0°C (Figure 12). The changes made in the column temperature and flow rate did not significantly affect the separation criteria, but the peak retention times were changed according to the mobile phase ratios. The developed test method was found to be robust.

4 | CONCLUSION

The impurity profiling of MDS was carried out primarily by using the stability-indicating HPLC and LC–MS methods. The developed method provided excellent separation between the closely eluting peaks of the MDS, all DP, excipient, and diluent peaks. The proposed method was validated as per ICH guidelines and found highly efficient in the quantitative estimation of MDS assay and its organic impurities with high precision and good repeatability. The forced stress testing of MDS was performed as per ICH guidelines; the drug was susceptible to hydrolytic, oxidative, thermolytic, and photolytic stressed conditions. The peak fractions of the four DPs (DP1–DP4) that were formed and detected under stress-testing conditions were isolated, and the chemical structure of DP1 was predicted using spectral data (UV, IR, LC/MS, LC–MS/MS, ^{1}H-NMR, and ^{13}C-NMR). DP1 was new, and moreover, it was not reported in the previously published literature of MDS, either in bulk drug or in any formulated drug products of MDS. The chemical structure of DP1 was identified as stauprimide (MDS oxo impurity) from experimental data. The spectral data of the other three DPs (DP2–DP4) obtained using UV and LC–MS/MS were discussed and presented.

ACKNOWLEDGMENT

The authors thank the management of Dr. SLN Laboratories Pvt. Ltd. for supporting this work by gifting samples for analysis and providing the facilities.

CONFLICT OF INTEREST

The authors have declared that they have no conflicts of interest.

DATA AVAILABILITY STATEMENT

Data available in article supplementary material: The data that supports the findings of this study are available in the supplementary material of this article.

ORCID

Narasimha Swamy Lakka https://orcid.org/0000-0002-2952-7493
Chandrasekar Kuppan https://orcid.org/0000-0002-3780-6222

REFERENCES

Ahmed, A., Tayyaba, M., & Sumaiyya, S. (2018). Development and validation of assay by RP-HPLC method. *International Journal of Pharmaceutical Sciences and Nanotechnology*, *11*(6), 4318–4322. https://doi.org/10.37285/ijpsn.2018.11.6.4

Bhaskar, R., Ola, M., Agnihotri, V., Chavan, A., & Girase, H. (2020). Current trend in performance of forced degradation studies for drug substance and drug Product's. *Journal of Drug Delivery and Therapeutics*, *10*(2-s), 149–155.

Blessy, M., Ruchi, D. P., Prajesh, N. P., & Agrawal, Y. K. (2014). Development of forced degradation and stability indicating studies of drugs – a review. *Journal of Pharmaceutical Analysis.*, *4*(3), 159–165. https://doi.org/10.1016/j.jpha.2013.09.003

Deepti, J., & Pawan, K. B. (2013). Forced degradation and impurity profiling: Recent trends in analytical perspectives. *Journal of Pharmaceutical and Biomedical Analysis*, *86*, 11–35. https://doi.org/10.1016/j.jpba.2013.07.013

Giorgio, C., Thomas, M., Andreas, F., Uwe, T., Helmut, M., & Doriano, F. (1994). Inhibitory activity and selectivity of staurosporine derivatives towards protein kinase C. *Bioorganic and Medicinal Chemistry Letters*, *4*(3), 399–404. https://doi.org/10.1016/0960-894X(94)80004-9

Handan, H., Phi, T., Helen, G., Vivienne, T., Jin, Z., Wen, L., Ewa, G., Kai, K., & Tycho, H. (2017). Midostaurin, a novel protein kinase inhibitor for the treatment of acute nyelogenous leukemia: Insights from human absorption, metabolism, and excretion studies of a BDDCS II drugs. *Drug Metabolism and Disposition*, *45*(5), 540–555. https://doi.org/10.1124/dmd.116.072744

ICH. (1995). Validation of Analytical Procedures: Text and Methodology Q2(R1), 1995.

ICH. (1996). Stability Testing: Photostability testing of new drug substances and products, Q1B, Current step 4 version, dated 6 November 1996.

ICH. (2003). Stability Testing of New Drug Substances and Products Q1A (R2), Current step 4 version, dated 6 February 2003.

Kumar, P. A., Kumar, Y. R., & Jayashree, A. (2016). Development and validation of a stability-indicating RP-HPLC method for the estimation of Erlotinib impurities by QbD approach. *Rasayan Journal of Chemistry*, *9*(2), 180–188.

Nageswara, R., Hassan, F., Prafulla, S., Muthumani, J., & Gangu, C. H. (2013). Development and validation of a stability-indicating assay including the isolation and characterization of degradation products of metaxalone by LC-MS. *Biomedical Chromatography*, *27*(12), 1733–1740. https://doi.org/10.1002/bmc.2987

Narasimha, S. L., & Chandrasekar, K. (2019). Principles of chromatography method development. In O.-M. Boldura, C. Baltă, & N. S. Awwad (Eds.), *Biochemical analysis tools – methods for bio-molecules studies* (Vol. 2019). IntechOpen. https://doi.org/10.5772/intechopen.89501

Narasimha, S. L., Chandrasekar, K., Kona, S. S., & Raviteja, Y. (2020). Separation and characterization of new forced degradation products of Dasatinib in tablet dosage formulation using LC–MS and stability-indicating HPLC methods. *Chromatographia*, *83*, 947–962. https://doi.org/10.1007/s10337-0

Narasimha, S. L., Chandrasekar, K., & Parathasarathi, R. (2019). Impurity profile of macitentan in tablet dosage form using a stability-indicating high performance liquid chromatography method and forced degradation study. *Chinese Journal of Chromatography*, *37*(1), 100–110. https://doi.org/10.3724/SP.J.1123.2018.06032

Narayanaswamy, H., Gejalakshmi, S., Hemalatha, C. N., & Pavankumar, V. (2020). RP-HPLC method development and validation for the estimation of Midostaurin in bulk and pharmaceutical dosage form. *International Journal of Research in Pharmaceutical Sciences*, *11*(2020), 5108–5112. https://doi.org/10.26452/ijrps.v11i4.3114

Philippe, B., Alexandre, A., Marie-Olivia, C., Fabrice, V., Christophe, M., Isabelle, H., Laure, C., Ana, C., Agnès, M., Laurent, F., Gandhi, D., Olivier, L., & Olivier, H. (2014). Liquid chromatography–tandem mass spectrometry assay for therapeutic drug monitoring of the tyrosine kinase inhibitor, midostaurin, in plasma from patients with advanced systemic mastocytosis. *Journal of Chromatography B*, *944*, 175–181.

Q3A(R2) (2006a). Impurities in new drug substances, Q3A(R2), Current step 4 version, dated 25 October 2006.

Q3B(R2) (2006b). Impurities in new drug products, Q3B(R2), Current step 4 version, dated 2 June 2006.

Rampurna, P. G. (2010). Soft gelatin capsules (softgels). *Journal of Pharmaceutical Sciences*, *99*(10), 4107–4148. https://doi.org/10.1002/jps.22151

Richard, F. S., & Sabine, K. (2018). Midostaurin: A Multiple Tyrosine Kinases Inhibitor in Acute Myeloid Leukemia and Systemic Mastocytosis. In U. Martens (Ed.), *Small molecules in hematology. Recent results in cancer research* (p. 212). Cham: Springer. https://doi.org/10.1007/978-3-319-91439-8_10

Roberto de Alvarenga, J. B., & Lajarim, C. R. (2019). Chemometrics approaches in forced degradation studies of pharmaceutical drugs. *Molecules*, *24*(20), 3804. https://doi.org/10.3390/molecules24203804

RYDAPT (midostaurin) – FDA. (2017). Reference ID: 4090671. https://www.accessdata.fda.gov/drugsatfda_docs/label/2017/207997s000lbl.pdf

Saranjit, S., Mahendra, J., Gajanan, M., Harsita, T., Moolchand, K., Neha, P., & Padmaja, S. (2013). Forced degradation studies to assess the stability of drugs and products. *Trends in Analytical Chemistry*, *49*, 71–88. https://doi.org/10.1016/j.trac.2013.05.006

Shoutian, Z., Heiko, W., Jian, W., Charles, Y. C., Xu, W., & Peter, G. S. (2009). A small molecule primes embryonic stem cells for differentiation. *Cell Stem Cell*, *4*(5), 416–426. https://doi.org/10.1016/j.stem.2009.04.001

Thomas, I., Hans-M, T., Christian, T., Martin, B., Markus, S., Eberhard, S., & Gerhard, E. (2007). A highly sensitive method for the detection of PKC412 (CGP41251) and its metabolites by high-performance liquid chromatography. *Journal of Pharmacological and Toxicological Methods*, *56*(1), 23–27.

United States Pharmacopeia, USP <1225>. (2020). Validation of compendia procedures. http://www.uspbpep.com/usp32/pub/data/v32270/usp32nf27s0_c1225.html

United States Pharmacopeia, USP <621> Chromatography. (2020). http://www.uspbpep.com/usp32/pub/data/v32270/usp32nf27s0_c621.html

Van Gijn, R., Havik, E., Boven, E., Vermorken, J. B., ten BokkelHuinink, W. W., van Tellingen, O., & Beijnen, J. H. (1995). High-performance liquid chromatographic analysis of the new antitumour drug N-benzoylstaurosporine (CGP 41 251) and four potential metabolites in micro-volumes of plasma. *Journal of Pharmaceutical and Biomedical Analysis*, *14*(1), 165–174. https://doi.org/10.1016/0731-7085(95)01616-3

Van Gijn, R., van Tellingen, O., de Clippeleir, J. J. M., Hillebrand, M. J. X., Boven, E., Vermorken, J. B., ten BokkelHuinink, W. W., Schwertz, S., Graf, P., & Beijnen, J. H. (1995). Analytical procedure for the

determination of the new antitumour drug N-benzoylstaurosporine and three potential metabolites in human plasma by reversed-phase high-performance liquid chromatography. *Journal of Chromatography. B, Biomedical Sciences and Applications*, *667*(2), 269–276. https://doi.org/10.1016/0378-4347(95)00037-J

Venkataraman, S., & Manasa, M. (2018). Forced degradation studies: Regulatory guidance, characterization of drugs, and their degradation products-a review. *Drug Invention Today*, *10*(2), 137–146.

SUPPORTING INFORMATION

Additional supporting information may be found in the online version of the article at the publisher's website.

How to cite this article: Lakka, N. S., Kuppan, C., & Ravinathan, P. (2021). Impurity profiling and stability-indicating method development and validation for the estimation of assay and degradation impurities of midostaurin in softgel capsules using HPLC and LC–MS. *Biomedical Chromatography*, e5222. https://doi.org/10.1002/bmc.5222

Received: 14 November 2021 | Revised: 12 December 2021 | Accepted: 22 December 2021

DOI: 10.1002/bmc.5325

RESEARCH ARTICLE

Biomedical Chromatography WILEY

Development and validation of liquid chromatography–tandem mass spectrometry method for the estimation of a potential genotoxic impurity 2-(2-chloroethoxy)ethanol in hydroxyzine

Narasimha S. Lakka[1] | Chandrasekar Kuppan[1] | Poornima Ravinathan[2] | Ashok Kumar Palakurthi[3]

[1]Division of Chemistry, Department of Sciences and Humanities, VIGNAN's Foundation for Science, Technology & Research, Vadlamudi, Guntur (Dist.), India

[2]Department of Sciences and Humanities, JMJ College for Women, Tenali, Guntur (Dist.), India

[3]Department of Analytical Research and Development, Aurex Laboratories LLC, East Windsor, NJ, USA

Correspondence
Chandrasekar Kuppan, Division of Chemistry, Department of Sciences and Humanities, VIGNAN's Foundation for Science, Technology and Research, Vadlamudi, Guntur (Dist.) 522213, India.
Email: ramachan16@gmail.com

Funding information
World Health Organization

Abstract

2-(2-Chloroethoxy)ethanol (CEE) belongs to the so-called cohort of concerns which were classified as highly potent mutagenic carcinogens by the World Health Organization. It is widely used in the synthesis of the essential anti-histamine drug hydroxyzine. In addition, it is used as a primary solvent in dyes, nitrocellulose, paints, inks and resins. Owing to its potential genotoxicity, an efficient liquid chromatography–tandem mass spectrometry method was developed for the quantitative estimation of CEE traces in an active pharmaceutical ingredients and in tablet dosage forms of hydroxyzine-free base. The chromatographic separation was achieved on a C_{18} column using a gradient elution mode with a binary solvent system (ammonium formate and methanol). Mass detection was performed for CEE using a positive mode with selected ion monitoring technique at *m/z* value of $[M + NH_4]^+$. The developed method was validated as per the International Conference on Harmonizaiton guidelines. The quantitation limit, linearity and recoveries were found to be 0.56 ppm, 0.56–7.49 ppm ($r^2 > 0.9985$) and 93.6–99.3%, respectively. The proposed method was highly compatible and was used effectively to estimate CEE traces in different stages of drug synthesis and in tablet dosage forms of hydroxyzine for routine and stability testing.

KEYWORDS
2-(2-chloroethoxy)ethanol (CEE), atmospheric pressure chemical ionization (APCI), hydroxyzine, liquid chromatography–tandem mass spectrometry (LC–MS/MS), potential genotoxic impurity (PGI)

1 | INTRODUCTION

Hydroxyzine is an anti-histamine medication used for treatment of itchiness, anxiety and nausea. It is chemically designated as "2-[2-[4-(*p*-chloro-α-phenylbenzyl)-1-piperazinyl]ethoxy] ethanol dihydrochloride" with the molecular formula $C_{21}H_{27}ClN_2O_2{\cdot}2HCl$ and molecular weight 447.83 g/mol (hydroxyzine-free base: 374.904 g/mol). The chemical structural of hydroxyzine is illustrated in Scheme 1 (a). The tablet dosage form of hydroxyzine hydrochloride is available on the market as 10, 25 and 50 mg forms. The recommended dose is 50 mg daily in divided doses for children under 6 years, and 50–100 mg daily in divided doses for patients over 6 years (FDA, 2021).

The genotoxic impurity 2-(2-chloroethoxy)ethanol (CEE) is predominantly utilized as a starting material in the early intermediate synthesis stages of hydroxyzine-free base (Scheme 1b). CEE has potential mutagenic properties and belongs to the so-called cohort of concern, which is a group of highly potent mutagenic carcinogens that have been classified by the World Health Organization. It causes skin

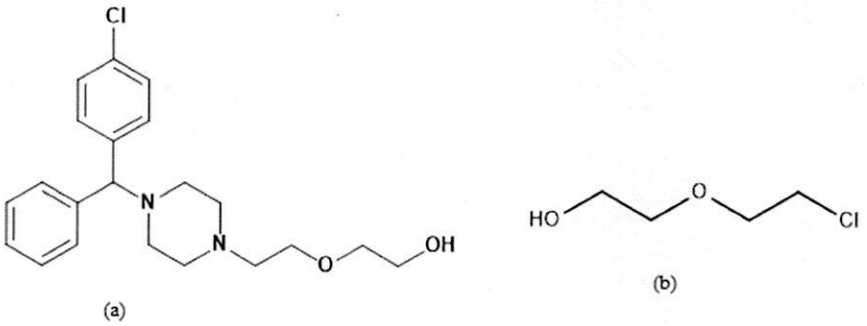

SCHEME 1 Chemical structure of (a) hydroxyzine and (b) 2-(2-chloroethoxy) ethanol

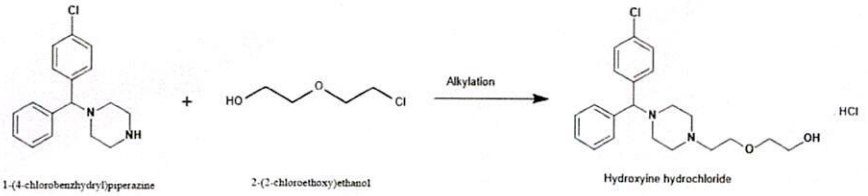

SCHEME 2 Route of synthesis of hydroxyzine

irritation, serious eye damage and respiratory system damage when in contacted with the skin. Thus, it is mandatory to estimate the residual amount of CEE present either in the final stage of an active pharmaceutical ingredient (API) or in formulated drug products (Scheme 2; Stolarczyk et al., 2007, 2011). The main aim of the study was to ensure the quality of the drug hydroxyzine-free base and patient safety.

CEE is a clear, colorless to pale yellow oily liquid which is essentially used in the synthesis of APIs such as (a) *o*-nitrophenylbromoacetaldehyde *bis*-2-(2-chloroethoxy)-ethyl acetal, (b) 2-(2-azidoethoxy)ethanol, (c) quetiapine and (d) bis(2-chloroethyl) ether, (Scheme 3(a–c); Ellis-Davies & Kaplan, 1994; Mespouille et al., 2007; Stolarczyk et al., 2007, 2011). It is also chemically known as diethylene glycol monochlorohydrin with the molecular formula $C_4H_9ClO_2$ and a molecular weight of 124.57 g/mol. CEE has a perceptible odor and is mostly formed as a major degradation product from the API *bis*(2-chloroethyl)ether (Scheme 3(d), McClay et al., 2007).

Many different purification processes are employed to obtain drug substances with the highest purity form possible, and the high-purity drugs are intended for use in pharmaceutical dosage forms by many drug makers, despite the chance of their containing genotoxic impurity residues carried over from the starting material to the final API. Thus, it is necessary to estimate the genotoxic impurities or mutagenic carcinogens using a suitable detection technique, even if they are present at trace level, at all possible synthesis stages from the raw materials to the final API and finished dosage forms (EMEA, 2006, 2010; FDA, 2008, 2018; Gosar et al., 2018; ICH, 1996, 2003, 2011, 2021b; Kirkland & Snodin, 2004; Müller et al., 2006).

As per the literature inclusive of official monographs and regulatory references, the specification limit for the CEE has not been reported and, to the best of our knowledge, no attempt has been made to calculate the limit for CEE impurities using the available guidance (International Conference on Harmonization, ICH, and US Food and Drug Administration, FDA; Stolarczyk et al., 2007, 2011). Based on the literature, the usage of hydroxyzine hydrochloride comes under the less-than-life-time exposure category for the establishment of risk. To address less-than-life-time exposures to mutagenic impurities in pharmaceuticals, an approach of maximum daily dosage is applied, and the concentration limit (in parts per million) of CEE was calculated as 3.75 ppm for hydroxyzine-free base in according with the ICH (2021b) guidelines, even though it falls under the category of process impurity as per the ICH guidelines (EMEA, 2006, 2010; FDA, 2008, 2018; Gosar et al., 2018; ICH, 1996, 2003a,b, 2011, 2017; Kirkland & Snodin, 2004; Müller et al., 2006).

To quantify such a low-level impurity in the API at all stages throughout the manufacture and production and in the drug product, highly sensitive and advanced analytical techniques like gas chromatography (GC), liquid chromatography–mass spectrometry (LC–MS) and liquid chromatography–tandem mass spectrometry (LC–MS/MS) are mandatory (Lakka et al., 2021; Narasimha et al., 2020; Narasimha & Chandrasekar, 2019; Petras et al., 2017; Pitt, 2009).

A literature search revealed that there was no LC–MS or LC–MS/MS method reported for the estimation of CEE in hydroxyzine, except for a few analytical methods for CEE determination in quetiapine using gas chromatography (Stolarczyk et al., 2007, 2011). However, these were found to be not suitable for CEE estimation owing to hydroxyzine matrix interference. Consider the need for better therapy, the authors have developed a new LC–MS/MS method for the estimation of CEE in the API and formulated drug product of hydroxyzine tablets. LC–MS/MS is a widely used powerful and sophisticated analytical technique that combines the separating power of chromatography with highly sensitive and selective mass analysis capability using triple quadruple mass spectrometry (Agilent, 2007, 2010; Colby & Thoren, 2020; Lakka

SCHEME 3 Chemical structure of (a) *o*-nitrophenylbromo-acetaldehyde bis-2-(2-chloroethoxy)-ethyl acetal, (b) 2-(2-azidoethoxy)ethanol, (c) quetiapine and (d) *bis*(2-chloroethyl)ether

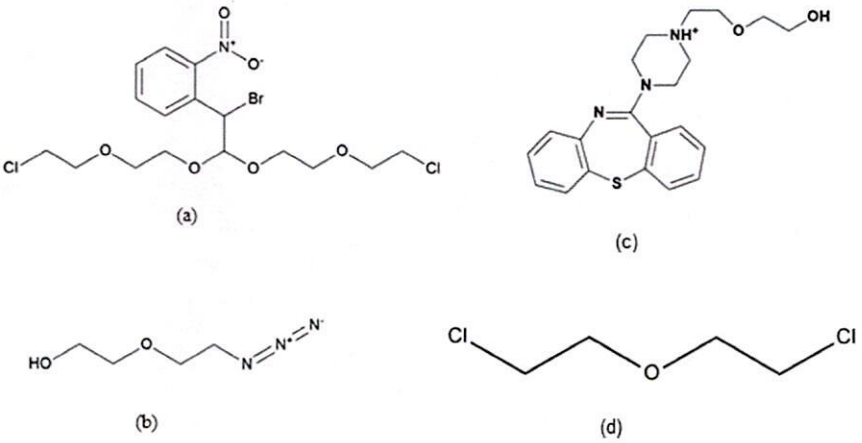

et al., 2021; Lee et al., 2015; Narasimha et al., 2020; Pitt, 2009; Thomas, 2019).

2 | EXPERIMENTS

2.1 | Reagents and materials

CEE standard and samples of hydroxyzine hydrochloride (drug substance, tablets and placebo samples) were kindly supplied by Manasa Life Sciences Pvt. Ltd (Hyderabad, India) and Dr SLN Laboratories Pvt. Ltd (Hyderabad, India). Ammonium formate and formic acid of analytical-reagent grade were purchased from Finar (Ahmadabad, India). Methanol of HPLC grade was purchased from the Qualigens (Thermo Fisher Scientific India Pvt. Ltd, Mumbai, India).

2.2 | Instruments

High-performance liquid chromatography (HPLC) equipped with a mass detector and diode array detector were utilized for the separation, identification and quantitative estimation of CEE (Agilent 6470, Triple Quad LCMS with 1260 Infinity HPLC system). MassHunter software was used for the output signal monitoring, processing and data analysis (Agilent, 2007, 2010). The analytical column used was a BDS Hypersil™ C_{18} (dimensions 100 × 4.0 mm, particle size 3 µm; Thermo Scientific, Lithuania). An analytical balance (GH-252, AND, Japan) was used for the weighing of samples and standards. Ultrapure water (electrical resistivity ≥ 18.2 MΩ cm at 25°C) was collected from a Millipore (Milli Q® IQ-7000, Merck, Molsheim, France) water purification system. The ultrasonic bath used for sample preparation was purchased from Labman (LMUC-6, Delhi, India). The gas chromatograph equipped with a flame ionization detector used for the initial method development trials was an Agilent 7890B (Agilent Technologies Inc., DE, USA). The GC column used was DB-264 (60 m × 0.32 mm, 1.8 µm; Agilent J&W, CA, USA).

2.3 | HPLC and LC–MS conditions

The LC–MS separation was achieved on a C_{18} column (BDS Hypersil™ C_{18}, 100 X 4.0 mm, particle size 3 µm) using the gradient elution mode with binary solvents [solvent A, aqueous ammonium formate (10 mM) with 0.2% (v/v) formic acid; solvent B, methanol]. The gradient run with a flow rate of 0.7 ml/min was programmed as [time (min)/B (%)]: 0.01/20, 5/20, 10/0, 12/0, 14/20 and 20/20. The column temperature and sampler temperature were maintained at 45 and 5°C, respectively. Aliquots of 50 µl of the standard and sample solutions of CEE were injected for analysis and the absorbance was monitored using a UV detector at 230 nm. The following MS/MS conditions were used for estimation of CEE: polarity, positive; ionization mode, atmospheric pressure chemical ionization (APCI); selected ion monitoring ion $[M + NH_4]^+$, 142.1; fragmentation temperature, 60°C; drying gas flow, 8.0 L/min; nebulizer pressure, 35 psig; drying gas temperature, 250°C; vaporizer temperature, 400°C.

2.4 | Standard solution

The standard stock solution (15 µg/ml) of CEE was prepared by dissolving 3.75 mg of CEE standard in 250 ml of diluent [formic acid, 0.1% (v/v) in water]. Further dilution (1.0 ml into 200 ml) was made in order to obtain the nominal concentration of 0.075 µg/ml (3.75 ppm) with respect to the sample concentration of 20 mg/ml.

2.5 | Sample solutions

For the final API and all of its stages, the sample solution was made by dissolving hydroxyzine hydrochloride equivalent to a 200 mg sample (i.e. reaction mass, mother liquor and final drug substance) in 10 ml of diluent to obtain the sample concentration of 20 mg/ml.

The sample solution of hydroxyzine hydrochloride tablet dosage form was made as follows: finely crushed sample powder as obtained from 10 tablets (25 mg/tablet) equivalent to 200 mg drug was weighed into a 10 ml volumetric flask; 5 ml of diluent was added and sonicated for 10 min (temperature maintained at 5°C in ultrasonic bath) and made up to the volume with diluent. This solution was filtered through a 0.22 μm PVDF membrane filter (Durapore, Merck Life Science Pvt. Ltd, Bangalore, India) and the clear filtrate was used for LC–MS/MS analysis. The placebo solution for hydroxyzine tablets was prepared using the same procedure as implemented for the sample solution.

3 | RESULTS AND DISCUSSION

3.1 | Evaluation of literature methods

The gas chromatography method reported in the literature was tested during the initial experiments for the estimation of CEE in hydroxyzine-free base, but the diluting solvent peak interfered with the CEE peak (Stolarczyk et al., 2007, 2011). GC conditions used were: oven, 150°C, 0.0 min/230°C, 5 min/240°C, 40 min; carrier gas, nitrogen, 3 ml/min; inlet, split, 2:1 at 150°C; detector, flame ionization detector at 260°C, H_2 at 40 ml/min, O_2 at 400 ml/min, N_2 makeup at 25 ml/min; detector signal, 50 Hz; retention time, 10.6 min; run time, 16.25 min. Moreover, the peak response as obtained from the gas chromatography was very low and multiple peaks were detected owing to the sample matrix of hydroxyzine. In fact, several optimization trials were conducted to obtain a better separation for the quantitative estimation of CEE, although the hydrazine matrix peak, CEE peak and solvent peak were not separated well. Thus, the method development was carried out using the LC–MS/MS for the estimation of the amount of CEE in hydroxyzine (Table 1).

3.2 | Method development and optimization trials using LC–MS/MS

The main aim of the work is to quantitatively estimate the CEE impurity traces in the API and finished tablets dosage form of hydroxyzine using the liquid chromatography–tandem mass spectrometry (LC–MS/MS) method. In the proposed method, chromatographic separation was achieved as discussed in the following sections.

3.2.1 | Selection of mobile phase

The method development trails were conducted using HPLC–MS/MS and a diode array detector in the presence of buffers (such as ammonium acetate, ammonium formate, formic acid, trifluoroacetic acid and their combinations), which were compatible with mass spectrometry.

The selected chromatographic conditions—mobile phase A [ammonium formate buffer with 0.2% (v/v) formic acid] and mobile phase B (methanol) in a gradient run [time (min)/B (%)] of 0.01/20, 5/20, 10/0, 12/0, 14/20, and 20/20, with flow rate 0.7 ml/min and column temperature 45°C—were well suited for the estimation of CEE in hydroxyzine samples. The CEE peak, which was eluted at retention time of 2.5 min, was separated well from the sample matrix peaks of hydroxyzine. The organic modifier acetonitrile, which is most frequently used in liquid chromatography, was not chosen as the mobile phase in the present study, as it is not compatible with APCI technique, owing to the reduction of nitrile to carbon during the negative ionization.

3.2.2 | Selection of diluting solvent

Different diluting solvents (such as water, ammonium formate buffer, formic acid buffer, acetonitrile and methanol) were tried during the

TABLE 1 Method feasibility and optimization trials of GC method reported in literature

Experiment	GC conditions	Observation	Result
Trail 1	Injection volume 1.0 μl	Rt, 8.175 min Peak area, 0.783 (μV s)	CEE peak eluted in the tailing of the diluting solvent peak, but its response was very low so this trial was rejected
Trail 2	Injection volume 2.0 μl	Rt, 8.215 min Peak area, 1.421 (μV s)	CEE peak eluted in the tailing of the diluting solvent peak, but its response was very low so this trial was also rejected
Trail 3	Injection volume 3.0 μl	Rt, 8.2565 min Peak area, 1.895 (μV s)	CEE peak eluted in the tailing of the diluting solvent peak, but its response was very even with 3.0 μl injection volume so this trial was also rejected
Trail 4	Injection volume 3.0 μl	Rt, 8.271 min CEE area, 1.8 (μV s) Diluent peak area, 0.8 (μV s)	Blank (diluting solvent) peak interfered with CEE peak. Moreover, multiple unwanted peaks were eluted owing to the sample matrix, so this trial was also rejected

CEE, 2-(2-Chloroethoxy)ethanol; Rt, retention time.

preliminary experiments but the aqueous formic acid solution (0.1%, v/v) was chosen as a final diluent owing to its compatibility with the mass detector and mobile phases. Moreover, the CEE was solubilized completely, which gave good peak shape when compared with other solvents.

3.2.3 | Selection of wavelength and injection volume

The chromatogram of CEE and hydroxyzine was monitored using the HPLC equipped with a diode array detector at a wavelength of

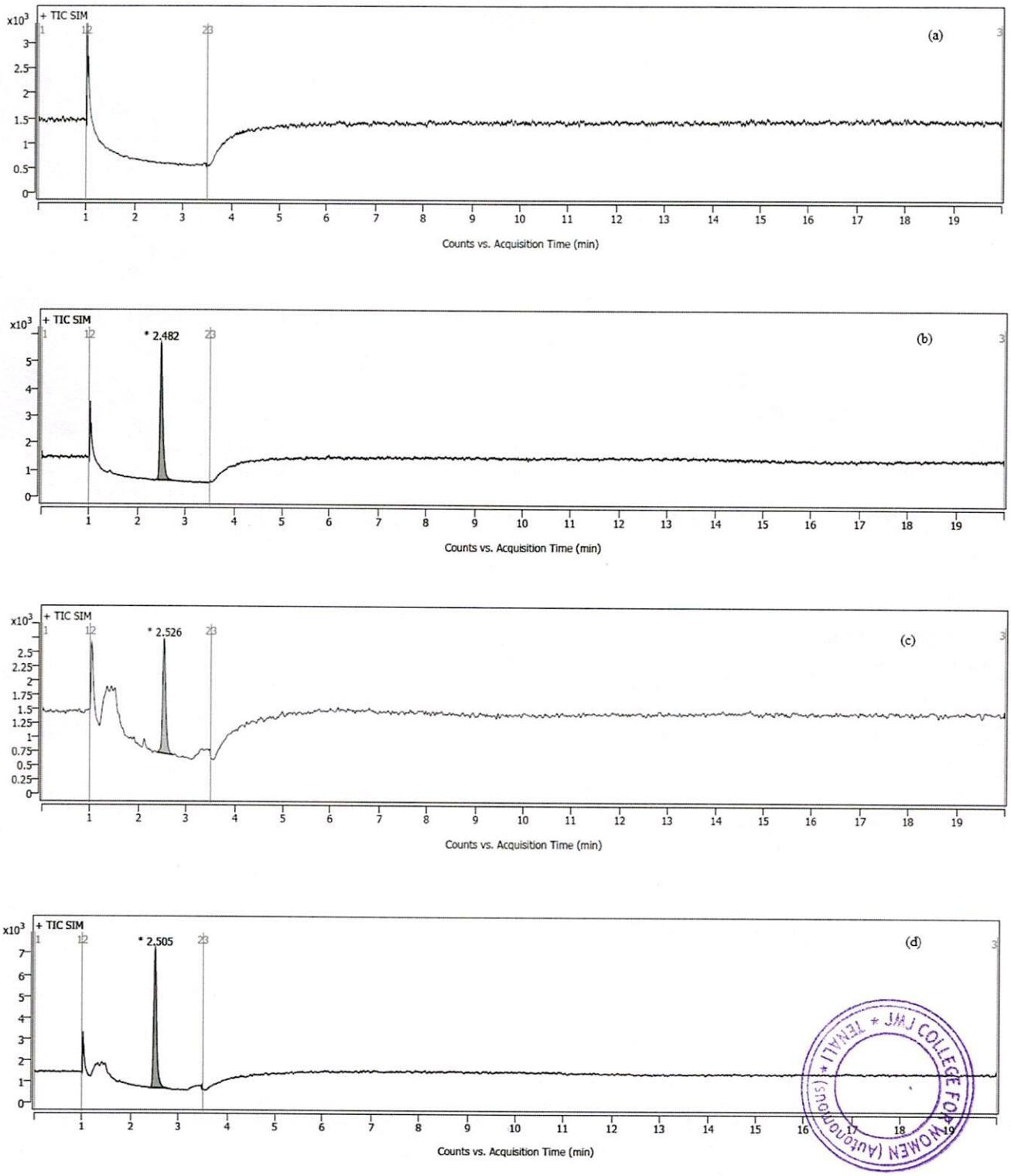

FIGURE 1 (a) LC chromatogram of diluent, (b) LC chromatogram of standard solution [2-(2-chloroethoxy)ethanol, CEE], (c) LC chromatogram of control sample of hydroxyzine hydrochloride and (d) LC chromatogram of spiked sample (100%) of hydroxyzine hydrochloride

230 nm. The selected injection volume of 50 µl gave higher sensitivity and a reliable response for CEE.

3.2.4 | Effect of oven temperature

The effect of the column oven temperature on the separation and estimation of CEE was established by varying column temperature (45 ± 2°C), and the respective changes made did not affect much the peak elution (retention time) and peak response (i.e. 43°C, 2.55 min; 45°C, 2.53 min; 47°C, 2.52 min).

3.3 | Optimization of MS conditions

3.3.1 | Selection of MS detector

In this study, a mass detector was chosen for the detection and quantitative estimation of CEE because it had several advantages and a capacity to detect numerous molecules, even those that do not have a chromospheric nature (i.e. ultraviolet active functional groups).

3.3.2 | Selection of ionization parameters

Selected ion monitoring mode was used to estimate the CEE traces with high-quality precision and sensitivity. Atmospheric pressure chemical ionization, which is similar to electrospray ionization technique, was chosen for the CEE estimation, as it worked effectively for the estimation of small and liquid molecules with lower polarities (Colby & Thoren, 2020; Lee et al., 2015; Thomas, 2019). A drying temperature of 250°C and a vaporization temperature of 400°C were applied to de-solvate the buffer rapidly into aerosol droplets in a stream of nitrogen gas. The LC chromatogram and respective mass spectra (*m/z*) obtained from LC–MS/MS are depicted in Figures 1(a–d) and 2(a–c).

The mass-to-charge ratio (*m/z*) of CEE was observed at 142.1 corresponding to the mass value of $[M + NH_4]^+$ (in which 124.56 is

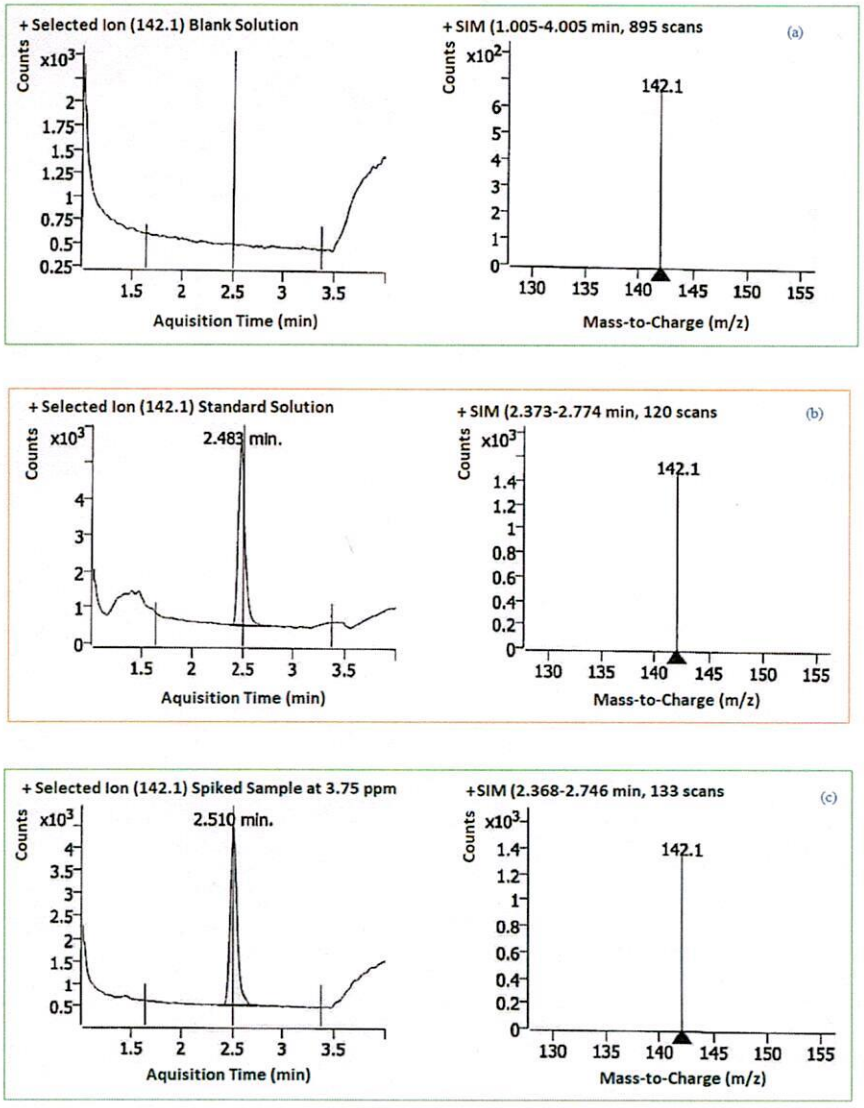

FIGURE 2 (a) LC chromatogram and mass spectra of blank (diluent), (b) LC chromatogram and mass spectra of standard (CEE) and (c) LC chromatogram and mass spectra of the sample (CEE spiked in the sample at 100% level)

the mass value of CEE and 18 is the mass value of the ammonium ion, NH_4^+) in the positive mode of selected ion monitoring and with APCI technique.

As shown in Table 2, various trials were carried out by changing the nebulizer gas (N_2) pressure, drying gas (N_2) flow rate, drying gas (N_2) temperature and vaporizer temperature, but all of the changes made, except for the nebulizer gas pressure, under ionization parameters did not have any influence on the detection and estimation of CEE.

In order to de-solvate and generate aerosols for reliable and high-quality intensity, the nebulizer gas pressures were varied and finally the nebulizer gas pressure 35 psi was chosen for the optimal condition.

3.4 | Establishment of the CEE limit

In accordance with the ICH, FDA, European Medicines Agency (EMEA) and other guidance (EMEA, 2006, 2010; FDA, 2008, 2018; Gosar et al., 2018; ICH, 1996, 2003, 2003a,b, 2011, 2017, 2021a; Kirkland & Snodin, 2004; Müller et al., 2006), the specification limit (in ppm) for the potential genotoxic impurity (CEE) obtained from the manufacturing processes (starting material stage or intermediate stage) of hydroxyzine was estimated using the following: the allowable concentration limit (ACL, in ppm) is equal to the threshold of toxicological concerns (TTC) (μg/day)/dose (g/day), where the TTC is 1.5 μg/ml (ICH, 2021b) and the maximum daily dosage of the hydroxyzine drug product is 0.4 and 0.8 g/day, respectively, i.e. the ACL of CEE of 3.75 ppm was calculated for hydroxyzine [ACL = TTC (1.5 μg/day)/dose (0.4 g/day)], and the CEE traces were estimated in the API (at different synthesis stages) and formulated drug product (tablet dosage form) of hydroxyzine using the developed LC–MS/MS method. In addition, the method validation study was performed using an ACL of 3.75 ppm of CEE in the hydroxyzine-free base.

3.5 | Method validation

The developed method was validated as per the ICH guidelines for specificity, linearity, and quantitation limit (QL), accuracy, precision and solution stability (ICH, 2005). The method validation experiments carried out for CEE are discussed in the following sections.

3.5.1 | Specificity

The specificity of the developed test method was proven by injecting blank and placebo solutions. The study results indicated that the blank and placebo did not show any interference at the retention time of 2.5 min for CEE, and there was no spectral interference peak found at the *m/z* of $[M + NH_4]^+$ at 142.1 (Figures 1 and 2).

3.5.2 | Linearity

The linearity study of the developed LC–MS/MS method was proved by preparing a series of linearity solutions containing CEE at five different concentrations (0.56–7.49 ppm), which covered the QL of 15–200% of the target limit concentration of 3.75 ppm for hydroxyzine. The calibration curve of CEE impurity was drawn by plotting the peak response (counts) vs. concentration (Figure 3). The correlation coefficient (r) obtained was found to be >0.999 (r^2 > 0.998) for CEE (Table 3).

TABLE 2 Optimization of ionization parameter in MS/MS

Experiment	MS conditions	Observation	Result
Trail 1	Nebulizer gas pressure, 25 psi; drying gas (N_2) flow rate, 7.0 L/min; drying gas (N_2) temperature, 240°C; vaporizer temperature, 380°C	Low intensity	Rejected
Trail 2	Nebulizer gas pressure, 30 psi; drying gas (N_2) flow rate, 7.0 L/min; drying gas (N_2) temperature, 240°C; vaporizer temperature, 380°C	Low intensity	Rejected
Trail 3	Nebulizer gas pressure, 35 psi; drying gas (N_2) flow rate, 7.5 L/min; drying gas (N_2) temperature, 240°C; vaporizer temperature, 380°C	Moderate intensity	Rejected
Trail 4	Nebulizer gas pressure, 35 psi; drying gas (N_2) flow rate, 7.5 L/min; drying gas (N_2) temperature, 250°C; vaporizer temperature, 385°C	Good intensity	Tentatively accepted
Trail 5	Nebulizer gas pressure, 35 psi; drying gas (N_2) flow rate, 8.0 L/min; drying gas (N_2) temperature, 250°C; vaporizer temperature, 390°C	Good intensity	Tentatively accepted
Trail 6	Nebulizer gas pressure, 35 psi; drying gas (N_2) flow rate, 8.0 L/min; drying gas (N_2) temperature, 250°C; vaporizer temperature, 400°C	Good intensity	Accepted

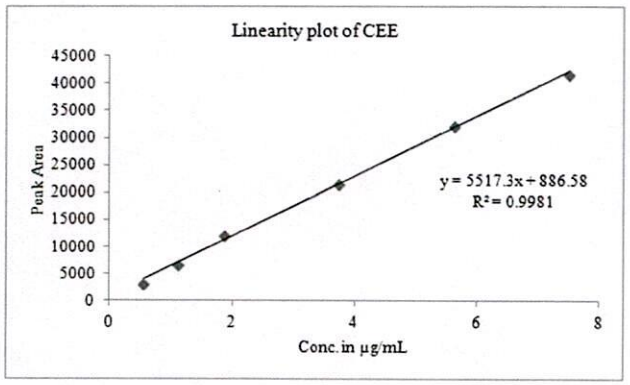

FIGURE 3 Linearity plot of CEE (obtained from the concentration in ppm vs. peak area counts)

TABLE 3 Linearity results of CEE (by LC–MS/MS method)

Item	Observed value
QL concentration, µg/ml	0.5625 µg/ml
Concentration range, µg/ml	0.5625–7.49 µg/ml
Trend line	$y = 5517.3x + 886.58$
Correlation (r^2)	0.999
Regression (R) (Stolarczyk et al., 2007))	0.998

$y = mx + c$, where m is the slope value, c is the intercept value obtained from the linear regression line (concentration vs. peak response) and x is the unknown concentration of target analyte.
r^2, Correlation coefficient is obtained from the linear regression plot of the respective component.
R (Stolarczyk et al., 2007), Linear regression coefficient obtained from the linear regression plot of the respective component.
QL, Concentration of the quantitation limit is calculated using the slope method as per ICH guidelines.

3.5.3 | Quantitation limit

The QLs for CEE were established based on the standard deviation (SD) of the response and slope (s) of the regression line as obtained from the linearity (which was calculated as per ICH guidelines; ICH, 2005). The slope value of CEE was calculated from the linearity study: $QL = 10 \times \sigma/s$ where, σ = SD. The residual sum of squares obtained from the linearity regression data was used as the SD (STEYX in Microsoft Excel spreadsheet; Alquadeib, 2019; Miller, 1991; Thompson et al., 2002; Vogelgesang & Hädrich, 1998). The concentration of the QL for CEE impurity was 0.56 ppm (Table 3). The concentrations of QL were verified by performing the accuracy and precision analyses of solutions in six replicates and were <5.0% (RSD, relative standard deviation).

3.5.4 | Accuracy and precision

The accuracy and precision of the developed test method were proved by preparing 12 spiked samples at three different concentrations, viz. 15–150% of the target concentration of 3.75 ppm for hydroxyine. The percentage recovery, mean percentage recovery and percentage RSD were calculated from the data obtained from the liquid chromatography–tandem mass spectrometry (Table 4). The recovery values observed were in the range 93.6–99.3% (limit 80.0–120.0%) from all 12 preparations ($n = 12$). The RSD results (1.5%) confirmed that the developed test method is precise and accurate.

3.5.5 | Solution stability

The solution stabilities of the CEE standard and sample solution (100% spike level) were established by storing the standard solution (3.75 ppm) and spiked sample of CEE (concentration of hydroxyzine, 20 mg/ml) with a known impurity concentration of 3.75 ppm in clear volumetric flasks at ambient temperature and in the refrigerator (2–8°C). The analyses of standard and sample were done at 24 and 48 h. The results obtained confirmed that the CEE standard solution and sample solution are stable for up to 48 h when stored in the refrigerator. Thus, the sample oven temperature was established as 5 ± 3°C.

3.5.6 | Batch analysis

The sample solutions of hydroxyine obtained from the different stages of synthesis followed by the finished tablet dosage forms were analyzed by applying the optimized LC–MS/MS conditions and the test results were found to be below the QL concentration (≤15%). Since the detected CEE in the final API and tablets dosage form was found to be below the QL and <30% of the specified limit (0.56 ppm), there is no significant impact on the quality of the drug either in its pure form (API) or in the finished tablet dosage form of hydroxyzine.

TABLE 4 Results of accuracy and method precision for the determination of CEE

	Spike level (in ppm) and recovery (%)			
Preparation	0.56	1.875	3.75	5.625
1	93.6	96.2	98.0	96.4
2	99.3	97.8	98.5	96.8
3	96.5	98.2	97.7	96.1
Mean ($n = 3$)[a]	96.5	97.4	98	96.6
RSD, % ($n = 3$)	2.94	1.09	0.41	0.49
Overall recovery ($n = 12$)[b]	97.1			
Overall RSD, % ($n = 12$)[c]	1.54			

[a]Mean of recovery, percentage of three replicates at each concentration level. Recovery covered at four different levels: −0.56 ppm (15%), 1.875 ppm (50%), 3.75 ppm (100%) and 5.625 ppm (150%).
[b]Overall mean recovery of all four different concentration levels (three preparations made at each level).
[c]Relative standard deviation of all recoveries done at four different concentration levels.

4 | CONCLUSION

A new and highly selective liquid chromatograph–tandem mass spectrometry method was developed for the quantitative estimation of residual genotoxic CEE impurity in API and finished tablet dosage form of hydroxyzine hydrochloride. The developed method was validated in according with guidelines of the ICH (2005). The QL was established as 0.56 ppm (15% with respect to CEE concentration 3.75 ppm in hydroxyzine). The linearity study was proved in the concentration range 0.56–7.49 ppm ($r^2 > 0.9985$), which covered 15–200% of the target limit concentration of 3.75 ppm. High-quality recoveries were found in range of 93.6–99.3%, which covered 0.56–5.625 ppm (15–150% of the target concentration of 3.75 ppm). The proposed method is effectively used for the routine testing of CEE impurity traces in the different stages of API and finished tablets dosage forms of hydroxyzine hydrochloride.

ACKNOWLEDGEMENT

The authors thank the management of Dr SLN Laboratories Pvt. Ltd for supporting this work by gifting samples for analysis and providing the facilities.

CONFLICT OF INTEREST

The authors declare no conflict of interest.

DATA AVAILABILITY STATEMENT

The data that supports the findings of this study are available in this article (manuscript).

ORCID

Narasimha S. Lakka https://orcid.org/0000-0002-2952-7493
Chandrasekar Kuppan https://orcid.org/0000-0002-3780-6222
Ashok Kumar Palakurthi https://orcid.org/0000-0001-5658-8622

REFERENCES

Agilent. (2007). *Familiarization guide. Agilent MassHunter workstation software data acquisition for 6200 series TOF and 6500 series Q-TOF* (2006–2007. 1st ed.) (pp. G3335–G90029). Agilent Technologies, Inc.

Agilent. (2010). *Familiarization guide. Agilent MassHunter workstation software quantitative analysis. Agilent Technologies, Inc. (2007–2010, 4th edn)* (pp. G3335–G90061). Agilent Technologies, Inc. https://www.agilent.com/cs/library/usermanuals/Public/G3335_90061_Quant_Familiarization-EN.pdf

Alquadeib, B. T. (2019). Development and validation of a new HPLC analytical method for the determination of diclofenac in tablets. *Saudi Pharmaceutical Journal.*, *27*, 66–70. https://doi.org/10.1016/j.jsps.2018.07.020

Colby, J. M., & Thoren, K. L. (2020). Applications of mass spectrometry in the clinical laboratory. In *Contemporary Practice in Clinical Chemistry* (Fourth ed.) (pp. 351–363). Academic Press. https://doi.org/10.1016/B978-0-12-815499-1.00021-1

Ellis-Davies, G. C., & Kaplan, J. H. (1994). Nitrophenyl-EGTA, a photolabile chelator that selectively binds Ca2+ with high affinity and releases it rapidly upon photolysis. *Proceedings of the National Academy of Sciences of the United States of America*, *91*(1), 187–191. https://doi.org/10.1073/pnas.91.1.187

EMEA. (2006). Guideline on the limits of genotoxic impurities. CPMP/SWP/5199/02 EMEA/CHMP/QWP/251344/2006. European Medicines Agency Evaluation of Medicines for Human Use. https://www.ema.europa.eu/en/documents/scientific-guideline/guideline-limits-genotoxic-impurities_en.pdf

EMEA. (2010). *Safety working group, questions and answers on the 'Guideline on the limits of genotoxic impurities'*. 23 September 2010. EMA/-CHMP/SWP/431994/2007 Rev. 3 Committee for Medicinal Products for Human Use (CHMP) Safety Working Party (SWP). Academic Press. https://www.ema.europa.eu/en/documents/scientific-guideline/questions-answers-guideline-limits-genotoxic-impurities_en.pdf

FDA. (2008). *FDA draft guidance, genotoxic and carcinogenic impurities in drug substances and products: Recommended approaches* (242th ed., Vol. 73, pp. 76361–76362). USA: U.S FDA. https://www.govinfo.gov/content/pkg/FR-2008-12-16/pdf/E8-29674.pdf

FDA. (2018). *M7(R1): Assessment and control of DNA reactive (mutagenic) impurities in pharmaceuticals to limit potential carcinogenic risk, guidance for industry*. U.S. Department of Health and Human Services Food and Drug Administration, Center for Drug Evaluation and Research (CDER), Center for Biologics Evaluation and Research (CBER). https://www.fda.gov/media/85885/download

FDA. (2021). Hydroxyzine hydrochloride, accessed on July 25, 2021. https://www.accessdata.fda.gov/drugsatfda_docs/label/2014/088617Orig1s043,088618Orig1s043,088619Orig1s044lbl.pdf

Gosar, A., Sayyed, H., & Shaikh, T. (2018). Genotoxic impurities and its risk assessment in drug compounds. *Drug Designing & Intellectual Properties International*, *2*(4), 227–232. https://doi.org/10.32474/DDIPIJ.2018.02.000143

ICH. (1996). Stability testing: Photostability testing of new drug substances and products, Q1B, current step 4 version, dated 6 November 1996. https://database.ich.org/sites/default/files/Q1B%20Guideline.pdf

ICH. (2003). *Stability testing of new drug substances and products Q1A (R2), current step 4 version, dated 6 February 2003*. ICH. https://database.ich.org/sites/default/files/Q1A%28R2%29%20Guideline.pdf

ICH. (2021a). *Impurities: Guideline for residual solvents Q3C(R8), current step 4 version, dated 22 April 2021*. ICH. https://database.ich.org/sites/default/files/ICH_Q3C-R8_Guideline_Step4_2021_0422_1.pdf

ICH. (2021b). *M7(R1) Assessment and control of DNA reactive (mutagenic) impurities in pharmaceuticals to limit potential carcinogenic risk*, accessed on 20 July, 2021. ICH. https://database.ich.org/sites/default/files/M7_R1_Guideline.pdf

ICH. (2005). Q2(R1) Validation of analytical procedures: Definitions and methodology. Incorporated in Q2(R1)

ICH. (2011). S2(R1) Genotoxicity testing and data interpretation for pharmaceuticals intended for human use.

Kirkland, D., & Snodin, D. (2004). Setting limits for genotoxic impurities in drug substances, threshold-based and pragmatic approaches. *International Journal of Pharmaceutical Medicine*, *18*, 197–207. https://doi.org/10.1097/00124363-200418040-00001

Lakka, N. S., Kuppan, C., & Ravinathan, P. (2021). Impurity profiling and stability-indicating method development and validation for the estimation of assay and degradation impurities of midostaurin in softgel capsules using HPLC and LC–MS. *Biomedical Chromatography*, *e5222*, e5222. https://doi.org/10.1002/bmc.5222

Lee, H.-R., Kochhar, S., & Shim, S.-M. (2015). Comparison of electrospray ionization and atmospheric chemical ionization coupled with the liquid chromatography–tandem mass spectrometry for the analysis of cholesteryl esters. *International Journal of Analytical Chemistry*, *2015*, 1–6. https://doi.org/10.1155/2015/650927

McClay, K., Schaefer, C. E., Vainberg, S., & Steffan, R. J. (2007). Biodegradation of *Bis*(2-chloroethyl) ether by *Xanthobacter* sp. strain ENV481. *Applied and Environmental Microbiology*, *73*, 6870–6875. https://doi.org/10.1128/AEM.01379-07

Mespouille, L., Vachaudez, M., Suriano, F., Gerbaux, P., Coulembier, O., Degée, P., Flammang, R., & Dubois, P. (2007). One-pot synthesis of well-defined amphiphilic and adaptative block copolymers via versatile combination of "click" chemistry and ATRP. *Macro Molecular Rapid Communications*, *28*(22), 2151–2215. https://doi.org/10.1002/marc.200700400

Miller, J. N. (1991). Basic statistical methods for analytical chemistry. Part 2. Calibration and regression methods. A review. *The Analyst*, *116*, 3–14. https://doi.org/10.1039/AN9911600003

Müller, L., Mauthe, R. J., Riley, C. M., Andino, M. M., De Antonis, D., Beels, C., DeGeorge, J., De Knaep, A. G. M., Ellison, D., Fagerland, J. A., Frank, R., Fritschel, B., Galloway, S., Harpur, E., Humfrey, C. D. N., Jacks, A. S., Jagota, N., Mackinnon, J., Mohan, G., … Yotti, L. (2006). A rationale for determining, testing, and controlling specific impurities in pharmaceuticals that possess potential for genotoxicity. *Regulatory Toxicology and Pharmacology*, *44*(3), 198–211. https://doi.org/10.1016/j.yrtph.2005.12.001

Narasimha, S. L., & Chandrasekar, K. (2019). Principles of chromatography method development. In O.-M. Boldura, C. Balta, & N. S. Awwad (Eds.), *Biochemical analysis tools—Methods for bio-molecules studies*. IntechOpen. https://doi.org/10.5772/intechopen.89501

Narasimha, S. L., Chandrasekar, K., Kona, S. S., & Raviteja, Y. (2020). Separation and characterization of new forced degradation products of Dasatinib in tablet dosage formulation using LC–MS and stability-indicating HPLC methods. *Chromatographia*, *83*, 947–962. https://doi.org/10.1007/s10337-0

Petras, D., Koester, I., Da Silva, R., Stephens, B. M., Haas, A. F., Nelson, C. E., Kelly, L. W., Aluwihare, L. I., & Dorrestein, P. C. (2017). High-resolution liquid chromatography tandem mass spectrometry enables large scale molecular characterization of dissolved organic matter. *Frontiers in Marine Science*, *4*(405). 1–14. https://doi.org/10.3389/fmars.2017.00405

Pitt, J. J. (2009). Principles and applications of liquid chromatography–mass spectrometry in clinical biochemistry. *Clinical Biochemist Reviews*, *30*, 19–34. https://www.ncbi.nlm.nih.gov/pmc/articles/PMC2643089/pdf/CBR_30_19.pdf

Stolarczyk, E. U., Groman, A., & Maruszak, W. (2011). Validation of GC method for quantitative determination of residual 2-(2-chloroethoxy) ethanol (CEE) and *N*-methyl-2-pyrrolidinone (NMP) in pharmaceutical active substance. *Acta Poloniae Pharmaceutica. Drug Research*, *68*(2), 161–167.

Stolarczyk, E. U., Groman, A., Groman, A., Kaczmarek, L. S., & Gołebiewski, P. (2007). GC method for quantitative determination of residual 2-(2-chloroethoxy) ethanol (CEE) and *N*-methyl-2-pyrrolidinone (NMP) in quetiapine. *Acta Poloniae Pharmaceutica*, *64*(2), 187–189.

Thomas, S. N. (2019). Mass spectrometry. In *Contemporary Practice in Clinical Chemistry* (4th ed.) (pp. 171–185). Academic Press. https://doi.org/10.1016/B978-0-12-815499-1.00010-7

Thompson, M., Ellison, S. L. R., & Wood, R. (2002). Harmonized guidelines for single-laboratory validation of methods of analysis (IUPAC technical report). *Pure and Applied Chemistry*, *74*(5), 835–855. https://doi.org/10.1351/pac200274050835

Vogelgesang, J., & Hädrich, J. (1998). Limits of detection, identification and determination: A statistical approach for practitioners. *Accreditation and Quality Assurance*, *3*, 242–255. https://doi.org/10.1007/s007690050234

How to cite this article: Lakka, N. S., Kuppan, C., Ravinathan, P., & Palakurthi, A. K. (2022). Development and validation of liquid chromatography–tandem mass spectrometry method for the estimation of a potential genotoxic impurity 2-(2-chloroethoxy)ethanol in hydroxyzine. *Biomedical Chromatography*, e5325. https://doi.org/10.1002/bmc.5325

PRINCIPAL
JMJ COLLEGE FOR WOMEN (Autonomous)
TENALI

JMJ COLLEGE FOR WOMEN (Autonomous) TENALI

International Journal of Early Childhood Special Education (INT-JECSE)
ISSN: 1308-5581 Vol 14, Issue 03 2022

THE ELEMENT OF EMOTIONAL INTELLIGENCE AND THEIR IMPACT ON SOCIAL RELATION

P. Hemalatha[1], Dr. K Ram Chandra [2],Dr. Shakila Azim [3],Dr. B. Annapurna [4], Dr. V. Nagalakshmi [5], Dr. M. Esther Kalyani[6]

[1]Associate Professor, Department of Home Science, JMJ College for Women (A), Tenali, Andhra Pradesh, India
[2] Professor and Head, Department of English,V R Siddhartha Engineering College (A), Vijayawada, A.P, India
[3]Associate Professor, Department of Psychology, MDDM College, Muzaffarpur, Bihar, India
[4] Associate Professor, Department of CSE, Aditya College of Engineering Surampalem,A.P, India
[5] Associate Professor, Department of Chemistry, Ch.S.D.St.Theresa's College for Women (A), Eluru, A.P, India
[6] Reader in History, Ch.S.D.St.Theresa's College for Women (A), Eluru, A.P, India

ABSTRACT: Particularly the most basic and significant aspect of human experience is our capacity to experience emotions. Humans can feel a myriad of emotions can be joy, pleasure anger, stress. Defining emotion is a complicating task but the concept somewhere lies between the field of psychology, philosophy, and neuroscience. In this paper, we are discussing emotions from the perspective of psychology. Emotions and intelligence have different meanings and roles from the viewpoint of psychology but after combining both words, EI can be referred to as an ability that provides an advantage in the world to deal with many negative emotions and in spread harmony. Emotional intelligence has drawn the attention of many researchers in every field. The Emotional intelligence first article was published by Salovey& Mayer in 1990 after that so much work has been done in the academic area of professional relations, instruments, or Scales for EI. So, the researcher decided to study factors of emotional intelligence and its role in social relationships. [1] [2]

KEYWORDS: Social relation, Emotional intelligence

1. INTRODUCTION

"Emotional intelligence is your ability to recognize and understand emotions in yourself and others, and your ability to use this awareness to manage your behavior and relationships".[3]

Emotional intelligence is a widely used concept of psychology. This term is used by many researchers to study the EI of human beings in various settings. The emotional intelligence term emerged from the theory of 'social intelligence' which is given by Robert Thorndike in the late 1930 Emotional intelligence (EI) deals with the competence of an individual to perceive, control, and evaluate emotions of themselves and others. Emotional intelligence is important for the person for coping with dynamic change in our social settings. It can be understood as an association among individual emotions and cognition that support a person coping with surrounding and understanding others around them. Researcher contradicts the adaptability of EI, few of them says EI can be improved through learning, and few claims that it is an inborn quality of an individual. EI is important for a human being not only for personal development but also for relationship management with others, social skills development. An emotional intelligence person has generally shown few traits like Emotional awareness, employing emotions to understand, and solving problems. Skilled in emotion management of oneself and others as well.[4]

"Emotional intelligence is an educational, permanent, and continuous process that intends to boost the development of emotional competencies as an essential element of human development to qualify individuals for life and to increase personal and social well-being."(Bisquerra, 2009) [5]

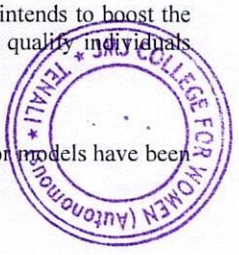

2. WORKING PRINCIPAL AND THEORIES OF EMOTIONAL INTELLIGENCE

Many psychologists and sociologists have talked about emotional intelligence but three major models have been acknowledged for the concept and component of emotional intelligence. They are:

1. Performance model: Goleman's
2. Competencies model: Bar-On's
3. Ability model: Mayer, Salovey, and Caruso's

DOI: 10.9756/INT-JECSE/V14I3.555

The performance model of EI by Goleman's: In 1995Daniel Goleman haswritten a book on EI. Daniel Goleman expressed Emotional intelligence as "the capacity for recognizing our feelings and those of others, for motivating ourselves, and for managing emotions well Ourselves and in our relationships". Goleman's model defines elements of EI for interrelationship and intrarelationship. He has mentioned four Components of emotional intelligence that are Important in recognizing and managing self-Emotions and Social relationships. In four Categories self-awareness is about understanding Emotions and deciding on that basis. the second category is self-management including Adaptivity in changing Environment. The third category talks about social awareness which incorporates the skill in a person to understand and deal with others' emotions refers to how individuals hold relationships and recognize feelings, and concerns of others in social networks. The fourth category Is Relationship Management involves skills and adaptability for relationship Management. [6]The Goleman model Component can be better Explained through a matrix of four categories through an image which is given below:

Emotional Competencies		
	Self (Personal Competence)	Other (Social Competence)
	Self-Awareness	**Social Awareness**
Recognition	• Emotional Self-Awareness • Accurate self-assessment • Self-confidence	• Empathy • Service orientation • Organizational awareness
	Self-Management	**Relationship Management**
Regulation	• Emotional self-control • Trustworthiness • Conscientiousness • Adaptability • Achievement drive • Initiative	• Developing others • Influence • Communication • Conflict Management • Visionary Leadership • Catalyzing change • Building bonds • Teamwork & Collaboration

Figure 1: The performance model is given by Goleman

Competencies model of EI by Bar-On's: In 1998 Bar-On named EI as emotional quotient. He explained Emotional intelligence as "an array of non-cognitive abilities, competencies, and skills that influence one's ability to succeed in coping with environmental demands and pressures". Specifically in his explanation of EI, he emphasizes on one understanding of feelings & emotions and knowledge to express oneself, managing the emotion of own self and others, coping with change in a social environment, and problem-solving behavior for others and oneself. Bar on model emphasized process rather than outcome, he mentioned a person having less emotional intelligence can lack in achieving success in life. [6]Bar on a model have mentioned five components and fifteen sub-component of emotional intelligence which are given below:

DOI: 10.9756/INT-JECSE/V14I3.555

Components	Sub-Components
Intrapersonal	Self Regard Emotional Self-Awareness Assertiveness Independence Self-Actualization
Interpersonal	Empathy Social Resonsibility Interpersonal Relationship
Adaptability	Reality Testing Flexibility Problem Solving
Stress Management	Stress Tolerance Impulse Control
General Mood Components	Optimism Happiness

Figure 2: Model of Emotional Intelligence: Bar-On's[7]

The ability model of EI by Mayer, Salovey, & Caruso's: Salovey and Mayer explained EI as "the ability to perceive emotions, to access and generate emotions to assist thought, to understand emotions and emotional knowledge, and to reflectively regulate emotions to promote emotional and intellectual growth." Ability Model talks about the development of Emotional intelligence as an ongoing Process from childhood to adulthood. Which is defined through four branches They are Emotional Management, Emotional Understanding, Emotional Perception, Emotional facilitation. The first branch of this model refers to understanding Emotions through the face and body language, understanding oneself and others. Emotional facilitation concerned with concrete thinking differentiates between different Emotions like anger, mood swing, etc. focuses on Prioritizing thinking and decision. The third branch is Emotional Understanding refers to Processing and Understanding Emotions. The last branch is Emotional Management, which is about Managing Emotions for oneself and social effectiveness.

Figure 3: The four branches of the Ability Model.

Objective:
The study aims to understand the importance of emotional intelligence in social relationships.

DOI: 10.9756/INT-JECSE/V14I3.555

Hypothesis:
There is a significant level of emotional intelligence that is essential in impacting social relations for individuals.

Operational definition of Keyword:
Emotional intelligence: It is a set of skills, abilities that are important to understand and deal with our feelings as well as others, improve and uphold social connections, cope with difficult situations, and use emotional intelligence to deal with the various condition in meaningful and effectful ways.[8]

Social relationship: Social relationship can be defined as an individual relationship with others in a different setting like the workplace, community, etc.

3. LITERATURE SURVEY

R.Trigueros, E.Sanchez-Sanchez, I Mercader et al. did a study on the Relationship between EI, Social Skills, on secondary school students of the Spanish school. This research aims to identify the influence of social skills and emotional intelligence on bullying in peer groups. The result of this study mentioned that there is positive relation in social skills have higher empathy which creates a positive relationship among the peer group. So, the study mentioned variables are predictors for best social functioning whereas the negative result of the study shows that those who didn't have optimal emotional intelligence are involved in bullying because of bad emotional management. So appropriate development of emotional intelligence can support adolescents in managing their behavior in society and prevent them from violent actions.[1]

A.Petrovici, T.Dobrescu conducted a study to evaluate the importance of EI in skills and communication. The study mentioned the previous research related to the domain. In this study 250 subjects are taken as a sample which includes student faculties from very domains. The evaluation instrument of the study consists of 10 items. As result, this study states that women show better results in showing emotional intelligence, they are better at expressing emotions compare to men. This study concluded by saying that the best level of emotional intelligence can be achieved by linking empathy with self-control and increasing the level of understanding of others' feelings and nurturing these traits may become a challenge for the future.[9]

.Behbahani,Done a study on the correlation among EI and Employee's Performance variables. This study includes 160 employees as a sample from the physical education department in Iran. The tool included a Questionnaire by Cyberia-Shrink, including Steinmetz-Todd Capabilities Questionnaire for Collecting the data of Study. The result of this Study Shows emotional intelligence is one of the major factors in establishing relationships among managers and Employees. It can foster motivation, appropriate Communication, and health relation at the workplace. Having good emotional intelligence can evade anger or any negative feeling in a person. The researcher mentioned the Statement of Goleman (1988) that Emotional intelligence is important for adaptation, job performance, and a good relationship in his Conclusion.[10]

P.Lopes, M.Brackett, J.Nezlek, et.al has been done a study on Emotional intelligence and social interaction in which he discusses the role of Emotional intelligence and social interaction. This study suggested that Emotional abilities and Personality traits are helpful for social adjustment and adaptation This Study unused the MSCEIT test to understand the relationship between quality of social interaction and Emotions management. As a Sample, the researcher has Collected 118 Students Sample for the study The result Concluded that those who have higher scores in managing Emotions are positively related to social interaction. [11]

P.Roy, I. Chandi, Conducted a quantitative study to investigate the ability of emotional intelligence in a social relationship in the growing period of adulthood, and also looking for the connection between social relationship and emotional intelligence. The sample of the study is 60 adult of which 15 are urban male 15 female or 15 rural male and 15 female who falls between 19 to 30 age group. stratified random sampling technique is used for the study. the tool is used for the study is a standardized tool as well as a researcher also opts for the self-made tool according to the study. interpretation of the study is done through descriptive and inferential statistics. As a result of the study, the researcher found that emotional intelligence and social skill are directly related to social relationships. But also mention that other factors are also important to build a social relationship in adulthood.[12]

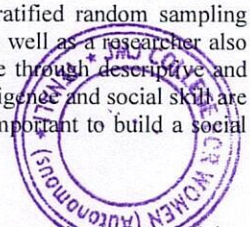

4. APPROACH FOR RESEARCH

The data facts, the figure of this study are gathered from secondary sources like research studies, articles, reports, websites, etc.

The implication of the study:
The purpose of the present study is to help others to understand the role and impact of EI in maintaining social relationships and also revealing the importance of EI for social harmony.

DOI: 10.9756/INT-JECSE/V14I3.555

5. CONNEXION AMONG EMOTIONAL INTELLIGENCE AND SOCIAL RELATIONSHIP

The social relation is a term that means a personal connection with another individual, group, an organization in any setting of our society. It can be maintained through any means of communication like physical or verbal. It is said that "humans are social animals" mean we are part of the society and survival of human beings is not possible without being a part of society. We play different roles and responsibilities in our social relations. many people maintain good relations in society and many are not able to do so. But when we study the factors of maintaining relationships, we may know that few skills are necessary for keeping good relations in our social context.

Emotional intelligence comprises mostly intelligence which includes factors like interpersonal, understanding others' emotions, intrapersonal, knowing one's own emotions, both factor plays a very significant role in maintaining and influencing social relation. Emotional intelligence is considered a key element for social interaction because it helps in understanding Others' feeling, thoughts, intentions encourage communication that supports the social function. Ultimately emotional management talks about a person who can manage their own emotions as well as be able to understand and manage other emotions. If a person is socially responsible and able to manage relationships it impacts positively in their social relationship. It can be understood through the diagram given below:

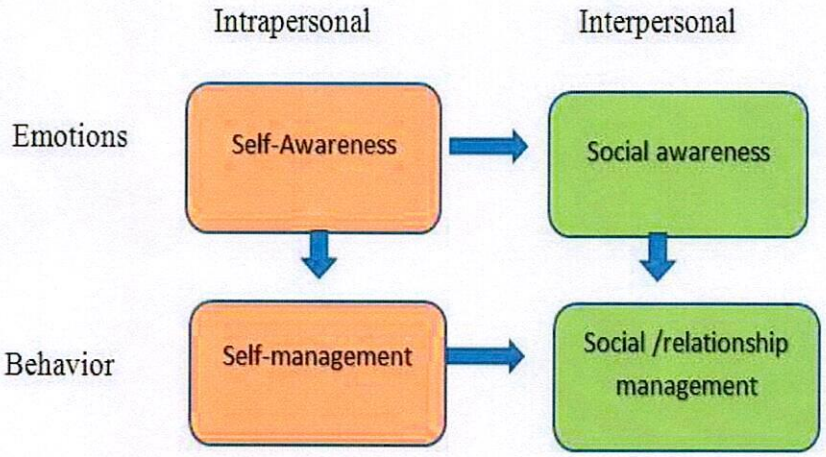

Figure 4: Interconnection of emotions and behavior in social relations.

If a person is self-aware can understand their own emotions and effect when using that feeling through which he can evaluate the outcome or impression of the decision. An individual who can self-management of their behavior can adapt to the changing situation and control their negative attitude or any emotions. A socially aware person does not react before thinking about others feeling. They don't make uncomfortable others and also respect the feeling of another person. A person who can understand others' problems can easily solve them through effective communication without raising conflict can also influence others and positive way can have a strong social relationship. Hence emotional intelligence skills ease our social behavior adjustment and performance in society.

Emotional intelligence performs a major role in managing society's mental health and well-being. which nurtures relationships in a positive manner. It can influence a person's behavior and its consequences in many fields either in personal relations or professional relations. An emotionally intelligent person can manage intra-personal things and foster interpersonal relationships. People in social and professional life giving value emotional intelligence more than intellectual intelligence. Many researches, articles have proven the importance of EI in one's life for professional and personal growth, signifying graphical representation of the studies:

DOI: 10.9756/INT-JECSE/V14I3.555

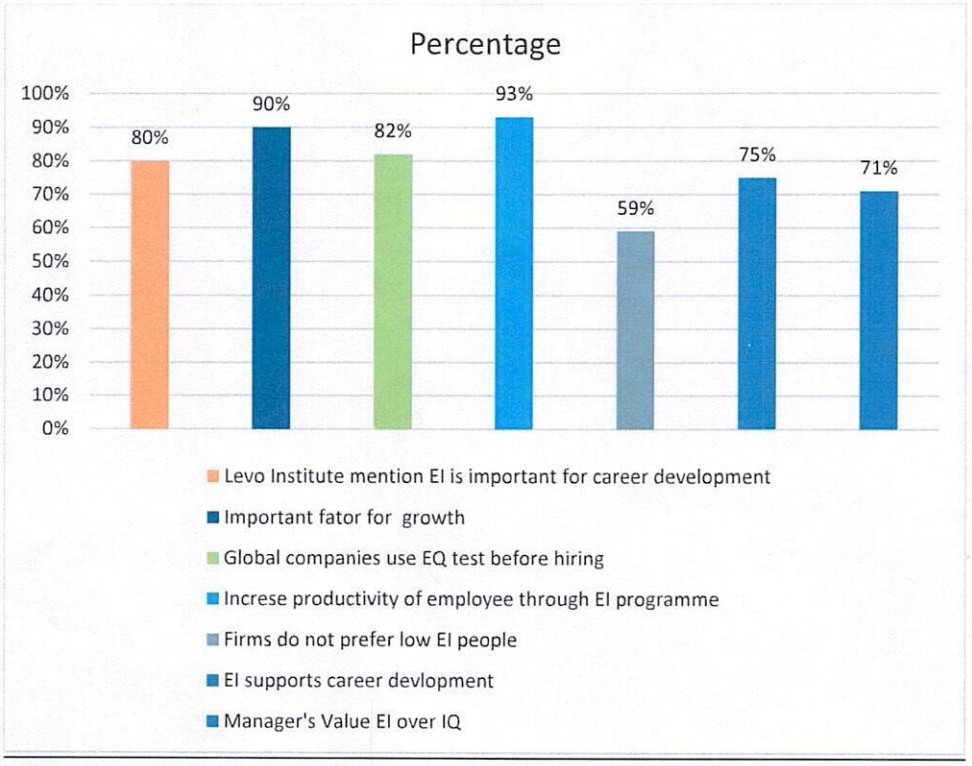

Figure 5: Representation of studies [13][14][15]

6. CONCLUSION

Through the studies done in the same field, we can understand the value of emotional intelligence. Emotional intelligence in a human being is capable of managing stress, evaluating situations, and understanding them from various perspectives, always carrying a positive and problem-solving attitude who can deal with crisis adopt a coping attitude in any difficult situation, respect others and themselves as well. these people's behavior helps them in achieving goals and they also help others to progress in their life. they also contribute to balancing peace and harmony in their social relationship. An empathic person utilizes their skills to help others for cultivating positive emotions & attitudes. Nowadays Emotional Intelligence is important in every field of our society whether that is a workplace, school, or personal relationship. Erik Erikson talks about the person's psychological need for relation with society. this time researcher found that emotional intelligence and its components: perform a major part in maintaining impactful relationships with society. Emotional intelligence makes a person aware of oneself, makes them able to manage emotions of one other, ability to handle an interpersonal relationship.[16]

7. REFERENCES

[1]. R. Trigueros et al., "Relationship between Emotional Intelligence, Social Skills and Peer Harassment. A Study with High School Students," Int. J. Environ. Res. Public Health, vol. 17, no. 12, pp. 1–10, Jun. 2020, doi: 10.3390/IJERPH17124208.

[2]. S. Malekar and R. P. Mohanty, "Factors affecting emotional intelligence: an empirical study for some school students in India," Int. J. Manag. Educ., vol. 3, no. 1, pp. 8–28, 2009.

[3]. "Emotional Intelligence", 4 Emotional Intelligence Skills for Handling Crises, www.kornferry.com.

[4]. "Difference Between Social Intelligence and Emotional Intelligence | Compare the Difference Between Similar Terms." https://www.differencebetween.com/difference-between-social-intelligence-and-emotional-intelligence/ (accessed Jan. 28, 2022).

[5]. C. Salavera, P. Usán, and L. Jarie, "Emotional intelligence and social skills on self-efficacy in Secondary Education students. Are there gender differences?," J. Adolesc., vol. 60, pp. 39–46, Oct. 2017, doi: 10.1016/J.ADOLESCENCE.2017.07.009.

DOI: 10.9756/INT-JECSE/V14I3.555

[6]. S. Mehta and N. Singh, "A Review paper on emotional intelligence: Models and relationship with other constructs," Int. J. Manag. Inf. Technol., vol. 4, no. 3, pp. 342–353, Jul. 2013, doi: 10.24297/IJMIT.V4I3.772.
[7]. "Emotional Intelligence Test, Emotional Intelligence Concepts, Emotional Intelligence Definition."https://www.civilserviceindia.com/subject/General-studies/notes/emotional-intelligence-concepts.html
[8]. "BPCS-183 Emotional Intelligence."
[9]. A. Petrovici and T. Dobrescu, "The Role of Emotional Intelligence in Building Interpersonal Communication Skills," Procedia - Soc. Behav. Sci., vol. 116, pp. 1405–1410, Feb. 2014, doi: 10.1016/J.SBSPRO.2014.01.406.
[10]. A. A. Behbahani, "A comparative study of the relation between emotional intelligence and employee's performance," Procedia - Soc. Behav. Sci., vol. 30, pp. 386–389, 2011, doi: 10.1016/J.SBSPRO.2011.10.076.
[11]. P. N. Lopes, M. A. Brackett, J. B. Nezlek, A. Schütz, I. Sellin, and P. Salovey, "Emotional Intelligence and Social Interaction," 2004, doi: 10.1177/0146167204264762.
[12]. P. Roy and | SwarupChandi, "Impacts of Emotional Intelligence on Social Relationships in Adulthood: A Normative Survey Study," Res. Pap. E-ISSN, Accessed: Jan. 28, 2022. [Online]. Available: https://ssrn.com/abstract=3978007.
[13]. "30 Interesting Statistics on Emotional Intelligence." https://blog.dtssydney.com/30-interesting-statistics-on-emotional-intelligence (accessed Feb. 01, 2022).
[14]. "Mentorprise | Emotional Intelligence." https://mentorprise.be/emotional-intelligence/ (accessed Feb. 01, 2022).
[15]. "EQ (Emotional Intelligence) and the Future of Work | Mitrefinch Inc." https://mitrefinch.com/blog/eq-future-work/ (accessed Feb. 01, 2022).
[16]. "What is Business Emotional Intelligence?" https://www.ebwonline.com/about-the-ebw/all-about-the-ebw-model (accessed Jan. 28, 2022).

PRINCIPAL
JMJ COLLEGE FOR WOMEN (Autonomous)
TENALI

JMJ COLLEGE FOR WOMEN (Autonomous) * TENALI *

DOI: 10.9756/INT-JECSE/V14I3.555

కావేరి ప్రత్యేక సంచిక

Journal of Literary, Culture & Language Studies

Vol. 19 - Issue. 3 - Spl. Edition - March 2022 - ISSN No. : 2456-4702

తెలుగు సాహిత్యం - వికాసం

అంతర్జాల జాతీయ సదస్సు

3-4 మార్చి 2022

నిర్వహణ:

తెలుగు శాఖ, IQAC మరియు పూర్వ విద్యార్థుల సంఘం వారి సంయుక్త ఆధ్వర్యంలో

ప్రభుత్వ డిగ్రీ కళాశాల : చేబ్రోలు, గుంటూరు జిల్లా.

శ్రీ వైష్ణవీ & కె ప్రభుత్వ డిగ్రీ కళాశాల : కోవూరు, నెల్లూరు జిల్లా.

మార్చి 2022

అంతర్జాల జాతీయ సదస్సు
3-4 మార్చి 2022

భావేచిత ప్రత్యేక సంచిక

తెలుగు సాహిత్యం - మహిళ

ప్రభుత్వ డిగ్రీ కళాశాల: చేబ్రోలు

(ఆచార్య నాగార్జున విశ్వవిద్యాలయ అనుబంధ కళాశాల)

చేబ్రోలు, గుంటూరు జిల్లా, ఆంధ్రప్రదేశ్, ఇండియా.

శ్రీ వై.కె.ఆర్ & కె ప్రభుత్వ డిగ్రీ కళాశాల: కోవూరు

(విక్రమ సింహపురి విశ్వవిద్యాలయ అనుబంధ కళాశాల)

కోవూరు, నెల్లూరు జిల్లా, ఆంధ్రప్రదేశ్, ఇండియా.

BHAVAVEENA Spl. Issue
Vol. 19, Issue. 3, March 2022
ISSN No. : 2456-4702 - RNI No. APTEL/2003/12253
భావవీణ
UGC CARE List Group - 1
under Arts and Humanities

మహాభారతంలో సహనం కలిగిన స్త్రీమూర్తులు

– డా॥ ఖి. మేరికుమారి, అధ్యాపకురాలు, తెలుగు విభాగం, జె.యం.జె. మహిళా కళాశాల,

సత్యవతి :

ఈమె దాశరాజు కూతురు. పడవ నడిపేది. పరాశరుడు అనే ముని వల్ల వ్యాసుడు పుడతాడు. పిల్లవాడు 12 ఏళ్ళ ప్రాయంతో పుట్టి, నువ్వు ఎప్పుడు కోరుకున్నా నేను అప్పుడు ప్రత్యక్షమౌతానని చెప్పి వెళ్ళిపోయాడు. తరువాత శంతనుడు గంగా తీరానికి వెళ్ళినపుడు ఈమె కన్పిస్తుంది. ఈమెను మోహించి ఆమెతో వివాహం జరిపించమని ఆమె తండ్రిని అడుగుతాడు. అందుకు దాశరాజు నీ మొదటి భార్యకు పిల్లవాడు వున్నాడు. ఇప్పుడు నా కూతురుని ఇచ్చి పెళ్ళి జరిపిస్తే నా కూతురుకు పుట్టే పిల్లలకు రాజ్యాధికారం ఉండదు కదా అంటాడు. ఈ విషయం తెలుసుకున్న గాంగేయుడు దాశరాజుతో మాట్లాడి సత్యవతికి, శంత నుడికి పెళ్ళి జరిపిస్తాడు. తర్వాత ఈమెకు చిత్రవీర్యుడు, విచిత్ర వీర్యుడు అనే ఇద్దరు కుమారులు పుడతారు. వీరిద్దరు చనిపోతారు. తర్వాత తన వంశం నిలబడదని గాంగేయుడిని వివాహం చేసుకోమంటుంది. అతను చేసుకోను అని చెప్పటంతో, అతనికి తన గతం చెప్పి వ్యాసుడిని పిలిపించి, వ్యాసుడు ద్వారా వంశాన్ని నిలబెట్టి స్తుంది. వ్యాసునికి ధృతరాష్ట్రుడు, పాండురాజు, విదురుడు అనే ముగ్గురు కొడుకులు పడతారు. ఈవిధంగా ఆరిపోతున్న వంశాన్ని నిలబెట్టిన వనితగా గుర్తించవచ్చు. తనకు వచ్చిన కష్టాలను ధైర్యంగా ఎదుర్కొన్న స్త్రీగా తెలుసుకోవచ్చు.

కుంతి :

మహాభారతంలో కుంతి అసలు పేరు పృధ. కుంతి భోజుడనే రాజు కూతురు. కనుక ఈమెకు కుంతీదేవి అనే పేరు వచ్చింది. ఆమె పాండవుల తల్లి. పాండురాజు భార్య, వసుదేవుని చెల్లెలు, శ్రీకృష్ణుని మేనత్త, యాదవుల ఆడబిడ్డ. పువ్వు పుట్టగానే పరిమళిస్తుంది. కుంతి చిన్ననాడే చాలా బుద్ధిమంతురాలు అనిపించుకుంది. అ
చూస్తే పెద్దలకు ముద్దు పచ్చేది. తండ్రి ఆజ్ఞ
ఇంటికి వచ్చిన అతిథికి పాదాభివందనం చేసేవాడు.
ఆకస్మికంగా దుర్వాసుడనే ఋషి వచ్చాడు. అ
చూస్తే అందరికి భయమే. ఆయనకు కోపం ముక్కు
ఆయన శపిస్తే తిరుగలేదు. అలాంటి దుర్వా
ఓర్పుతో సేవచేసి ఓర్పులో భూదేవి వంటి
అనిపించుకున్నది. ఆమె చేసిన పరిచర్యకు
సంతోషపడి నీకు ఏమి కావాలో అడుగు ఇస్తాను అన్
నాకు కావలసినది ఏమున్నది మీరు ప్రసన్నులయ్
అదే పదివేలు అని అన్నది. నీవు పసిదానవు
తెలియదు. అడుగలేకున్నావు నీకు ఒక మంత్రాన్ని చెప్
తీసుకో. నీవు ఏ దేవుడిని పిలిస్తే ఆ దేవుడు నీ
వస్తాడు. నీకు వరాన్ని ప్రసాదిస్తాడు అని చెప్తాడు. కు
మారు మాటాడకుండ మంత్రంను స్వీకరించింది.

ఒకనాడు ప్రొద్దుపొడుపున స్వామీ! సహజ కుం
లతో వజ్ర కవచంతో మిరమిట్లు గొలిపే తేజస్సుతో
చూడ ముచ్చటగా ఉండే కుమారుని నాకు
దిస్తారు? అంటూ అప్రయత్నంగా దుర్వాసుడు
మంత్రం జపించింది. సూర్యభగవానుడు ప్ర
మయ్యాడు. ఇంతపని జరుగుతుందని నేను అనుకో
'అయ్యా'! నేను కన్యను, నేను గర్భవతినైతే తల్లిదండ్రు
చుట్టుప్రక్కల నున్న వారు నన్ను చూసి నవ్వు
నేను బ్రతకలేను నన్ను రక్షించు అంటుంది
సూర్యుడు కమలాక్షి ! నీ కన్యత్వం చెడదు. నీకు
వాదం రాదు నేను వరమిస్తున్నాను. అన్నారు.
బిడ్డ లోకంలో ఎవరికైనా జన్మించాడా? నాకు
చాడు. ఇది భాగ్యం అనుకోవాలా, అని లోలోపల
పోయింది. లోకోపవాదం భయం ఆమెను
చుట్టు ముట్టింది ఆమె మనసులో మెరిసిన
బాలుడిని బుట్టలో పెట్టి అశ్వనది ప్రవాహం

ప్రతిలింది. నీవుఎక్కడ వున్నా నీ చెవిపోగులు తళతళలాడే ముఖ పర్చను చూసి నిన్ను గుర్తు పడతాను అని అంటూ బావురమని చెప్పింది. బావురుమని ఏడ్చింది.

కుంతికి పాండురాజుతో పెళ్ళి అయిన దగ్గర నుండి కష్టాలు మొదలయ్యాయి. ఆమెకు పుట్టిన ముగ్గురు కుమారులు కూడ మంత్ర ప్రభావంతో పుట్టినవారు భర్త పాండురాజు చనిపోయాక భీష్మని ఆజ్ఞ ప్రకారము పంచ పాండవులను తీసుకుని హస్తినా పురానికి వచ్చింది. కౌరవులు, పాండవులను రకరకాల కష్టాలకు గురి చేసినప్పుడు ఓర్పుతో సహించింది. అర్జునుడు ద్రౌపదిని తీసుకొని వచ్చినప్పుడు పండులాగా భావించి అందరు పంచుకోండి అని చెప్పింది. కొడుకులతోపాటు అరణ్య వాసానికి వెళతాను అని ధృతరాష్ట్రుని అడిగినప్పుడు నీవు మా దగ్గరే ఉంటానని మాట ఇచ్చాపు అంటాడు. యుద్ధంలో తన కొడుకుల కోసం, చిన్నప్పుడు పదిలిపెట్టిన కర్ణుడు తన కొడుకేనని తెల్సుకుని అతని దగ్గరకు వెళ్ళి ప్రాణ దానం చెయ్యమని బ్రతిమిలాడుతుంది. పాండవులకు, కౌరవులకు కురుక్షేత్రం జరుగుతుంది అని అనుకున్నప్పుడు మీరు రాకుమారులు, ఒక రాజ పుత్రులు, మీ కర్తవ్యాన్ని మీరు నిర్వహించండి అని కుమారులకు ధైర్యం చెప్తుంది. ఈ విధంగా చరిత్రలో కుంతు అంటే సహనానికి ప్రతీక అని బిడుగురు పిల్లలకు తల్లి అని, ప్రజలు మెచ్చుకునే రాకుమారులకు తల్లి అయిందని కీర్తిస్తారు.

ద్రౌపది :

ద్రౌపది ద్రుపద మహారాజు పుత్రిక. పాండవుల భార్య, దృష్టద్యుమ్నుడు సోదరి ద్రౌపదికి వివాహం చేయటానికి పాండవులు చనిపోయారని ద్రపదుడు స్వయంవరం ఏర్పాటు చేశాడు. ఆ స్వయంవరంలో పాండవులలో మధ్యముడైన అర్జునుడు దక్కించుకొని ఇంటికి వచ్చి తల్లి అయిన కుంతితో చెప్పగా ఆమె పంచుకోమని చెప్తుంది. ఆవిధంగా ద్రౌపదికి బిడుగురు భర్తలు అయ్యారు. వివాహము చేసుకున్నప్పటి నుండి కష్టాలను అనుభవిస్తూనే ఉంది ధర్మరాజు మాయా జూదంలో ఓడిపోయినపుడు ద్రౌపదిని, అతని తమ్ముళ్ళను కూడా జూదంలో పెట్టి ఓడిపోయాడు. అందువల్ల దుర్యోధనుడు ద్రౌపదిని బానిస అని అంతపురంలో ఉన్న ఆమెను తీసుకొని రమ్మంటాడు. ఆ సమయంలో నేను రాకూడదు అని చెప్పినా వినిపించుకోకుండా జుట్టుపట్టుకొని లాక్కొస్తాడు దుశ్శాసనుడు. దుర్యోధనుడు పచ్చి ఆమెను తన తొడల మీద కూర్చోమంటాడు. ఆమె భర్తల ముందే ఆమె వస్త్రాన్ని లాగేయగ శ్రీకృష్ణుడు ఆమెను కాపాడినాడు. భర్తలతోపాటు ఆమె అరణ్య వాసం, అజ్ఞాతవాసం చేసింది. ఈ అజ్ఞాతవాసంలో విరాట రాజు భార్యకు దాసీగా పనిచేసింది.

విరాటరాజు బావమర్ది కీచకుడు కన్నుశైరంధ్రి మీద పడడంతో భీముడు అతన్ని చంపి ద్రౌపదిని రక్షించాడు. వనవాసం పూర్తి అయ్యాక, సంధి విషయంలో వెనుకకు తగ్గవద్దని ధర్మాన్నే కోరుకుంటున్నానని శ్రీకృష్ణునితో చెప్పింది. యుద్ధంలో దుశ్శాసనుని రక్తంతో తన యొక్క వెంట్రుకలను శుద్ధి చేసుకుంటుంది. అశ్వత్థామ తన పుత్రులను చంపినపుడు, భర్తలతో అతనిని చంపి పగతీర్చు కొమ్మని చెప్తుంది. అశ్వత్థామ ఓడిపోయి తలపై ఉన్న చూడామణి కోసి ఇవ్వటంతో ఆమె కోపం చల్లారుతుంది. యుద్ధం అయిపోయాక ధర్మరాజుని పట్టాభిషేకానికి ఒప్పించే బాధ్యత ద్రౌపది తీసుకోవలసి వచ్చింది తర్వాత కొంతకాలం హస్తినాపురానికి పట్టమహిషిగా జీవించింది. చరిత్రలో ఎవ్వరికి జరగని అవమానాలు అవహేళనలు అన్ని అధిగమించి చివరి గమ్యానికి చేరుకుంది. ఈమెకు కూడా ఓర్పు ఎక్కువ, తనకున్న ధర్మ సంకటాలు అన్ని శ్రీకృష్ణుడిని, వ్యాసుడిని అడిగి తీర్చుకునేది. ఇంతటి ఓర్పు కలిగి స్త్రీ మూర్తులు భారతంలో ఇద్దరే ఇద్దరూ వారు ఒకరు కుంతీదేవి, మరొక ఆమె ద్రౌపది. వీరిద్దరి మధ్య తేడాయని బంధం కన్పిస్తుంది. ఒకామె ఐదుగురు పుత్రులకు తల్లిగా పేరు తెచ్చుకున్నది. మరొక ఆమె ఐదుగురు భర్తలకు భార్యగా జీవన యాగం పూర్తి చేస్తుంది.

ఆధార గ్రంథాలు : మహాభారతం

WORLD JOURNAL OF PHARMACY AND PHARMACEUTICAL SCIENCES
SJIF Impact Factor 7.632
Volume 11, Issue 6, 1872-1881 Research Article ISSN 2278 – 4357

MUCORMYCOSIS: ASSESSMENT OF RISK FACTORS IN A SUBJECT SUFFERING FROM CONGENITAL HAEMOPHILIA

Baratha Jyothi N.[1]*, Aruna M.[2] and B. Karuna Harika[3]

[1]Lecturer, Dept. of Zoology, [3]Dept.of Hindi, Maris Stella College (Autonomous) Vijayawada, A. P. India.

[2]HOD, Dept. of Zoology, JMJ College for Women (Autonomous) Tenali, A.P. India.

Article Received on
14 April 2022,
Revised on 04 May 2022,
Accepted on 24 May 2022
DOI: 10.20959/wjpps20226-22364

***Corresponding Author**
Dr. Baratha Jyothi N.
Lecturer, Dept. of Zoology, Maris Stella College (Autonomous) Vijayawada, A. P. India.

ABSTRACT

The present paper communicates a rare presentation of COVID-19 infection in a 32-year-old male patient, who presented with black fungus infection after recovery from corona infection during second lock down period and development of the classic symptoms for COVID-19. Subject is suffering from congenital Haemophilia of Factor IX and diabetes. COVID-19 infection has been associated with fungal infections. Mucormycosis is more often seen in immunocompromised individuals, and complications of orbital and cerebral involvement are likely in diabetic ketoacidosis and with concomitant use of steroids. Rhinocerebral mucormycosis is a **rare opportunistic infection of the sinuses, nasal passages, oral cavity, and brain caused by saprophytic fungi**. The infection can rapidly result in death. Rhinocerebral mucormycosis commonly affects individuals with diabetes and those in immunocompromised states. **CT brain scan showing the appearance of** a cerebral infarct. CT scan of a patient who is suspected of having mucormycosis shows extensive involvement of the right orbit and adjacent sinuses. There was total ophthalmoplegia of the right eye. He incidentally tested positive for COVID-19. An emergency functional endoscopic sinus procedure was done, which confirmed mucormycosis on histopathological examination. After 1 week of conventional amphotericin B and antibiotics, repeat CT brain showed improvement in mucosal thickening and sinusitis. This case is a rare presentation of mucormycosis associated with rapid progression to orbital apex syndrome with brain infarction in a patient with non-

ketotic diabetes and COVID-19. Early diagnosis and treatment are essential to prevent further end-organ damage.

KEYWORDS: Haemophilia of Factor IX, Mucormycosis, mucosal Thickening and Sinusitis, amphotericin B.

INTRODUCTION

Over the past few decades, several blood-borne viruses have targeted haemophilia patients requiring treatment with clotting factors derived from human plasma. In haemophilia B, also known as "Christmas disease," the person lacks clotting factor IX. Haemophilia occurs in around 1 in every 20,000 males born worldwide.

Mutations in the *F8* or *F9* gene lead to the production of an abnormal version of coagulation factor VIII or coagulation factor IX, or reduce the amount of one of these proteins. The altered or missing protein cannot participate effectively in the blood clotting process. As a result, blood clots cannot form properly in response to injury. These problems with blood clotting lead to continuous bleeding that can be difficult to control. The mutations that cause severe haemophilia almost completely eliminate the activity of coagulation factor VIII or coagulation factor IX. The mutations responsible for mild and moderate haemophilia reduce but do not eliminate the activity of one of these proteins.

What is mucormycosis?

Mucormycosis is a very rare infection. It is caused by exposure to mucor mould which is commonly found in soil, plants, manure, and decaying fruits and vegetables. "It is ubiquitous and found in soil and air and even in the nose and mucus of healthy people.

It affects the sinuses, the brain and the lungs and can be life-threatening in diabetic or severely immunocompromised individuals, such as cancer patients or people with hemophilia of Factor VIII or Factor IX.

History

Symptoms of rhinocerebral mucormycosis are often nonspecific, complicating early diagnosis. The most common presentation includes facial pain, headache, lethargy, visual loss, proptosis, and/or palatal ulcer. Perinasal cellulitis and paresthesia are also common early clinical signs of rhinocerebral mucormycosis. The incubation period is measured in days. The

clinical course can progress from normal to symptomatic in a week and from sinus opacification to uncal herniation and death in just a few days.[1,2,3]

General symptoms of rhinocerebral mucormycosis include the following:

- Headache
- Nausea
- Fever
- Lethargy

Facial symptoms of the disease include the following:

- Weakness
- Numbness
- Pain

Nasal symptoms of rhinocerebral mucormycosis include:

- Purulent drainage
- Stuffiness and rhinorrhea
- Epistaxis
- Nasal hypoesthesia

Ocular symptoms include the following:

- Periorbital or retro-orbital pain
- Diplopia and blurred vision
- Amaurosis (unilateral or bilateral)
- Possible rapid progress to blindness

CNS symptoms include the following:

- Convulsions

This emerging coronavirus (SARS-CoV-2) virus, spreading from person-to-person via respiratory droplets, is mainly responsible for respiratory tract infections and potentially fatal pneumonia in more frail patients. Current available data show that the mortality is very low in those less than 20 year of age but much higher, up to 20 %, in older patients presenting with co-morbidities. This may have consequences on medical follow-up, assessment consultations, specific treatments (immune tolerance induction), therapeutic education programs, and diagnostic procedures including lab testing. Treatment centres must rapidly adapt to this

reality by taking advantage of all means of distance communication such as telemedicine and maintain regular contacts with patients, especially those who require more attentive and regular follow-up. Elective surgeries have been postponed in areas where hospitals need to conserve resources for the overwhelming onslaught of COVID-19 patients.

MATERIALS AND METHODS

The study was a retrospective record based and observational study carried out of a 32 year old Haemophilia patient May 10th 2021 to April 2022. Permission from the subject and family members was taken and the data is highly reliable. The clinical profile of the subject during the study period was noted. He was admitted to Gandhi hospital, Hyderabad.

RESULTS

MRI BRAIN, PNS AND ORBITS (PLAIN & CONTRAST)

TECHNIQUE:
T1,T2, FLAIR AXIAL , T2 SAGITTAL; SWI, DWI.
T1, T2 FAT SAT CORONALS, T1 FAT SAT , T2 FAT SAT AND OBL SAGITTAL T2.
POST CONTRAST: T1 AXIAL, CORONAL AND SAGITTALS.

FINDINGS:

BRAIN:
Sulcal and cisternal spaces are normal.

Ventricular system is normal in size and signal intensities.

Cerebellum and brain stem show normal signal intensity.

Sellar and para sellar regions are normal.

Cerebral parenchyma show normal signal intensity.
No abnormal enhancing areas noted on contrast administration.

No haemorrhage/infarcts

No shift of midline structures.

MRI PNS AND ORBITS:

Known case of invasive fungal sinusitis - status post surgery.

Fluid signal intensity noted in bilateral mastoid air cells - Bilateral Mastoiditis.

Partial maxillectomy with resection of medial walls of bilateral maxillary sinuses and resection of left inferior and middle turbinates.

Heterogeneously enhancing mucosal thickening in sphenoid sinus, bilateral ethmoidal air cells, right maxillary sinus and frontal sinuses.

Minimal mucosal thickening with enhancement on contrast on left maxillary sinus.

Signal changes in bilateral zygomatic bones with enhancing periosseous soft tissue enhancement of bilateral masticator muscles, enhancement in right retroantral region and right pterygopalatine fossa.

Enhancement noted in left orbital apex, retroorbital fat with enhancement of left optic nerve sheath and medial and lateral rectus muscles.

Soft tissue thickening with enhancement in bilateral preantral regions.

Evidence of dural enhacement noted in left anterior temporal region.

Fig. 1: Case report of haemophilia subject.

NATURE OF SPECIMEN FOR EXAMINATION:

C.S.F. ANALYSIS		**SERUM PROTEINS**	
Globulin:		(i) Total :	gm%
Protein :	mg%	(ii) Albumin : 3.19	gm%
Sugar:	mg%	(iii) Globulin:	gm%
Chlorides:	mg%	(iv) Fibrinogen:	mg%
ASCITIC FLUID		**SERUM BILIRUBIN**	
Total Proteins :	gm%	(i) S.V.B.R.	
PLEURAL FLUID		(ii) T.S.B. 0.62	mg%
Total Proteins :	gm%	(iii) T.T.T.	Unit
BLOOD SUGAR = 126.8		**PROTHROMBIN TIME** PT= 27 INR 2.2 27	
(i) Fasting :	mg%	Test Sec:	Sec.
(ii) Post prandial :	mg%	Control:	IU/L
(iii) Random :	mg%	S.G.P.T	IU/L
Blood Urea: 24.35	mg%	S.G.O.T.	KAU/100ml
Serum Cholesterol :	mg%	Acid Phosphatase :	/100ml
Serum Creatinine : 0.58	mg%	Alakaline Phosphatase 195 KAU	U/100ml
Serum Calcium :	mg%	Amylase:	
Serum Phosphorus :	mg%	**SERUM ELECTROLYTES**	
Serum Uric Acid :	mg%	Sodium : 122	mEq/L
PT-INR -		Potassium : 4.6	mEq/L
		Chloride : 85	mEq/L
		Bicarbonate :	mEq/L
		Serum Iron :	ug/100ml.

Fig. 2: Biochemical parameters of haemophilia subject.

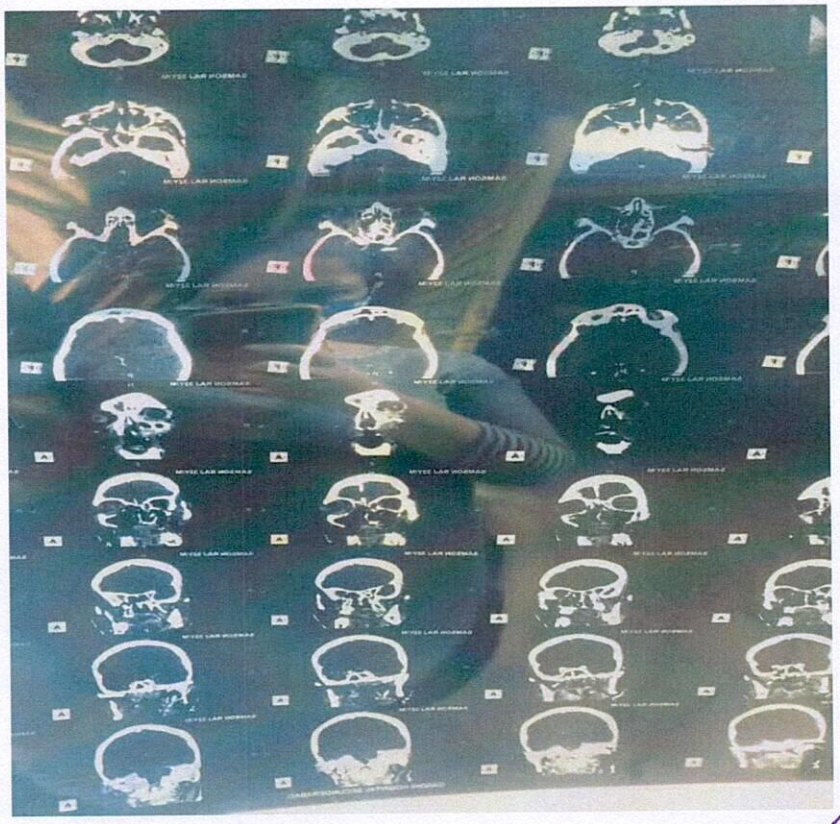

Fig. 3: Cross-sectional image of MRI brain showing acute infarct of the parieto-occipital lobe. ADC, apparent diffusion coefficient; DWI, diffusion weighted image.

Treatment

He was initiated on conventional amphotericin B (given for 11 days) and aspirin for acute cerebral infarct. Post FESS, CT paranasal sinus imaging was done after 1 week of treatment

with antifungal therapy and showed a reduction in the diffuse opacification of the left ethmoid, frontal and maxillary sinuses.

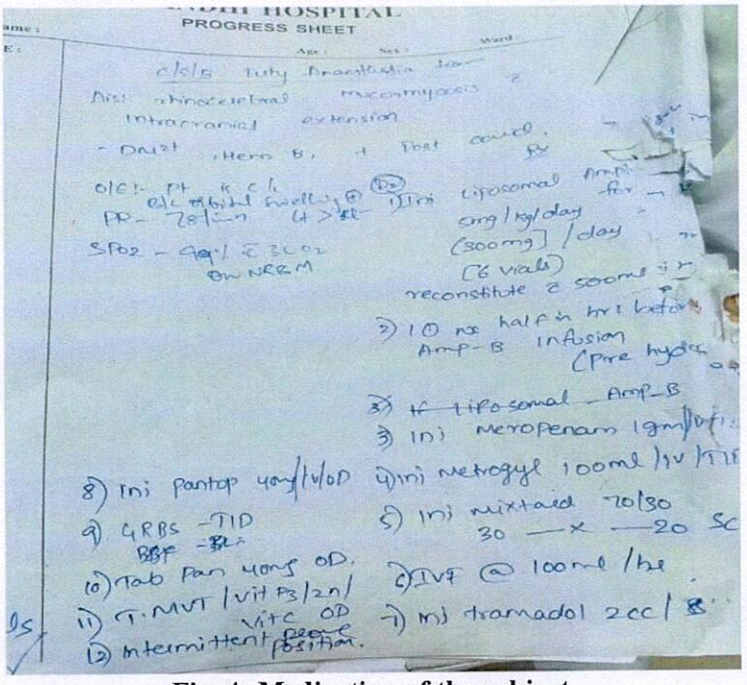

Fig. 4: Medication of the subject.

DISCUSSION

An active search of literature reviewed few reported rhino-orbitary cases associated with COVID-19.[4,5,6] Diabetes mellitus is an independent risk factor for rhino-orbital–cerebral mucormycosis in a meta-analysis of 600 series with 851 cases. The most common species isolated was *Rhizopus* species, with an overall mortality of 46%.[7] A case of COVID-19 with rhino-orbital mucormycosis co infection associated with ketoacidosis was reported in a patient with recent-onset diabetes mellitus.[8] A case series in the Indian subcontinent reported six cases of rhino-orbital–cerebral mucormycosis following COVID-19 infections.[8]

Control of hyperglycemia, early treatment with liposomal amphotericin B and surgery are essential for the successful management of mucormycosis. Thus, the use of glucocorticoids in mild COVID-19 cases (without hypoxaemia) or the utilisation of higher doses of glucocorticoids should be avoided. Further, in the absence of a clear benefit, drugs targeting immune pathways such as tocilizumab should be discouraged. For successful management of mucormycosis, a high index of clinical suspicion, low threshold for diagnosis in patients with risk factors, neuroimaging and specific diagnostic tests with a coordinated effort from a

multidisciplinary team including ophthalmology, otorhinolaryngology, infectious diseases, neurosurgery, critical care, microbiology and pathology department are crucial. A delay of even 6 days in initiating treatment doubles the 30-day mortality from 35% to 66%.

Simple tests like vision, pupil, ocular motility and sinus tenderness can be part of routine physical evaluation of a patient with COVID-19 hospitalised with moderate to severe infection or diabetics with COVID-19 or those receiving systemic corticosteroids. Visual prognosis, however, continues to remain poor.

Doctors believe mucormycosis, which has an overall mortality rate of 50%, may be being triggered by the use of steroids, a life-saving treatment for severe and critically ill Covid-19 patients.Steroids reduce inflammation in the lungs for Covid-19 and appear to help stop some of the damage that can happen when the body's immune system goes into overdrive to fight off coronavirus. But they also reduce immunity and push up blood sugar levels in both diabetics and non-diabetic Covid-19 patients.

It's thought that this drop in immunity could be triggering these cases of mucormycosis. Eleven of them had to lose an eye, and six of them died. Most of her patients are middle-aged diabetics who were struck down by the fungus two weeks after recovering from Covid-19. "We are already seeing two to three cases a week here. It's a nightmare inside a pandemic," she told me. In the southern city of Bangalore, Dr Raghuraj Hegde, an eye surgeon, tells a similar story. He has seen 19 cases of mucormycosis in the past two weeks, most of them young patients. "Some were so sick that we couldn't even operate on them."

Doctors say they are surprised by the severity and the frequency of this fungal infection during the second wave, compared to some cases during the first wave last year.

Dr Nair says he has come across not more than 10 cases in Mumbai in the past two years. "This year is something different," he says. **Present study subject from this deadly infectious disease after using proper medication.**

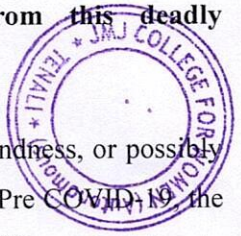

If not treated early and aggressively, it can spread to the eyes causing blindness, or possibly involve the central nervous system causing seizures and leading to death. Pre COVID-19, the rate of prevalence of mucormycosis ranged between 0.005 and 1.7 per million population in different countries, except India, where the number of reported cases were far greater at 140 cases per million population. Now with 27 million COVID-19 cases in India (as of May 23,

2021), 77 million diabetics and the use of steroids for treatment, there has been an exponential increase in the reported cases of mucormycosis.[8,9,10,11,12,13] Of note, COVID-19 associated mucormycosis showed that 94% of patients had diabetes, suggesting the number of mucormycosis cases will continue to rise in India and globally. For the many patients affected with mucormycosis, the outcome is poor. About half of the affected patients will die and many will sustain permanent damage to their health.

The recommended treatment against mucormycosis involves the intravenous application of amphotericin B (preferably liposomal formulation) in initial dose of 5 mg per kg body weight per day, and 10 mg per kg body weight per day at advanced stage of the disease. Depending on the severity of the disease, each patient needs 60–100 injections (each vial containing 50 mg). With each injection costing from 5000 to 10,000 rupees, the projected cost of the treatment can be more than a million rupees, and even then, a successful outcome is not certain. Such high dosage of drug is administered due to the intravenous application of amphotericin B, which leads to dilution of the drug in the plasma. In the case of cerebral mucormycosis, further complications are attributed due to the highly selective blood-brain barrier and poor penetration of amphotericin B to reach the central nervous system and target the fungi. This results in the application of higher doses of the drug to accomplish minimum inhibitory concentration to target the epicentre of infection.

CONCLUSION AND RECOMMENDATIONS

Even today, many haemophilia patients and their families still retain painful and indelible memories of HIV and hepatitis C infections or are confronted with the progressive health consequences of these infections. Even as a deadly second wave of Covid-19 ravages India, doctors are now reporting a rash of cases involving a rare infection - also called the "black fungus" - among recovering and recovered Covid-19 patients. It is indeed possible to cure haemophilia by using viruses, deprived of most of their content and infectivity, as vectors to transport genetic material and permit long term, endogenous production of Factor VIII or Factor IX by the transduced liver in quantities sufficient to maintain hemostasis.Indeed, very few of the aforementioned cogent unsolved questions can be tackled by studies done in single, albeit large, haemophilia centres.Judicial use of immunosuppressive therapy in COVID-19 infection should be considered particularly in regard to treatment of fungal coinfections.

ACKNOWLEDGEMENT

All three authors were involved in patient care directly. Writing the initial manuscript was done by NBJ. Selecting appropriate image templates was done by AM. The necessary corrections and final outcome of the article were done under the guidance of BKM.

REFERENCES

1. Kimberly P Liang, Imad M Tleyjeh, Walter R Wilson, Glenn D Roberts, Zelalem Temesgen. Rhino-orbitocerebral mucormycosis caused by Apophysomyces elegans. Journal of Clinical Microbiology, 2006; 44(3): 892-8.
2. Murat Songu, H Halis Unlu, Kivanc Gunhan, S Sami Ilker, Nalan Nese. Orbital exenteration: A dilemma in mucormycosis presented with orbital apex syndrome. American Journal of Rhinology, 2008, 22(1): 98-103
3. Mahi M, Chaouir S, Amil T, Hanine A, Benameur M. Rhino-orbito-cerebral mucormycosis. Journal de Radiologie, 2002; 83(2): 165-7.
4. Mehta S, Pandey A.. Rhino-Orbital mucormycosis associated with COVID-19. Cureus, 2020; 12: e10726. pmid:http://www.ncbi.nlm.nih.gov/pubmed/33145132. doi:10.7759/cureus.10726
5. Mekonnen ZK, Ashraf DC, Jankowski T. Acute invasive rhino-orbital mucormycosis in a patient with COVID-19-associated acute respiratory distress syndrome. Ophthalmic Plast Reconstr Surg, 2021; 37: e40–80. pmid:http://www.ncbi.nlm.nih.gov/pubmed/33229953.doi:10.1097/IOP.0000000000001889
6. Mekonnen ZK, Ashraf DC, Jankowski T. Acute invasive rhino-orbital mucormycosis in a patient with COVID-19-associated acute respiratory distress syndrome. Ophthalmic Plast Reconstr Surg , 2021; 37: e40–80. pmid:http://www.ncbi.nlm.nih.gov/pubmed/33229953. doi:10.1097/IOP.0000000000001889
7. Jeong W, Keighley C, Wolfe R. The epidemiology and clinical manifestations of mucormycosis: a systematic review and meta-analysis of case reports. Clin Microbiol Infect, 2019; 25: 26–34.
8. Sen M, Lahane S, Lahane TP, et al. Mucor in a viral land: a tale of two pathogens. Indian J Ophthalmol, 2021; 69: 244–52.

9. Reference method for broth dilution antifungal susceptibility testing of filamentous fungi: approved standard-second edition. CLSI document M38-A2. Clinical and Laboratory Standards Institute, Wayne, PA: CLSI, 2008.
10. Hanley B, Naresh KN, Roufosse C, Nicholson AG, Weir J, Cooke GS, et al. Histopathological findings and viral tropism in UK patients with severe fatal COVID-19: a post-mortem study. *Lancet Microbe,* 2020; 1(6): e245–e253. doi: 10.1016/S2666-5247(20)30115-4.
11. Mehta S, Pandey A. Rhino-orbital mucormycosis associated with COVID-19. Cureus, 2020; 12(9): e10726.
12. Chen N., Zhou M., Dong X., Qu J., Gong F., Han Y. Epidemiological and clinical characteristics of 99 cases of 2019 novel coronavirus pneumonia in Wuhan, China: a descriptive study. Lancet, 2020.
13. Zhou P., Yang X.L., Wang X.G., Hu B., Zhang L., Zhang W. A pneumonia outbreak associated with a new coronavirus of probable bat origin. Nature, 2020.

PRINCIPAL
JMJ COLLEGE FOR WOMEN (Autonomous)
TENALI

JMJ COLLEGE FOR WOMEN (Autonomous) TENALI

International Journal of Early Childhood Special Education (INT-JECSE)
DOI:10.9756/INTJECSE/V14I5.317 ISSN: 1308-5581 Vol 14, Issue 05 2022

PESTICIDE SPRAYING ROBOT: THE MECHATRONICS APPROACH TO AGRICULTURE

Dr. S V G V A Prasad[1*], C.M. Anitha[2], Dr. K Ram Chandra[3],Dr. BBRG.Vijaya Lakshmi[4]
Dr. Ravi Chandran[5*], Dr. B. Annapurna[6]
[1] S G Lecturer, Department of Physics, Pithapur Rajah's Government Autonomous College Kakinada, A.P, India
[2] HOD, Departmen of Physics, JMJ College for Women (A), Tenali, A.P, India
[3] Professor and Head, Department of English,V R Siddhartha Engineering College (A), Vijayawada, A.P, India
[4] Associate Professor in Botany, Ch.S.D.St.Theresa's College for Women (A), Eluru, A.P, India
[5] Guest Assistant Professor, Department of Physics, B.M.D. College, Dayalpur, Bihar, India
[6] Associate Professor, Department of CSE, Aditya College of Engineering Surampalem, A.P, India
E-Mail: [1]dr.svgvaprasad@gmail.com, [5]goforchandran@gmail.com

ABSTRACT: Herbicides, nematicides, molluscicides, rodenticides, fungicides, insecticides, and other pesticides are all classified as pesticides. Pesticides were designed to kill specific organisms such as insects, pests, rodents, fungi, and so on, but they cause serious harm to human neurological systems and tissues. Pesticides used in Asia accounts for 50% of all pesticide manufacturing worldwide. After China and Turkey, India is the third-largest pesticide consumer in Asia **[1]**. Pesticides have a significant impact on farmers' health since they frequently come into contact with pesticides and there is currently no way to protect them. They are extremely harmful and should be banned immediately, but pest infestation and agricultural destruction will have a disastrous effect on the population of the country. This would not be a good choice in a situation where India's ranking on the global hunger index is constantly declining, but there is a need to identify alternative solutions. Our proposed project involves the use of robots to automate pesticide spraying tasks across a wide area using the Internet of Things. With the help of the Internet of Things, the robotic device is navigated, controlled, and trained to spray insecticide on plants. As a result, farmers are protected from the effects of pesticides as the physical presence of a human is not present in this scenario. The spray robot has the worldwide coverage of information update and video multicast, additional MQ-135 Air Quality Sensors provide many advantages compared to conventional pesticide spraying robots.

IndexTerms—Pesticides, ESP8266, Internet of Things (IoT)

JEL Codes: I18, I11, I15

1. INTRODUCTION

Food, housing, and clothes are the three most fundamental requirements for human survival. It is always considered necessary to look forward to feeding every individual, regardless of how powerful a country is. For millennia, India has been famed for its agricultural riches. Farmers in India are the backbone of its rich agricultural heritage. Pesticide use is unavoidable since pests cause significant crop damage, making it necessary for farmers to treat them with the appropriate chemicals and pesticides. Herbicides and insecticides are the two major types of pesticides that are made up of a mix of natural and synthetic substances. Components of insecticides such as organochlorines, creosote, and sulfallate induce cancer, whereas organochlorines DDT, chlordane, and lindane cause tumours, according to multiple previous studies [2]. Human cells and tissues are highly reactive to these substances. They induce acute irritability, skin problems, and cancer in many circumstances. The vast majority of farmers take the necessary precautions. Even so, pesticides infiltrate their bodies and create serious problems. The Punjab region of India has recently received national attention as a result of multiple incidences of blood cancer among farmers [3]. Insecticides account for the majority of pesticides used in India. Pesticides that cause major tumours and cancer have already been banned in India, but the pesticides that are still allowed have extremely harmful side effects. Our proposed system deals with a pesticide spraying robot that has IP Camera based live feed, Wireless controlled navigation and also Bluetooth controlled robotic pesticide spray.

2. PREVIOUS WORKS

There have been several studies in the field of pesticides and different efficient ways to deliver them to plants with safety. Below are some of the work which matches our domains.

ArasoTayeWaktola et al. performed the work to create an efficient pesticide spraying robot that is practical enough for real-time implementation. The system is based on live mobility and manual control. Their team's system is built on the concept of Bluetooth-based robotic control and plant spraying. It was created for real-time use and proved to be quite valuable in the development of our system. The water tank was attached to the robot's body. This tank served as a pesticide reservoir for the sprayed insecticide. In our study, we employed the attached pesticide tank in the same way. Their work is quite similar to our proposed work, but our paper includes an extra IP camera, an air quality monitoring device, which is a significant improvement over their earlier work. [4].

The Pesticide Sprayer Robot was designed by A.M. Kassim et al. with larger wheels and a more realistic approach. Their robotic system uses an Arduino Mega System, which is similar to the Arduino Nano System. The ultrasonic sensor series is utilized to autonomously navigate the path. Their module can handle a payload of up to 20 kg. The pesticide robot benefits from the greater torque provided by the four-wheel-drive system, but it also necessitates a large power supply. To reduce power usage, the arrangement employs high-capacity 12V and 7AH batteries. Pesticides are sprayed on plants using 12V/70W diaphragm pumps. Mist nozzles of various lengths are used to spray pesticides on plants of various lengths. The diaphragm pumps and BLDC motors are turned on and off by the electromagnetic relay. The technology is quite remarkable, and it must be applied in real-time. In the paper, the ultrasonic sensor setup is particularly impressive [5].

In their study, PvrChaitanya et al. described a pesticide spray robot based on machine vision. The majority of their work is based on machine learning techniques. The image stream is collected by the camera and then processed by the machine learning process. The pesticide spraying nozzle is used to spray pesticides on exposed regions where disease, pests, or diseases are found. The technology uses a machine learning approach to forecast viable cures. The L293D motor diver IC, like our proposed cent, controls the robot's robotic movement. Embedded apps are run on the Raspberry Pi3 system. The code is written in Python and provides a training set for the robot to detect any anomalies on leaves, stems, or plants. The PC and its applications can control the robotic system. This provides the spraying system with an edge of intelligence to actively detect the area to target the pesticide for spray. It helps to save the pesticide and reduce wastage. [6].

3. SYSTEM DESIGN AND SPECIFICATIONS

This technique is intended to address the major problem of pesticide poisoning, which causes significant harm to farmers' hands, legs, and eyes. Pesticide poisoning has invasive consequences such as cancer, organ failure, and, in some cases, death. Many farmers have no idea what they are dealing with; they mistakenly think of pesticide poisoning as mild skin rashes, fever, and the typical cough and cold, but when properly examined, it turns out to be a life-threatening disease. This section contains the exact specifications for creating a pesticide bot. The entire system is broken down into six modules.

DOI:10.9756/INTJECSE/V14I5.317 ISSN: 1308-5581 Vol 14, Issue 05 2022

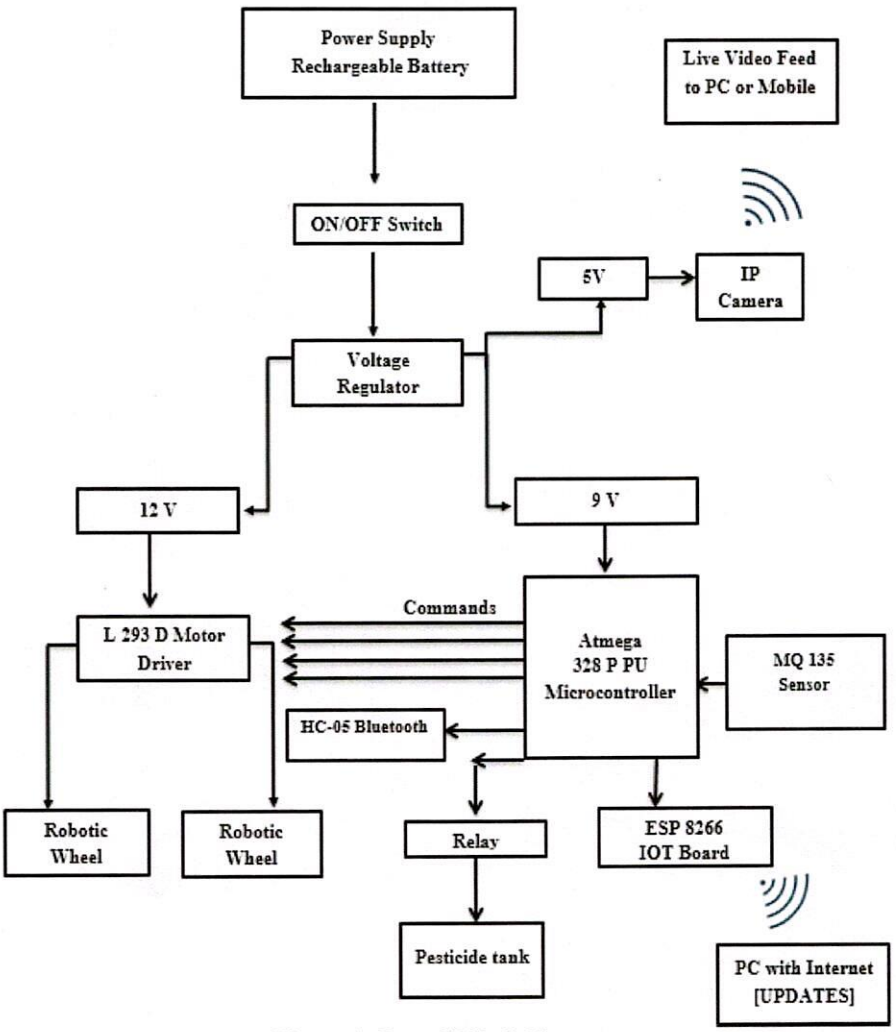

Figure 1: Overall Block Diagram

Power Supply Module: The module for supplying power uses a rechargeable battery as a power source to provide all of the system's energy needs. Various voltage regulators are used to regulating the voltages for various components and their requirements.

Motor Driver Module: The Motor Driver is built around the L293D motor driver IC. The primary responsibility of the motor driver is to regulate the power supply to the wheel motors [7]. The motor driver receives a 12V power supply. When the microprocessor sends 5V directives to the motor driver, the motor driver supplies this 12V power supply to the wheels. We use motor driver ICs to execute such jobs since microcontrollers cannot offer 12V power.

TABLE I: Motor Driver Logic

PIN	STATUS	Motor Movement
A	ON	Motor 1 Clockwise
B	ON	Motor 1 Anticlockwise
C	ON	Motor 2 Clockwise
D	ON	Motor 2 Anticlockwise

Controller Module: The controller module serves as the brain of the entire system. Embedded C code is used to write the overall program logic. The microcontroller we're using is the Atmega 328 P PU, which is a high-

performance 32-Kbyte flash program memory microcontroller. It is inexpensive and uses very little energy. It is simple to program using the Arduino IDE. The microcontroller is capable of efficiently and accurately managing all of the modules [8].

Data transmission and reception module:
The data transmission and reception module of our robotic system is divided into two sections.
The IoT transmission module comes first, followed by the Bluetooth data transceiver module.
IOT Transmission Module: The IoT transmission module is in charge of transferring all environmental data collected from the city to a central cloud server. The module updates the dedicated website with information such as the moment the robotic system started working, how long the pesticide sprayer operated, how much pesticide was sprayed, data acquired from an air quality sensor to assess toxic air levels, and so on. To complete the task, we use an ESP8266 IOT board, which is a WI-FI based IoT system that may be powered by a dedicated Wi-Fi system or even mobile phone hotspots [9].
The HC-05 Bluetooth module: The HC-05 Bluetooth module is used to connect the robot to the Android applications from a safe distance. Bluetooth is a lag-free technology that allows our robot to be extremely solid and steady when performing tasks in the field. The serial data provided by the Android phone is decoded into data series, received by Bluetooth, and forwarded to the microcontroller, where it is matched with the given task according to the system's program logic [10].
Switching Module: Relays and relay drivers make up the Switching Module. To drive 12V relays from 5V microcontroller commands, we used the ULN 2003 IC [11]. The magnetic field formed in the coils as a result of applied electric charges causes the electromagnetic relays to move. The coil movement activates and deactivates relay switching between the NO and NC pins, which is used to switch pesticide spraying motors and other components.
Sensor Module: Our project also includes an MQ-135 air quality sensor, which can detect a variety of toxic and hazardous substances in the atmosphere. It can give us information about the air we breathe, such as whether it is safe to breathe or not. It can detect NH3, NOx, alcohol, benzene, smoke, and CO2, among other gases [12]. This sensor is utilized to detect the presence of dangerous gases in our project, particularly when pesticides are employed.

4. RESULT AND DISCUSSION

The proposed robotic system is installed on a sunmica body with appropriately attached components for easy operation. The large 10x4 CM wheels are coupled to a 60 RPM geared motor to provide great torque while maintaining optimal speed. The system is efficient enough that this can work as Sanitizer sprayer in Covid type of pandemics [13][14].

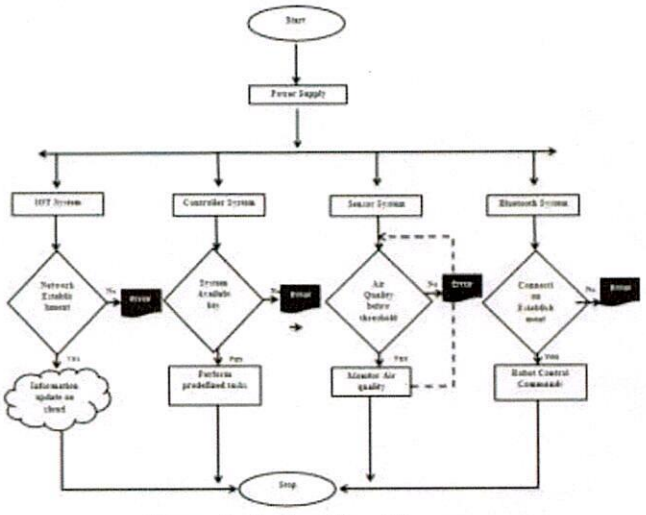

Figure 2: System Flow Diagram

The system is capable of completing the task assigned to it. The water pump motor is a DC pump system that delivers a water jet as a spray to the plant, allowing the pesticide to reach the intended area. The entire arrangement is put through its paces in real-time.

Figure 3: Spray Pump Setup

The overall system implementation is present below, some components are beneath the sunmica body to provide a neat look to the overall setup.

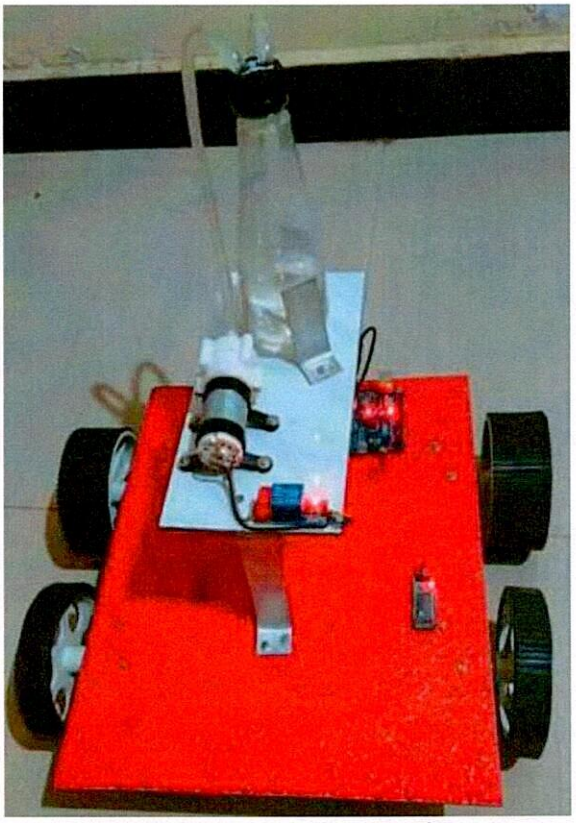

Figure 4: Overall Implementations

The simple design makes it easily fabricable for regular usage. There are several possibilities to enhance the system design as the wheels can be changed with tracked wheels, the connection range can be enhanced with RF or Zigbee System and the metallic body can be further strengthened by using fibre.

5. CONCLUSION

Thus we developed a system of pesticide spraying robots to help farmers to come out of the ill effects of pesticides. Pesticides are the important ingredients of the agriculture system and it's not possible to stop using pesticides. Of course, its usage should be minimized to avoid its ill effects and our robotic system is the technology that can efficiently operate. There is a huge possibility of enhancement in our project in future like increasing its range, weight loading capacity, intelligence and battery power but the present system helps us to estimate the enhancement possibilities in real-time.

REFERENCES

[1] "View of PESTICIDES AND INDIAN AGRICULTURE- A REVIEW | International Journal of Research -GRANTHAALAYAH." https://www.granthaalayahpublication.org/journals/index.php/granthaalayah/article/view/3930/3978 (accessed Dec. 20, 2021).

[2] J. Dich, S. H. Zahm, A. Hanberg, and H. O. Adami, "Pesticides and cancer," *Cancer Causes Control*, vol. 8, no. 3, pp. 420–443, 1997, doi: 10.1023/A:1018413522959.

[3] "Cancer ravages rural Punjab due to chemicals in pesticides; govt assistance fails to improve situation-India News ,Firstpost." https://www.firstpost.com/india/cancer-ravages-rural-punjab-due-to-chemicals-in-pesticides-govt-assistance-fails-to-improve-situation-6228451.html (accessed Dec. 20, 2021).

[4] A. T. W. Raushan Kumar Singh B. Annapurna J. Saravanan, "An Efficient Utilization of Robotics and IoT to Overcome Threats of Pesticides," *SCOPUS - Int. J. Innov. Technol. Explor. Eng.*, vol. 9, no. 2S3, pp. 411–415, 2019.

[5] A. M. Kassim*et al.*, "Design and Development of Autonomous Pesticide Sprayer Robot for Fertigation Farm," *IJACSA) Int. J. Adv. Comput. Sci. Appl.*, vol. 11, no. 2, 2020, Accessed: Jan. 05, 2022. [Online]. Available: www.ijacsa.thesai.org.

[6] P. Chaitanya, D. Kotte, A. Srinath, and K. B. Kalyan, "Development of Smart Pesticide Spraying Robot," *Int. J. Recent Technol. Eng.*, no. 5, pp. 2277–3878, 2020, doi: 10.35940/ijrte.E6343.018520.

[7] "L293D Motor Driver IC Pinout, Equivalent ICs, Features and Datasheet." https://components101.com/ics/l293d-pinout-features-datasheet (accessed Jan. 22, 2022).

[8] "ATmega328P 8-bit AVR Microcontroller with 32K Bytes In-System Programmable Flash DATASHEET."

[9] "ESP8266 Wi-Fi MCU I Espressif Systems." https://www.espressif.com/en/products/socs/esp8266 (accessed Jan. 22, 2022).

[10] "Sensors Modules Bluetooth Module Hc 05 | Sensors Modules." https://www.electronicwings.com/sensors-modules/bluetooth-module-hc-05- (accessed Jan. 22, 2022).

[11] "ULN2003A data sheet, product information and support | TI.com." https://www.ti.com/product/ULN2003A (accessed Jan. 22, 2022).

[12] "Air Quality Sensor (MQ135) : rhydoLABZ INDIA." https://www.rhydolabz.com/sensors-gas-sensors-c-137_140/air-quality-sensor-mq135-p-1115.html (accessed Jan. 22, 2022).

[13] D. R. C. Kalluri, "Effects of COVID-19 : The Psychosocial Impact on Schools and College Admissions," *J. Appl. Sci. Comput.*, vol. 8, no. 10, 2021.

[14] D. C. W. D. Dr. K. Ram Chandra Dr. Omprakash H. M., Dr. JavedAlam, Dr. K. S. V. K. S. Madhavi Rani, Dr. V. Nagalakshmi, "Education Beyond COVID-19- The world Academic Coalition," *Ann. R.S.C.B*, vol. 25, no. 2, p. 15, 2021.

PRINCIPAL
JMJ COLLEGE FOR WOMEN (Autonomous)
TENALI

JMJ COLLEGE FOR WOMEN (Autonomous) TENALI